

https://dspace.org/

Fracture control in the hangingwall and the interaction between the support system and the overlying strata

Herrmann, Dean Albert.

2015-01-27
http://hdl.handle.net/10539/16778

Downloaded from a DSpace repository. https://dspace.org/

FRACTURE CONTROL IN THE HANGINGWALL AND THE INTERACTION BETWEEN THE SUPPORT SYSTEM AND THE OVERLYING STRATA

Dean Albert Herrmann

A dissertation submitted to the Faculty of Engineering, University of the Witwatersrand, Johannesburg, in fulfilment of the requirements for the degree of Master of Science in Engineering.

Johannesburg, 1987

DECLARATION

I declare that this dissertation is my own, unaided work. It is being submitted for the Degree of Master of Science in Engineering in the University of the Witwatersrand, Johannesburg. It has not been submitted before for any degree or examination in any other University.

(Signature of Candidate)

this 1st day of October 1987

ABSTRACT

Stress-induced rock fracture is common in deep-level gold mines. Various orientations of fractures result in the formation of unstable blocks of rock which can be a danger and hindrance to mining activities. A study of the effects of an alteration in stope geometry and the influence of two different support systems on the overlying strata was performed. The stresses developed in the rock above an active support load were found to be significantly higher than those predicted by elastic theory. The cutting of a hangingwall dip slot in the back areas of a stope and the allowing of progressive collapse of the strata has been shown to cause large tensile strain changes in the hangingwall and to steepen the dip of extension fractures. Such procedures can be employed to produce competent, stable hangingwall conditions.

DEDICATION

To my parents, Herbert and Ginette,

with thanks

Tot Facienda

- Parum Factum

ACKNOWLEDGEMENTS

The author gratefully acknowledges the assistance and advice given him by his supervisor, Professor S. Budavari of the Department of Mining Engineering of the University of the Witwatersrand.

In addition the author would like to express his sincere thanks to the following:-

- Dr. Arthur Atkins, former director of the Rock Mechanics Laboratory, Chamber of Mines of South Africa, for his continual encouragement and advice during the course of the study.

- Mr. Joe de Klerk and Mr. Hennie Enslin and their staff at Hartebeestfontein Gold Mine, in particular Kingsley Kamanga, for their invaluable assistance with every aspect of the underground experimental work.

- Mr. Gieljam Oberholzer of the Rock Mechanics Laboratory, Chamber of Mines of South Africa, for conducting the laboratory tests on underground core samples.

- My colleagues at the Rock Mechanics Laboratory, in particular Matthew Mullins and Mike Roberts for

their assistance in many aspects of the research programme.

- The staff of the library at the Chamber of Mines Research Organization for their cheerful assistance in obtaining technical papers.

- Mrs. Joan Taylor, who speedily deciphered my scribbled text and turned it into a neat, typed manuscript.

Most sincere and grateful thanks to two people who untiringly gave of their best:

- Mr. Stephen Hall of the Rock Mechanics Laboratory, for his assistance in the day-to-day operation of underground experiments

and Mr. Richard Brummer, for his friendship, guidance and advice throughout the course of this study, and without whom much of this work would never have been completed.

The work described in this dissertation was carried out as part of the research programme of the Research Organization of the Chamber of Mines of South Africa.

Sola Deo Gloria

CONTENTS

		Page
DECLARATION		ii
ABSTRACT		iii
DEDICATION		iv
ACKNOWLEDGMENTS		v
CONTENTS		vii
LIST OF FIGURES		ix
LIST OF TABLES		xiv
LIST OF PLATES		xv
1	INTRODUCTION	1
1.1	Problem Definition	1
1.2	Scope of Work	2
1.3	Structure of this Dissertation	4
2	SUMMARY OF PREVIOUS WORK	7
2.1	Block Stability	7
2.2	Caving	12
2.3	Numerical Modelling of Rock Behaviour	24
2.3.1	The boundary element method (BEM)	25
2.3.2	The finite element method (FEM)	26
2.3.3	The distinct element method	28
2.4	Summary	29
3	ROCK FRACTURE AND DEFORMATION AROUND DEEP-LEVEL STOPES	31
3.1	Primary or Shear Fractures	34
3.2	Secondary or Extension Fractures	35
3.3	Parting Planes	37
3.4	Rock Deformation Around Stopes	37
3.5	Summary	46
4	BLOCK STABILITY	48
4.1	Keyblocks and their Importance in Excavation Stability	48
4.2	Stability Analysis	50
4.3	Discussion	53
4.3.1	Comparison with physical models	53
4.3.2	Parametric studies	55
4.4	Summary	60
5	EXPERIMENTAL DETERMINATION OF HANGINGWALL STRATA BEHAVIOUR	63
5.1	Measurement and Instrumentation	64
5.1.1	Strain measurement	64
5.1.2	Vertical displacement measurement	70
5.1.3	Closure and ride measurement	74
5.1.4	Surface dilation measurement	76

CONTENTS

		Page
5.1.5	Borehole observations	78
5.2	Location of the Experimental Site	79
5.2.1	Regional geology of the Klerksdorp Goldfield	79
5.2.2	Experimental site	79
5.2.3	Local geology of the second experimental site	83
5.3	Experimental Procedure	83
5.4	Laboratory Testing	89
5.4.1	Laboratory testing of rock samples	92
5.5	Summary	98
6	NUMERICAL MODELLING	104
6.1	The 'GOLD' Finite Element Suite	104
6.2	Finite Element Analyses	108
6.3	Effects of Slot-Cutting	109
6.3.1	Influence on stresses	109
6.3.2	Influence on displacements	113
6.4	Effects of Support Systems	121
6.4.1	Influence on stresses	121
6.4.2	Influence on displacements	125
6.5	Summary	128
7	RESULTS AND DISCUSSION	129
7.1	Individual Support Load Effects	129
7.1.1	Determination of the structure of the hangingwall	129
7.1.2	Induced stresses in the hangingwall	132
7.1.3	Induced displacements in the hangingwall	141
7.1.4	Young's modulus for broken rock	150
7.2	Support System Effects	152
7.2.1	Inclination of hangingwall fractures	152
7.2.2	Stress relaxation	164
7.2.3	Bedding separation	177
7.2.4	Closure and ride	188
7.2.5	Surface dilations	198
7.3	Summary of Results	202
8	CONCLUSIONS AND RECOMMENDATIONS	206
9	REFERENCES	214

LIST OF FIGURES

Figure		Page
2.1	Observations of hangingwall fracturing under different support densities. (After Morgan and Theron, 1963).	21
2.2	Sketch showing the changing pattern of fractures after commencement of 'caving'. (After Deacon, 1963).	22
3.1	Fracture classification and distribution around a typical stope face. (After Adams et al., 1981).	33
3.2	Diagram illustrating the zones of formation of primary and secondary fractures ahead of an advancing stope face. (After Brummer and Rorke, 1984).	36
3.3	Deformational mechanisms around a stope. (After Brummer, 1986a).	39
3.4	Tensile zones above and below an isolated tabular excavation at great depth. (After Salamon, 1974).	41
3.5	Elastic predictions of vertical and horizontal stresses ahead of a stope face. (After Peirce, 1981).	43
3.6	Zones of fracture formation ahead of an advancing stope face. (After Adams and Jager, 1979).	44
4.1	Keyblocks around an excavation in jointed rock. (After Goodman and Shi, 1985).	49
4.2	Isolated block in a rock stratum, showing applied forces.	51
4.3	Geometry of physical model tested by Crawford and Bray (1983). (After Yow, 1985).	54
4.4	Back analysis of required pullout stresses for a confined plaster wedge.	56
4.5	Stability curves for blocks with varying frictional properties.	58

LIST OF FIGURES

Figure		Page
4.6	The relationship between the F/W ratio and symmetric block geometry for different values of horizontal confinement.	61
4.7.	The relationship between the F/W ratio and block geometry for symmetric and non-symmetric blocks.	62
5.1	Schematic layout of a closure/ride monitoring station.	77
5.2	Plan of the experimental site, 6-shaft, Hartebeestfontein Gold mine.	82
5.3	Stratigraphic section from stope hangingwall.	84
5.4	Schematic strike section of stope showing face progression and support systems used.	88
5.5	Constitutive behaviour of quartzite. (After Stavropoulou, 1982).	90
5.6	Load path followed in triaxial extension test.	96
5.7	Failure envelopes for hangingwall quartzites.	99
6.1	Rheological analogue for elasto-viscoplastic material behaviour.	106
6.2	Mohr-Coulomb failure envelope with tension cut-off.	107
6.3	Finite element mesh for stope analysis.	110
6.4	Principal stress plot for conventional stope layout.	111
6.5	Principal stress plot for stope with hangingwall slot.	112
6.6	Vertical and horizontal stresses in stope hangingwall with and without the slot.	114
6.7	Horizontal displacement of the hangingwall surface.	115

LIST OF FIGURES

Figure		Page
6.8	Absolute dilation profile for rock ahead of a stope face. (After Brummer, 1986a).	118
6.9	Predicted stope closure.	120
6.10	Vertical stress profiles in the immediate hangingwall.	122
6.11	Horizontal stress profiles in the immediate hangingwall.	124
6.12	Predicted horizontal displacement of the hangingwall with stope support.	126
6.13	Closure profile with stope support.	127
7.1	Stereographic fracture map of the hangingwall surface, panel 2S.	130
7.2	Petroscopic observations of fractures intersecting the hangingwall borehole, panel 2S.	131
7.3	Sectional layout of stress measurement site.	134
7.4	Upper hemisphere polar stereonet showing dominant fracture and measured principal stress orientations.	135
7.5	Relationship between the applied surface loads and induced stresses at 2,3 m depth.	136
7.6	Altitudes of the induced principal stresses at 2,3 m depth.	137
7.7	Azimuths of the induced principal stresses at 2,3 m depth.	138
7.8	Point load effects on an elastic medium.	142
7.9	Plan of relative bolt positions.	144
7.10	Relative surface deformations around the active support load.	145
7.11	Load-deformation characteristics for hangingwall as measured at bolt 'A'.	148

LIST OF FIGURES

Figure		Page
7.12	Load-deformation curve for rock joints. (After Sun et al., 1985).	149
7.13	Predicted elastic deformations for rock surface.	151
7.14	Inclinations of shear and extension fractures based on Kersten's (1969) observations. (After Brummer, 1986a).	153
7.15	Hangingwall extension fracture inclinations, panel 9N.	154
7.16	Hangingwall extension fracture inclinations, panel 10N.	158
7.17	Inclinations of hangingwall shear and extension fractures on a 5 m strike line.	162
7.18	Hangingwall extension fracture inclinations, panel 3S.	163
7.19	Petroscopic observations of fractures in the stope hangingwall : (a) panel 9N, (b) panel 10N.	166
7.20	Strike-parallel stress changes under conventional mining, panel 10N.	168
7.21	Strike-parallel stress changes under conventional mining, panel 9N.	169
7.22	Strike-parallel stress changes after cutting the slot, panel 10N.	171
7.23	Strike-parallel stress changes after cutting the slot, panel 9N.	173
7.24	Borehole axial extensions as measured by sonic extensometer, panel 10N.	178
7.25	Borehole axial extensions as measured by sonic extensometer, panel 9N.	179
7.26	Wire extensometer measurements of borehole axial elongation, panel 9N.	182
7.27	Wire extensometer measurements of borehole axial elongation, panel 10N.	183

LIST OF FIGURES

Figure		Page
7.28	Borehole axial extensions as measured by sonic extensometer after slot-cutting, panel 9N.	186
7.29	Borehole axial extensions as measured by sonic extensometer after slot-cutting, panel 10N.	187
7.30	Measured stope closure under conventional layout, panel 9N.	189
7.31	Measured stope closure under conventional layout, panel 10N.	190
7.32	Measured stope closure under 'caving' conditions, panel 9N.	191
7.33	Measured stope closure under 'caving' conditions, panel 10N.	192
7.34	Relative downdip ride of the footwall under conventional mining conditions.	195
7.35	Relative downdip ride of the footwall after cutting the hangingwall slot.	196
7.36	Strike ride of the footwall under conventional mining conditions.	197
7.37	Strike ride of the footwall after cutting the hangingwall slot.	199
7.38	Total linear extension of the hangingwall surface, panel 9N.	200
7.39	Total linear extension of the hangingwall surface, panel 10N.	201

LIST OF TABLES

Table		Page
5.1	Summary of Laboratory Test Results	100
(a)	Uniaxial compression test results on hangingwall quartzites, panel 2S, 4-shaft site, Hartebeestfontein Gold Mine.	100
(b)	Uniaxial compression and triaxial extension test results, panel 9N, 6-shaft site, Hartebeestfontein Gold Mine.	101
(c)	Uniaxial compression and triaxial extension test results, panel 10N, 6-shaft site, Hartebeestfontein Gold Mine.	102
(d)	Brazilian test results on hangingwall quartzites, 6-shaft site, Hartebeestfontein Gold Mine.	103
7.1	Measured Parameters for the Experimental Panels .	205

LIST OF PLATES

Plate		Page
5.1	'Doorstopper' strain cells	66
5.2	'CSIRO' triaxial strain cell	69
5.3	'IRAD GAGE' sonic probe and readout unit	71
5.4	Magnetic anchors for use with sonic extensometer	73
5.5	Wire extensometer	75

1 INTRODUCTION

1.1 Problem Definition

The gold mines of South Africa are currently amongst the deepest in the world, extending to depths over 3 000 m. Even at much shallower depths the rock pressure due to the overburden is sufficient to cause fracturing of the strata surrounding the excavations. In the deep-level mines of the Witwatersrand and Orange Free State, such fracturing is extensive and causes many difficulties in mining operations. Various orientations & combinations of these fractures result in the formation of blocks of rock, which under certain conditions are unstable and separate from each other, resulting in falls of ground. Apart from the obvious danger to mine workers, this may also be a hindrance to mining activities.

This problem is partially alleviated by the use of support systems. The support requirements of underground excavations vary according to the condition and type of strata to be supported. In addition, the characteristics of the support system itself affect the rock strata and may, to some extent, control rock deformations. A number of different support systems are in use in South African gold mines and some contention

as to their suitability and range of influence has arisen.

It is the object of the work discussed in this dissertation to address various aspects which influence the occurrence of falls of ground and means for alleviating them, including modifications to the mining method and the method of support.

1.2 Scope of Work

Mining personnel associated with deep-level mines have long been aware of the inherent dangers of a stope hangingwall with fractures dipping towards the face, often resulting in hangingwall instability and falls of ground (Morgan and Theron, 1963). In such cases some mines initiate hangingwall 'caving' or collapse in the back areas. This has been found to provide some degree of stress relief on the working face, aiding mining operations and permitting the formation of more steeply dipping fractures. Such fractures have been found to create more stable hangingwall conditions. It is thought that the cutting of a hangingwall slot or hangingwall dip gully in the back areas of a stope should have a similar effect, permitting horizontal stress release and allowing fracture formation at a steeper angle, with the associated improvement in

stability. Very little analytical work on such phenomena has been published.

Theoretical analyses and laboratory tests have shown that a rock sample under uniaxial compression tends to fail on a plane parallel to the applied load (a so called 'extension fracture'). When the axial load is accompanied by adequate lateral confinement, the failure plane is inclined at some angle to the major stress component (a 'shear fracture'). Some degree of hangingwall fracture control should thus be possible by altering the stress distribution or principal stress magnitudes and directions in the vicinity of the stope face.

Elastic theory indicates that a point or areal load, acting on the surface of a semi-infinite mass or finite layer, induces stresses within the material acting both parallel and perpendicular to the applied load. It may be reasoned then that a load applied to the stope hangingwall, such as an hydraulic prop (commonly used for stope support), should induce such stresses within the rock. In turn, these may affect the stress distribution and horizontal confinement within the strata.

This study had two aims: Firstly, to determine the effects of the aforementioned hangingwall dip slot on

horizontal stress relaxation and fracture formation in the strata and hence the hangingwall block stability, and secondly to determine the effects of support loads on the hangingwall strata. This comprised both individual support element effects and support system effects in a stope, in conjunction with the dip slot experiment. The influence and necessity of certain support systems has become a matter of contention and it is hoped that the author's study will provide some insight into the behaviour of stope hangingwall strata in conjunction with various support systems.

Throughout the text several terms applicable specifically to the mining industry are used without explanation. It is expected that the reader is familiar with such terminology.

1.3 Structure of this Dissertation

This dissertation is arranged as follows:

Chapter 2 presents a summary of the relevant literature on block stability analysis, hangingwall collapse (or 'caving') and numerical modelling in mining applications.

Chapter 3 describes the patterns of rock fracture and deformation that have been observed around deep-level tabular excavations.

Chapter 4 contains an analytical approach to determining the stability of a wedge-shaped block in the hangingwall, under varying geometries and confinements. Through parametric studies the significance of the inclination of the block sides in maintaining stability is shown.

Chapter 5 commences with a description of the instrumentation used in the course of the underground monitoring programme. The geology and location of the experimental site are then presented followed by a description of the procedures followed in implementing the experiments. The chapter concludes with a discussion on the laboratory testing of rock samples performed to obtain relevant material properties.

Chapter 6 describes the finite element code used in predictions of the effects of the geometrical alterations and support systems implemented underground, followed by results of the analyses.

Chapter 7 presents the results of the underground experimental programme and includes a discussion of the influences of the hangingwall slot and support systems on the overlying strata.

Chapter 8 contains the conclusions derived from the research work and provides recommendations for further studies.

The primary objective of this work has been to determine the effects of a hangingwall dip slot and two diffexent support systems on the stability and condition of stope hangingwall strata. The following chapter provides a review of relevant literature on the stability and 'controlled' collapse of hangingwall strata.

2 SUMMARY OF PREVIOUS WORK

The question of stope hangingwall stability may be viewed from two aspects; the behaviour of individual blocks or wedges in the strata and the overall behaviour of the hangingwall subject to its external influences. This chapter is divided into three parts, the first being a summary of some of the available literature on block stability while the second summarizes some of the published work on hangingwall caving and support-strata interactions. The third part is a short review of relevant literature on numerical modelling of rock behaviour.

2.1 Block Stability

While many authors have published work on the theory of elasticity, notably Timoshenko and Goodier (1970), and on structural element theory and indeed, it is a well-known and applied science, few have applied that theory to the rock mechanics application discussed here. Some authors have simplified the 'hangingwall problem' down to a single beam or cantilever while others have proposed an arching effect of the rock over the excavation. Authors such as Briggs (1929) and Dinsdale (1937) as quoted in Evans (1941) have presented work on sandstone beds spanning large excavations, relating to shallow-level mining operations, while Thorneycroft (1931) and Auchtmuty (1931) also quoted by

Evans, attributed surface disruptions over a coal mine to sandstone beams tilting or rotating, due to mining activities. A comment by Evans (1941), however, attempts to discredit Thorneycroft's argument by indicating that inconceivably high stresses would have to be withstood by the material to comply with his hypothesis. In the same paper, Evans noted that '...unwarrantably high bending strength has been attributed to massive rock strata...' and goes on to advance a solution incorporating 'voussoir-beams' that is '... competent to account for the relative stability of...strata that are too broken...to act as simple beams'.

Evans applied the principle of a voussoir-arch to a fractured beam - notably referring only to the first or first few layers of strata above the excavation although he concluded that the theory could be extended further into the hangingwall; the overall capacity of such beams to resist bending depending on the compressive strength of the material. A simplified deformation pattern consisting of bedding separation and transverse tensile cracks in roof beams has been presented by Beer and Meek (1982) who reformulated and extended the voussoir beam theory initiated by Evans (1941) with a view to formulating design curves for hangingwalls. In a comparison with geomechanics classification systems (Bieniawski, 1976; Barton, Lien and Lunde, 1974) the authors concluded that such systems are insensitive to

certain geological and geometrical factors whereas their own method allows concentration or emphasis on such parameters. The simplifications inherent in the voussoir beam model have however been eliminated in the computational model of Lorig and Brady (1983) in which a hybrid solution comprising distinct- and boundary element methods was used to represent the finite, joint-defined rock units of the near-field and the enclosing elastic continuum of the far-field respectively.

The science of block stability and block behaviour has undergone rapid advances with researchers having published work on many aspects of the discipline, notably Goodman and Shi (1985) who have provided a comprehensive insight into the applications of block theory to rock engineering. As regards roof stability, much of the thrust has been directed at identifying and analysing 'keyblocks' which are formed between joint or fracture sets and on removal allow progressive collapse of the excavation boundary. By determining the inherent stability of such blocks the support requirements may be found (Shi and Goodman, 1981; Goodman and Shi, 1982; Chan and Goodman, 1983). In their paper of 1982, Goodman, Shi and Boyle presented two important issues in support selection for excavations. Initially, they argued that it was only necessary to support the critical keyblocks which, in turn, maintained the overall roof integrity, and secondly, that the in-situ

stress field may act as support for potential keyblocks, where the faces of the rock wedge are nearly perpendicular to the excavation surface. Other authors have included similar confining stresses in models, employing symmetric and asymmetric wedges (Sofianos, 1986) and the plane strain condition (Elsworth, 1986), who concluded that ignoring the effect of in-situ stresses may result in over design of the support, as rock blocks may be partially or fully self-supporting.

Hoek (1977) expanded further on this principle, stating that when the height of a rock wedge is less than the excavation span, the in-situ stress in the rock mass is unlikely to influence the wedge stability. The author's findings as presented in Chapter 4 have indicated that the in-situ stress field can prove to be a de-stabilizing influence in such cases. Hoek did note however that when the wedge apex angle is acute, the normal stresses across the potential failure planes should be taken into account. Crawford (1982), who performed two-dimensional plane strain parametric studies on the influence of discontinuity normal- and shear stiffnesses on wedge stability, found definite improvements in stability with increasing joint stiffnesses. He found too that the presence of a stress field tangential to the face of an excavation has an important effect on wedge stability. Unfortunately this model was applied only to symmetrical wedges in two dimensions and the effects of the excavation process

have been ignored. A similar paper (Crawford and Bray, 1983) has shown the importance of a joint normal stress in mobilizing shear resistance on discontinuities and the de-stabilizing effect on upright roof wedges of a vertical stress field. Other parameters, such as the importance of asperities on discontinuity surfaces in effectively increasing the angle of friction have been reported by Goodman et al. (1982), Cording and Mahar (1974) and Brekke (1968).

Hoek (1977) noted that gravity falls of two-dimensional rock wedges occur when the apex lies within the base area of the block, whereas sliding occurs when the apex lies outside of the base area, provided that one of the discontinuity planes is steeper than the material angle of friction. A determination of the type of failure likely to occur was presented by Hocking (1976), who considered single- and double-plane sliding of a wedge. It has however been shown by Cruden (1978) that Hocking's method was in fact the same as that used by Panet (1969) and Goodman (1976).

A fairly comprehensive paper by Priest (1980) presents an inclined hemisphere projection method for the determination of block stability. In this work the author included polyhedral blocks at planar, bi-planar and curved excavation faces and made use of the principle of selecting the excavation geometry to suit the rock conditions. This is not however always

practical. A mathematical approach by Warburton (1981) to the vector stability analysis of a three-dimensional polyhedral block allowed for re-entrant surface features and any number of free faces. The method provides for the determination of movement direction and calculation of a safety factor against sliding.

2.2 Caving

Collapse of the hangingwall strata in the mined-out regions has been an integral part and problem of underground coal mining since its inception. Much study has been completed on this phenomenon and the benefits and disadvantages of the system are fairly well documented. The effects on mining, support, strata movement and stress distributions of 'caving' (as it is known) of the goaf have been published by several authors (Unrug and Szwilski, 1982; Schaller, 1979).

Caving in coal mines is practised as a form of strata control, involving bulking of the fallen rock, which provides support to the overlying strata. A 'revised' form of the method has been practised in the deep-level gold mines of the Transvaal and Orange Free State but little definitive information is available - save that under certain poor stope hangingwall conditions it has been found advantageous to initiate collapse of the overlying strata, which results in an improvement in the hangingwall condition.

In this case, the method, although not 'caving' in its strictest sense, allows collapse of the unsupported strata in the back areas of the stope. Although bulking does occur, the vertical extent of the falls of ground is insufficient to allow any supporting influence to be derived from the loose material. The applicability of conventional caving mechanisms (in both coal and massive orebody mining) to deep-level gold mining is thus debatable. This section, which presents a summary of some of the available literature on 'caving' is included for the sake of completeness and comparisons between caving in coal and gold mines are intentionally omitted.

Unrug and Szwilski (1982) observed that successful operation of longwall coal mining operations is well-served by good regular caving of the goaf. They noted that mechanical cutters operated more efficiently in the coal seam after the goaf had fallen, which was explained as a relief of the high pressures on the face. Schaller (1979) in his studies of strata behaviour in the Sydney Basin Coalfields, reported bending of hangingwall strata over the excavations and noted corrugation of the shaley roof and floor heave in roadways, thought to be a result of high lateral stresses surrounding the excavation. Subsequent 'dropping' of the hangingwall allowed stress redistribution and roof sag and reduced the deformation of the hanging- and footwall. In his paper of June 1978, Kendorski noted that the horizontal stress field

in a rock mass can influence the stability of the strata by locking rock blocks together and cancelling tensile forces that would loosen blocks and additionally by reducing the overall tendency to form tensile zones above excavations. A similar approach was adopted by Kidybinski (1977, 1979) in his 'caveability classification', using the resistance of the strata to vertical tensile forces as a criterion. In a later paper (Kidybinski, 1982) he proposed a further classification scheme for roof rocks, in order to determine longwall stability.

A paper by Bucky (1956) as quoted by Mahtab and Dixon (1976) states:

> 'The ability of a block to cave or fragment is a function of its strength in tension or shear and the value of applied forces.'

The latter authors noted that a lack of lateral confinement on the rock mass is necessary to ensure ease of caving. In the examples given (Kendrick, 1970), caving was generally applied to the overlying portions of a massive blocky orebody, with reduction of lateral confinement by some form of boundary weakening. Additionally, these authors noted that there was a general lack of quantitative relationships between the characteristics of fracture systems and the caveability of the rock mass.

King (1945) related caving characteristics to rock type and fracture spacing while the effects of joints in the rock were noted by Swaisgood, McMahon and West (1972), and Elisovetskii et al. (1978).

Several other authors have published work on the influence of the fracture system on block stability, including Kendorski (1978) who noted that for successful caving, the attitude of fractures is important as it determines the directional behaviour of the rock mass as it fails and the effectiveness of any arching, keying and interlocking of the blocks of rock. The beneficial influence of powered support on the mining face was also reported by Gorrie and Scott (1970). In a discussion on this paper, Shepherd (1970) noted that good caving of the goaf is often determined by the conditions (fractures) created in the zone ahead of the face.

Roof instability depends too on the properties of the rock mass, as under any form of loading these affect the fracturing and more intense fracturing decreases block stability. Numerical results (Mahtab and Dixon, 1976) have shown that a reduction in rock strength or stiffness increases the incidence of block failure. This was borne out by experimental results in two mines which showed that the hangingwall composed of the stronger rock type was less likely to fall in an unstable fashion than that in the weaker rock. These authors observed too, that a decrease in rock mass

modulus was accompanied by a decrease in the fracture spacing, while boundary weakening in the form of pre-fractured abutments showed an effective increase in the excavation span and an associated decrease in roof block stability.

In addition to the above rock mass stability factors, the influence of the inclination and surface irregularities or asperities of fracture planes has been found to markedly affect the stability of roof strata. Studies on a rhyolite block at San Manuel mine (Mahtab, Bolstad and Kendorski, 1973) showed that the lack of a horizontal joint or weakness in the rock mass increased the overall stability of the block. This occurrence was confirmed in two-dimensional finite element studies by Mahtab and Dixon (1976), from which it may be deduced that a near-vertical set of fractures in the immediate hangingwall may improve block stability. Further studies by the same authors (Mahtab and Dixon, 1976) predicted the formation of a larger tensile zone above the excavation in the presence of low angle fractures than with steeper angle fractures.

Summarizing, the above authors have determined that the factors influencing caveability include the in-situ stress field, the intact rock strength, fracture geometry, fracture strength properties, the excavation size and boundary conditions.

Although in the past several authors have published work on hangingwall stability and roof strata collapse or 'caving' in relation to the gold mine stopes of South Africa, little work has been published recently.

In the reply to, and discussion on, a paper by Heywood (1945), Morgan (1945) reported that the cutting of 1,5 m high hangingwall dip gullies at approximately 30 m intervals in stopes was found to be advantageous to mining operations in that an increased rate of face advance was achieved. This author also noted that 'at the time of a burst', lateral hangingwall expansion of the order of 75 mm was seen to occur into the abovementioned gully, which 'permits a considerable release of stress'. Morgan attributed the marked decrease in the frequency of rockbursts when hangingwall dip gullies were adopted into the layout, to the absorbant effects of the hangingwall slot and the regional wastefill. He concluded by noting that the breaking of the stope hangingwall by cutting dip gullies artificially creates fractures in such orientations and extent as to significantly improve the hangingwall conditions and stability.

In work carried out on the Sub-Nigel, Batty and Bell (1945) noted relative movement of the stope hangingwall away from the face after stress relief in the form of caving had occurred. In addition, favourable responses in the form of a decrease in pressure on the face (often

identified by a reduction in the frequency of drilling jumpers becoming wedged in the hole), vastly improved hangingwall conditions and a good face advance rate were observed. It is of interest that hangingwall bedding separation occurred up to 15 m above the stope. It is unfortunate that only a brief mention is made of the change in inclination of the hangingwall fracture planes which may have been a prominent part of the overall cause of improved hangingwall conditions. The authors conclude with a comment to the effect that permanent support may tend to maintain confining stresses in the rock and thus inhibit stress relief and its accompanying beneficial effects.

During the 1960's, similar 'caving-type' operations were conducted in the Klerksdorp and Welkom Goldfields.

Jooste (1963) in his work at Free State Geduld Mine reported hangingwall collapse and stress relief resulting in easier mining conditions on the face and safer working areas, with the proviso that 'the sooner the cave takes place the better. If the hangingwall tends to hold up, the cave must be induced'. This inducement was attempted in two ways; namely blasting of the hanging or strengthening of the back or breaker row of props. He noted too that an inadequate support density permitted excessive strata sag which was detrimental to caving. Where back area support in the form of skeleton packs was used, no release of pressure

on the face and poor hangingwall conditions were experienced.

Pearson (1963) at President Steyn Gold Mine reported regular, easy caving in stopes supported by five rows of props with the only difficulty experienced being in obtaining a controlled collapse above a shale layer.

Deacon (1965) observed stress increases on the face when caving of the stope hangingwall did not occur, particularly when the stope span was large. This he explained as the resistance to lateral movement due to the support system putting the hangingwall into tension, which resulted in local falls of ground. This explanation is debatable since any resistance to lateral movement produced by the support would tend to create compressional and not tensional forces in the hangingwall strata. Few indications of the increased stress on the abutments were given. Cutting of hangingwall dip gullies proved beneficial to roof strata conditions, with lateral strata movements observed at right angles to the advancing face.

Where hangingwall collapse was initiated in stopes in an attempt to destress the strata, rapid beneficial effects were noted (Morgan and Theron, 1963). The effects of various support (prop) densities on the stress build-up on the face and the fracture orientations in the stope hangingwall were reported by the above authors after

observations at Stilfontein Gold Mine, a summary of which is presented in Figure 2.1. They noted that under-supported panels were reluctant to cave and that in such cases the hangingwall fractures tended to dip towards the face possibly resulting in local fallout. Stiffer supports or a higher density were recommended along with the cutting of a hangingwall dip gully in the stope. This does however appear to contradict the findings of Deacon (1965) who noted that the denser or stiffer support system tended to inhibit caving.

In this paper (Morgan and Theron, 1963) the authors discredited an earlier presentation by Morgan (1945) on the effects of wastefill in relieving the intensity of rockbursts, by noting that the wastefill probably offset the beneficial effects of the hangingwall slots. This was borne out in a comment by Deacon (1963), who deduced that wastewalls were inhibiting lateral strain in a similar caving situation on Hartebeestfontein Gold Mine. Experimental results showed that the inclination of hangingwall fractures became much steeper after the initiation of caving (Figure 2.2). In further discussion on the paper, Briggs (1963) revealed that in similar work on the Sub-Nigel in the 1940's, simple removal of the back area support resulted in a stress release on the face and marked improvement in the hangingwall stability.

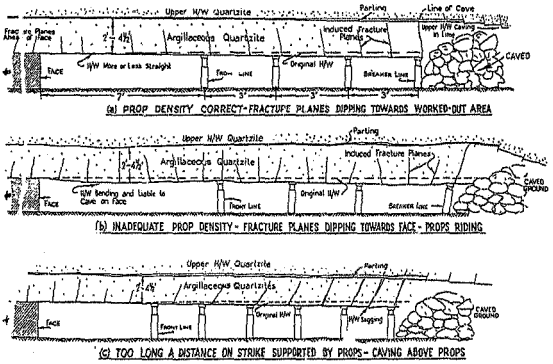

ure 2.1 Observations of hangingwall fracturing under different support densities.
(After Morgan and Theron, 1963)

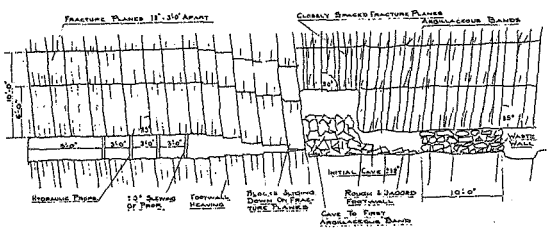

Figure 2.2 Sketch showing the changing pattern of fractures after commencement of 'caving'.

(After Deacon, 1963)

Closely related to the whole sphere of 'caving' or roof collapse is the effect and influence of the support system on the roof strata.

The action of the support system on the hangingwall has been studied by several researchers, largely however in the coal mining régime. The extent of zones of elastic, plastic and clastic material surrounding excavations is difficult to define, and roof collapse and the resulting mass expansion create a statically undefined support system (Unrug and Szwilski, 1982). In further discussion the above authors noted that the interaction between mechanical supports and the mine roof may be used as a method of controlling the overlying strata, as the support should counteract vertical displacement (bed separation) and limit horizontal movement by frictional resistance. Irresberger (1981) has shown that an increase in support resistance resulted in a lower frequency of large roof falls, but had little effect on the smaller falls. This suggests that active supports tend to influence the rock mass as a whole rather than affecting each individual block. In his work on fracturing in brittle rock mining environments, Kersten (1969) noted the importance of support types in controlling overlying strata movements. As described by Unrug and Szwilski (1982), the loads required to maintain or achieve hangingwall stability may depend on the height of the detached strata, the frictional resistance to sliding available between bedding planes,

the rock strength and the mining geometry; however no mention was made of the effect or importance of the fracture system.

In the mining of tabular seams such as narrow gold-bearing reefs, it is often impractical to drastically alter the mining geometry. When mining massive ore bodies however, a large degree of freedom of geometry is available. Numerical studies by Mahtab and Dixon (1976) using a Mohr-Coulomb criterion and idealized conditions on the influence of a boundary slot on tensile and shear zones above an excavation, showed a marked influence of the height of the slot on these zones. No attempt was made however to determine an optimum height for the slot. Hangingwall movement into a similar slot was used by Kersten (1969) to explain the steepening of the orientation of the maximum principal stress ahead of the excavation and the associated change in fracturing. Although certain positive trends were noted in his work, these were marred by the large scatter in individual values.

2.3 Numerical Modelling of Rock Behaviour

The field of numerical modelling of rock material has come into its own only in the last twenty years or so. While analytical techniques (Salamon, 1963, 1964; Salamon et al., 1964), provided displacement and stress information for points both near and remote from the

excavation, they simulated only elastic rock behaviour, which may be applicable in the far-field of undisturbed rock but do not realistically model the near-field of fractured, discontinuous material. 'Early' researchers were hampered too by the limitations on computational equipment available. The advent of powerful digital computers has vastly influenced the advances in numerical analysis techniques.

Of several numerical analysis techniques in use, three principal methods dominate in the rock mechanics field, namely the Boundary Element Method, the Finite Element Method and the Distinct Element Method.

2.3.1 The boundary element method (BEM)

This technique involves the division of the problem boundary into a number of elements, while ignoring the interior. Thus the size of the numerical problem is related only to its surface area. The method, involving integration of the derived equations to compute the distribution of stresses and induced displacements, has been extensively studied and applied in virtually every engineering discipline. In the particular field of rock mechanics, after the work of Crouch and Starfield (Crouch, 1976; Crouch and Starfield, 1983), many analytical and mine-design tools have been based on this method. The method, which may be formulated for both two- and three-dimensional problems has, until recently

been primarily involved in elastostatic solutions, since it is rather unsupportive of non-linear material behaviour.

Non-linear behaviour is difficult to model but attempts have been made by researchers such as Deist (1966) and Crouch (1970) as reported by Brummer (1986a), which permitted non-linear rock behaviour in the near vicinity of the mining excavations. More recently, work by Peirce (1983) and Peirce and Ryder (1983) applied the non-linear technique to simulation of rock fracture and deformation phenomena around mining excavations, while Ryder and Napier (1985) have implemented the technique in the analysis of large scale tabular excavations.

2.3.2 The finite element method (FEM)

It is in this field that perhaps most of the recent advances in non-linear solution techniques have been made. Unlike the boundary element method, the finite element method discretises the entire problem domain into individual elements (usually triangular or rectangular) and forms a system of equations which is solved to provide the displacements and stresses of certain discrete points in each element. The method is complex and has been documented by Zienkiewicz (1977). Development of the method for non-linear applications has been widsspread (Owen and Hinton, 1980; Duffett

et al., 1983) while several researchers have concentrated on its merits in geotechnical applications.

Pariseau et al. (1970) in an overview of elastic-plastic problems in the geological context described the importance of the load path in determining non-linear behaviour, while Reyes and Deere (1966) and Zienkiewicz et al. (1970) reported on the non-linear analysis of geotechnical problems in continuous and discontinuous media respectively. In 1968, Zienkiewicz et al. proposed a finite element solution for a fissured rock material prescribing a 'no-tension' criterion in which induced tensile stresses were relaxed during the iterative solution procedure. A similar, limited tension criterion has been included in recent developments of a finite element suite, 'GOLD', employing elasto-viscoplastic material behaviour, infinite and joint elements and a Mohr-Coulomb yield criterion with post-peak strength, designed specifically for application in the South African gold mining industry (Crook et al., 1984; Brummer and Crook, 1985; Brummer and Herrmann, 1986; Herrmann and Johnson, 1987).

A different approach to modelling the inelastic behaviour of the brittle rocks surrounding the deep-level excavations of South African gold mines has been made by Resende (1984). This author developed a constitutive model based on damage theory in an attempt to produce a model which includes the important

characteristics exhibited by brittle rocks in laboratory tests. This model, in which the material properties degrade as the damage parameter, measuring internal material damage, increases, is currently being tested by both the University of Cape Town and the Research Organization of the Chamber of Mines of South Africa.

2.3.3 The distinct element method

The distinct element method, which was initially described by Cundall (1971), is similar to the finite element method in that the entire region of interest is divided into a system of solid elements, separated by joints, with each element corresponding to an individual rock block. Distinct elements can however experience large-scale translations and rotations without encountering numerical instability (Lorig, 1984). Early researchers in this field confined their work to rigid block interactions with much research directed towards relaxation of induced stresses and damping in both the static and dynamic fields of application. Latest developments by Cundall (1980) and Cundall and Hart (1983) have produced a Universal Distinct Element Code (UDEC) which allows the rock blocks to be rigid, simply deformable or fully deformable, providing for stress distribution calculations and permitting blocks to crack.

A hybrid analysis method, combining boundary elements and distinct elements for use in jointed rock media has been presented by Lorig (1984), while an alternative solution algorithm for rigid block interactions related to stability analysis in jointed rock has been presented by Belytschko et al. (1984).

2.4 Summary

This chapter has shown that the stability of fractured rock beams spanning large excavations is a complex phenomenon which is difficult to analyse theoretically. Various attempts at doing so have met with limited success. Workers in the field of keyblock analysis and support requirements for fractured rock masses have determined that by ensuring the stability of critical keyblocks, the stability of the entire excavation may be assured. In addition, the importance of the in-situ stresses and the orientation of keyblock boundary fractures in maintaining block stability has been shown.

In the coal mining régime, several authors have noted an improvement in mining conditions and efficiency after the initiation of hangingwall collapse or caving in the back areas, which has been attributed to the reduction in lateral confinement on the strata above the excavation. Similar improvements in mining conditions have been reported from gold mines after experimental work in the form of cutting hangingwall dip gullies in

stopes. Stress relief in the form of 'caving' or collapse of the hangingwall has produced improved strata conditions and a decrease in pressure on the face. In such cases, the inclination of hangingwall fractures has been observed to change to dip away from the mining face. Stiffer support systems have been noted to inhibit hangingwall lateral strain (and thus stress relief), with an associated decline in hangingwall stability.

In recent years, large advances in non-linear numerical techniques to simulate rock behaviour under load have been made. Future developments should greatly improve on the current numerical mine-design tools available.

3 ROCK FRACTURE AND DEFORMATION AROUND DEEP-LEVEL STOPES

The rock mass surrounding deep-level operational excavations is continually subjected to changing stress fields and thus deformations. These deformations include failure and fracturing of intact rock as well as translations and rotations of the surrounding elastic continuum and the inelastic, discontinuous fractured rock mass. A study of the hangingwall strata and influences of support systems must therefore take account of the deformational processes involved. This chapter describes the predominant fracture systems formed around deep-level stopes and the various modes of deformation observed.

Since early mining days on the Witwatersrand, attempts have been made to classify the fracture systems formed in the brittle quartzites surrounding the gold-bearing reefs. Amongst the first to describe fracturing in deep-level mines were Leeman (1958) and Cook (1962), both of whom mentioned a shear type of failure surface in the rock, after observations underground and in the laboratory respectively. Kersten (1969), in describing the hangingwall fractures in a stope at Hartebeestfontein Gold Mine noted three particular fracture types; clean-cut tensile fractures, those exhibiting evidence of shear movement in the fracture plane and a class lying somewhere between the two. The

first two classes were however clearly defined and were observed to dip towards and away from the mining face respectively. The third group of fractures may have been of the former type, having subsequently undergone some shear displacement possibly due to settlement or bending of the stratum. A classification by McGarr (1971) interpreted the fracture formation procedures as the reverse of those by Kersten. In the same paper however, when noting the results of Brace et al. (1966), McGarr found the suggestion that his type I fractures may be tensile cracks rather than shear planes, particularly appealing.

Work by Roering (1978, 1979) as reported by Brummer (1986a) resulted in his three part classification system; type I fractures being steeply dipping and showing no evidence of shear displacement, type II fractures having slightly shallower dip, with definite signs of shearing, while type III fractures were of much shallower dip and similar to type I. A similar scheme was presented by Adams et al. (1981) and is illustrated in Figure 3.1. The terminology adopted by the author and used in this dissertation is that proposed by Brummer and Rorke (1984) in which the numerical classification scheme was discarded and the fractures were grouped as primary or secondary fractures, corresponding to shear or extension (tensile) type formation processes respectively.

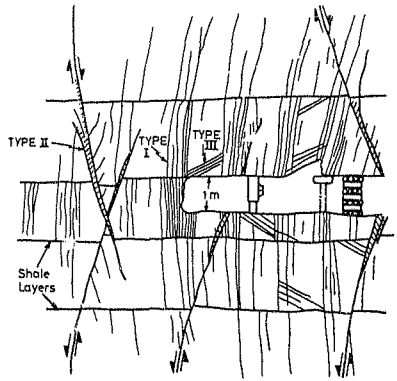

Figure 3.1 Fracture classification and distribution around a typical stope face. (After Adams et al.,1981)

3.1 Primary or Shear Fractures

Laboratory compression tests on rock samples have shown that shear-type failures generally occur under conditions of high confinement and at some angle to the major principal stress. Similar conditions may be found at some distance (6 m to 8 m) ahead of an advancing stope face in the highly stressed host rock, where in the otherwise unfractured rock, shear fractures have been observed to form (Brummer and Rorke, 1984; Legge, 1984). Hence in the chronological order of fracture formation, these fractures have been termed 'primary'. They form parallel to the general longwall direction and are not affected by local irregularities in the plan outline of the face. These shear fractures, which penetrate all stratum layers, usually occur in conjugate pairs, with those in the hangingwall dipping towards the excavation at some 60° to 80° and those in the footwall dipping away from it. They have been observed (Brummer, 1986b) to curve back towards the excavation at depths of the order of 7 m into the hanging- and footwalls, probably following the path of the major principal stress, and displaying a decreasing amount of shear displacement with distance from the excavation. Such fractures, which range in width from 5 mm to over 200 mm, contain a white powdery gouge and usually displace the strata across the fracture plane. Their formation is cyclic with a spacing of the order of 1 m to 1,8 m between successive fractures.

3.2 Secondary or Extension Fractures

Extension-type fractures, which may be likened to rock failure in a uniaxial compression test, form parallel to the major principal stress. Conditions of low confinement occur at small distances ahead of the stope face, where such fractures have been observed to form (Brummer, 1986a). Unlike shear fractures, they strike parallel to the immediate stope face and are clean-cut, of the order of 1 mm wide and exhibit no shear displacement. Extension fractures in the stope hangingwall are inclined at 80° to 120° to the horizontal, generally dipping towards the face with a spacing of 5 mm to 30 mm. They are truncated by parting planes and do not extend as far into the surrounding strata as do shear fractures. Extension fracturing may be observed in shallow mining operations where overburden stresses are lower, lateral confinement less effective and shear fractures do not occur. By their nature and mode of formation, extension fractures are sensitive to changes in the direction of the major principal stress.

The zones of formation of both primary and secondary fractures ahead of an advancing stope face is illustrated in Figure 3.2.

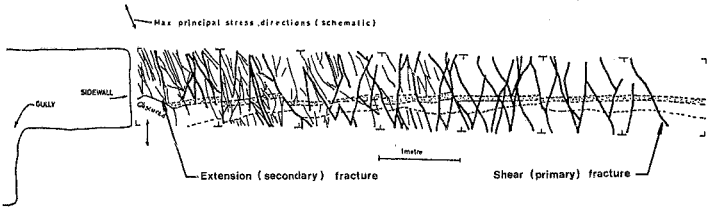

Figure 3.2 Diagram illustrating the zones of formation of primary and secondary fractures ahead of an advancing stope face. (After Brummer and Rorke, 1984)

3.3 Parting Planes

The quartzitic material surrounding the gold mine stopes generally occurs in bands or layers of the order of 50 cm in width separated by shaley argillaceous layers known as parting planes. These relatively flat planes, which average 3 cm to 5 cm in width, consist of soft, platy phyllosilicates having a low frictional coefficient and are in general, considerably weaker than the surrounding quartzites. As a result, horizontal movements can occur across these parting planes, enabling large dilations of the hangingwall strata to occur.

3.4 Rock Deformation Around Stopes

A rock mass deforms in response to an applied load which, in turn, may be altered by that deformation. In addition, the deformation of the rock around stopes both influences and is influenced by the pattern and mode of fracturing in the rock itself. The rock mass remote from an excavation has been found to behave elastically whereas that in the vicinity of the excavation acts in an inelastic fashion. The deformation of this material may be found to have an elastic and an inelastic portion and hence deformations are generally larger than those predicted by elastic theory. As no universal inelastic constitutive law has yet been established, the

prediction or determination of stresses in an inelastic zone is difficult.

Brummer (1986a) has identified seven different inelastic deformation mechanisms which may occur around a stope, (Figure 3.3):

1. Sliding on shear planes
2. Compression
3. Stope closure and ride
4. Bedding plane separation
5. Face dilation towards the excavation
6. Closure of gully sidewalls
7. Sliding on parting planes

Sliding on shear planes and the compression and deformation of rock material may be seen as influencing factors in the dilation of the rock ahead of the face. Such phenomena have been observed by Legge (1984), who conducted extensive measurements of the deformation of the rock strata surrounding deep-level stopes. He, unfortunately, was unable to determine absolute displacements due to his reference points being sited in ground that was still within the range of influence of the stress régime around the excavation.

Stope closure, defined as the reduction in distance between the hanging- and footwall strata has been a recent topic of contention in the design of stope

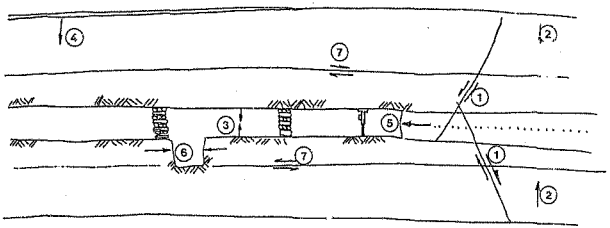

Figure 3.3 Deformational mechanisms around a stope. (After Brummer, 1986a)

(see text for explanation of numerals)

support systems. Associated with closure is the tangential movement of the hangingwall relative to the footwall, known as 'ride' which occurs when the stope plane is not horizontal. Such deformations have been reported by Ryder and Officer (1964). Theoretical elastic deformations are usually exceeded by the observed deformations around a stope particularly in the rate of closure, as has been confirmed in several independent studies by workers at the Chamber of Mines of frica and by Walsh et al. (1977). The dif may be interpreted as the inelast separatio of individual strata or bedding planes in th surrounding rock. This phenomenon, which should occur in accordance with the elastic prediction of tensile vertical stresses above a stope (Figure 3.4), has been frequently observed by the uthor to occur in the lower hangingwall, close to the excavation. Examples of such behaviour have been documented later in this dissertation.

Similar occurrences have been reported by Legge (1984) who observed open parting planes within the first 4,5 m of hangingwall rock, some 8 m behind the stope face at Blyvooruitzicht Gold Mine. In a separate experiment Legge (1984) noted that strata which had previously separated by 45 mm began closing up some 25 m behind the face. This may have been due to a redistribution of bending stresses in the hangingwall strata and compression of the hangingwall after total closure

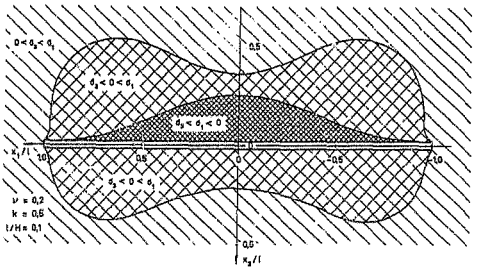

Figure 3.4 Tensile zones above and below an isolated tabular excavation at great depth. (After Salamon, 1974)

occurred at some point in the mined-out back areas. Recent measurements by Roberts (1986a) have indicated that similar separations occur in the footwall strata; these observations imply that the mechanism is not entirely gravity dependant.

The high vertical stresses developed ahead of an advancing stope face (Figure 3.5), should, according to elastic response theory cause rock movement away from the excavation. This is not observed in the underground situation, where dilation of the strata towards the stope is commonplace. It has been determined (Legge, 1984) that this dilation occurs primarily in the zones of fracture formation ahead of the face (as described by Adams and Jager, 1979, and illustrated in Figure 3.6) with the largest dilations occurring nearest the face, reducing to zero some 6 m ahead of the face. This movement is not confined to the rock in the reef plane as dilations of similar magnitude to those experienced in the rock ahead of the face have been measured in the over- and underlying strata (Legge, 1984). This movement has been seen to increase to the order of 40 mm for 3 m of face advance in footwall strata immediately below the reef in a stope where a dip gully was excavated in the footwall 40 m behind the face. Where no such gully was present, buckling of the footwall strata into the stope was observed (Legge, 1984). Such deformation indicates the presence of large horizontal stress in the strata.

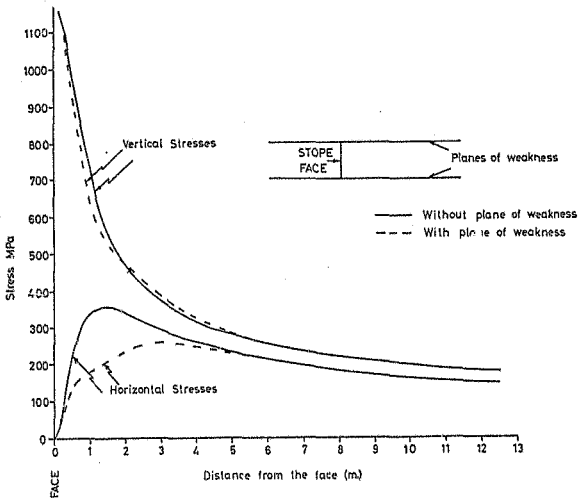

Figure 3.5 Elastic predictions of vertical and horizontal stresses ahead of a stope face (After Peirce, 1981)

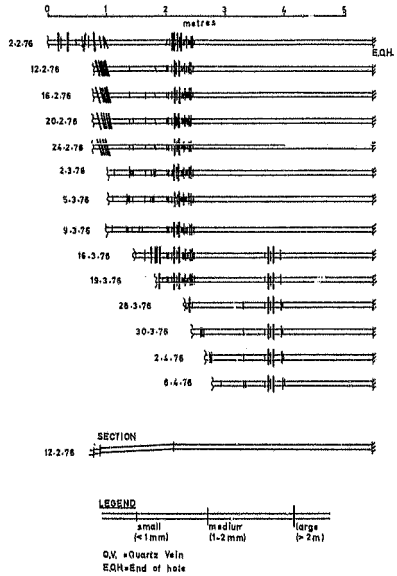

Figure 3.6 Zones of fracture formation ahead of an advancing stope face.
(After Adams and Jager, 1979)

It was proposed by Brummer (1986a) that the dilations caused by the crushing and fracturing of the rock ahead of the stope face are sufficient to generate significant horizontal stresses in the hangingwall and footwall strata, which may affect the fracture mechanisms in the material.

The compressive stresses so developed are in direct contradiction of elastic theory which predicts horizontal tensile stresses in the hangingwall above the excavation (see Figure 3.4). In measurements of horizontal rock deformations around the stope face, Legge (1984) noted that compression of the strata, indicated by contraction of the rock mass, occurred between 0,5 m ahead of the stope face and immediately behind it, which may be attributed to be a reaction to the dilation occurring a few metres ahead of the face. Further evidence for the existence of compressive stresses in the immediate hanging- and footwall strata is displayed by the relative stability of hangingwall blocks. Horizontal tensile stresses in the lower hangingwall stratum would cause opening of fractures and significant falls of blocks. It was proposed by Legge (1984) that the axial compressive forces in the hangingwall strata reduce the stability of these layers, due to sliding along face-parallel fractures inclined at acute angles to the plane of the stope and resulting in buckling of the strata into the excavation. The author has no measurements to substantiate this theory.

The importance of parting planes in assisting horizontal movements has been borne out by measurements of displacements in a diabase dyke devoid of parting planes, which showed reduced displacements compared to those in an adjacent layered quartzite (Legge, 1984). Biaxially-loaded physical models tested by Legge indicated a significant increase in the magnitude of horizontal slip between layers on the introduction of a dip gully in the footwall behind the face and when using lubricated interface surfaces. A point of significance observed in the models was that lateral deformation occurred not only in layers intersected by the dip gully but also in the adjacent layers below the gully. This indicates that the effect of such an excavation extends beyond its physical limits, to some depth in the surrounding material. Such perturbances led to the proposal (Brummer, 1986a) of an 'effective stope width', being somewhat wider than the actual excavation and comprising not only the stope itself, but also the relatively broken and discontinuous strata in the surrounding rock mass, bounded by the parting planes on which significant horizontal displacement occurs.

3.5 Summary

The fractures surrounding a deep-level stope have been classified as either primary (shear-type) or secondary (extension-type) according to their mode of formation. Some control over the inclination of secondary fractures

may be possible by altering the direction of the resultant stress acting on the rock. Seven inelastic deformation mechanisms around a stope have been identified and the influence of shaley parting planes in facilitating relative sliding of bedding layers discussed. The implications of such sliding include abnormally large dilations in the hangingwall and footwall strata and the generation of high horizontal stresses as a result of these dilations.

4 BLOCK STABILITY

The previous chapters have shown that improvements in hangingwall conditions have been achieved by stress relief methods and that the fracture formation mechanisms in the rock ahead of a stope face provide some opportunity for artificial control. This chapter provides a theoretical analysis on block stability and demonstrates the significant improvements in that stability which may be achieved by the alteration of the inclination of block boundary fractures.

4.1 Keyblocks and their Importance in Excavation Stability

A 'keyblock' as identified by Goodman and Shi (1985) is a rock block on which depends the stability of those surrounding it. The removal of a keyblock from a structure results in the progressive collapse of that structure. Figure 4.1 shows keyblocks around an excavation in jointed rock. Removal of the block labelled (1) allows adjacent blocks (2), (3) and (4) to fall, which progressively leads to collapse of the excavation. Hence the stability of such keyblocks is vital in maintaining the integrity and productivity of the excavation. Several methods of identification and analysis of such blocks have been published, a summary of which has been presented in Chapter 2. Yow (1985) identified such keyblocks for a mining environment and

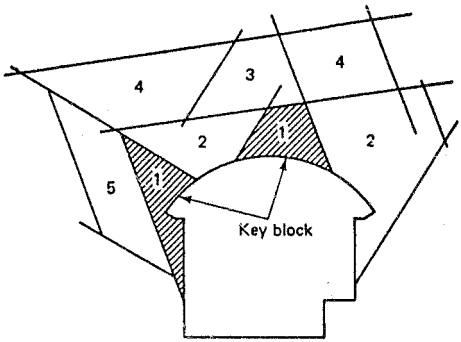

Figure 4.1 Keyblocks around an excavation in jointed rock.

(After Goodman and Shi, 1985)

presented both two- and three-dimensional numerical models simulating block behaviour.

4.2 Stability Analysis

In order to illustrate the significance of block geometry on its stability, a simplified, static, two-dimensional, rigid block analysis is presented. This analysis makes no allowance for the effects of joint stiffness or roughness, making use of friction as the sole source of resistance to block sliding on the laterally bounding fracture planes. In addition no allowance has been made for direct block falling nor any vertical load imposed by the overlying material. It should be noted that since the resultant forces on a block change with its displacement, an accurate analysis should include successive increments of block movement to determine whether ultimately the block becomes unstable.

Consider a trapezoidal block of free surface length ℓ_1 and height h with sides at angles θ_1 and θ_2 to the (horizontal) excavation surface as shown in Figure 4.2. For unit depth into the paper, the self-weight W of the block is given by

$$W = \Psi(h\ell_1 - \frac{h^2}{2} \text{ Cot } \theta_1 + \frac{h^2}{2} \text{ Cot } \theta_2) \qquad (4.1)$$

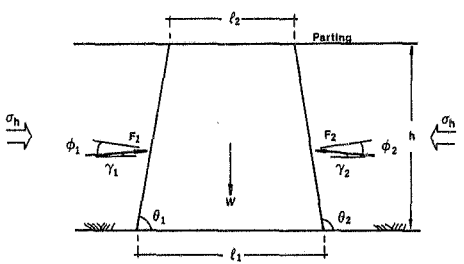

Figure 4.2 Isolated block in a rock stratum, showing applied forces.

where Ψ is the specific weight of the intact rock material.

It may be found by inspection that the block is inherently stable in the following situations:

(i)	$\theta_1 > 90°$	$\theta_2 < 90°$
(ii)	$\theta_1 > 90°$	$\theta_2 = 90°$
(iii)	$\theta_1 = 90°$	$\theta_2 < 90°$

The stability of other cases is dependent on various parameters.

At the point of failure or sliding, the maximum resultant force, F, on the block sides acts at φ, the angle of friction of the discontinuity, to the normal to the discontinuity surface.

Define $F_{1,2}$ as

$$F_{1,2} = \frac{\sigma_h \cdot h}{\cos \gamma_{1,2}} \qquad (4.2)$$

where γ is the angle F makes with the horizontal and σ_h is the horizontal confining stress.

Summing the activating forces

$$\Sigma F_a = W \qquad (4.3)$$

Summing the resisting forces

$$\Sigma F_r = F_1 \text{ Sin } \gamma_1 + F_2 \text{ Sin } \gamma_2 \qquad (4.4)$$

The effect of a cohesion, Cp, of the upper parting plane may be accounted for as a restraining force where

$$F_c = Cp.\ell_2 \qquad (4.5)$$

where $\ell_2 = \ell_1 + h(\text{Cot } \theta_2 - \text{Cot } \theta_1)$

The angles $\gamma_{1,2}$ may be expressed as follows

$$\gamma_1 = \varphi_1 + (\theta_1 - 90°) \qquad (4.6)$$

$$\gamma_2 = \varphi_2 - (\theta_2 - 90°) \qquad (4.7)$$

Resolving all forces in the vertical direction, the minimum horizontal confining stress to maintain block stability may be found:

$$\sigma_h = \frac{\gamma(\ell - h/2 \text{ Cot } \theta_1 + h/2 \text{ Cot } \theta_2) - Fc/h}{\text{Tan } \gamma_1 + \text{Tan } \gamma_2} \qquad (4.8)$$

4.3 Discussion

4.3.1 Comparison of physical models

The geometry of a model tested by Crawford and Bray (1983) in block pullout tests and later back-analysed by Yow (1985) is shown in Figure 4.3. These authors measured

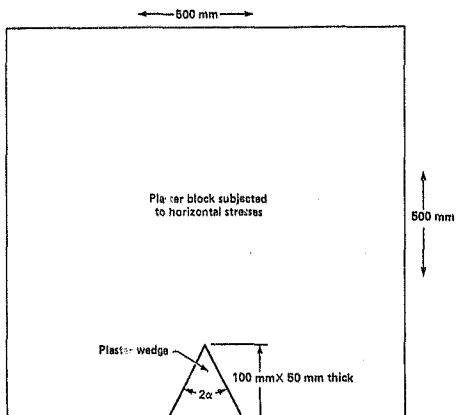

Figure 4.3 Geometry of physical model tested by Crawford and Bray (1983). (After Yow, 1985)

the force required to dislodge a wedge from the surrounding plaster block which was subjected to a horizontal compressive stress.

For comparative purposes the test geometry was used by the author in the numerical algorithm to determine the required pullout force on the wedge to cause sliding. The results, along with those of Crawford and Bray and numerical solutions by Yow (1985) are presented in Figure 4.4, for a wedge with included apex angle of 60° and boundary ion angles of 32°. The failure stress is the pull .orce divided by the area of excavation surface formed by removal of the wedge. A fairly close correlation with both experimental and numerical solutions may be observed. The difference in the gradient of the previous results from the present olution may be attributed to non-consideration in the present solution of joint stiffnesses and the effects of incremental block displacement on the required pullout force. The vertical offset of the experimental data from the numerical so ions, indicates inaccuracies in the physical model, probably due to difficulties in seating the wedge i he block, as described by the above authors.

4.3.2 Parametric studies

Rock blocks with both fracture planes at acute angles to the horizontal excavation surface may be seen to derive

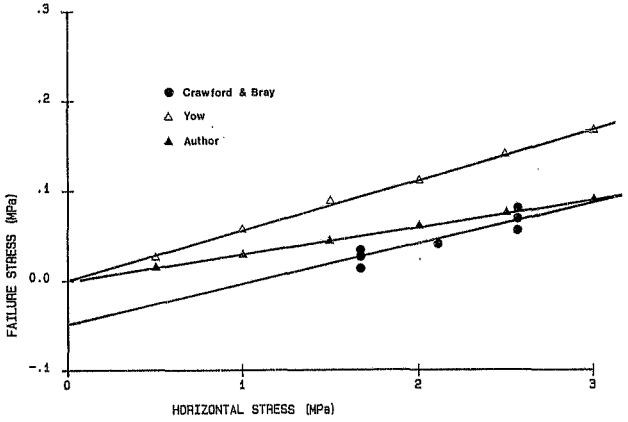

Figure 4.4 Back analysis of required pullout stresses for a confined plaster wedge.

additional resistance to failure from the supporting action of the underlying wedge, forcing failure to occur by sliding only. Such blocks may be regarded as being relatively stable.

The most critical block, as regards stability is that which is bounded by two fracture planes, being at an acute angle and an obtuse angle to the excavation surface on the left and right hand sides of the block respectively. In the studies presented below a block of height 0,5 m and free surface length 0,5 m was analysed.

The stability curves presented in Figure 4.5 tend towards an asymptote at an angle equal to $(90°-\phi')$ where ϕ' is the angle of friction of the discontinuity plane, which may include an angle of asperities, i, where

$$\phi' = \phi + i \qquad (4.9)$$

This indicates that a wedge-shaped block with sides inclined at angles greater than their angle of friction to the vertical cannot be held in place by confinement alone. It shows too that symmetrical wedge-shaped blocks with the limiting case of both fracture planes at right angles to the excavation surface, require the least horizontal confining stresses to remain stable. These stresses are fairly low, of the order of kilopascals (kPa), significantly lower than the induced stresses in the rock at the depths considered. The occurrence of falls of ground in deep-level excavations

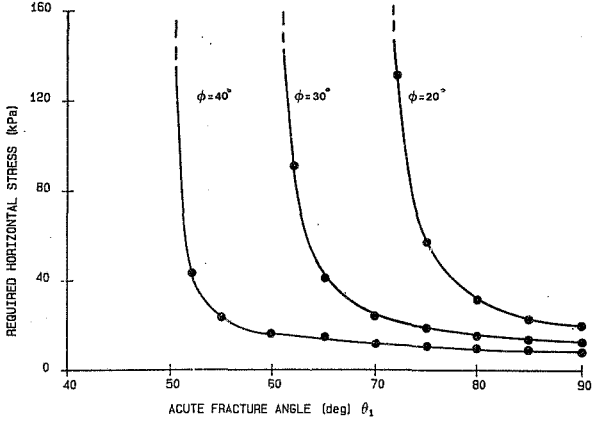

Figure 4.5 Stability curves for blocks with varying frictional properties.

indicates that the available confinement in the fractured rock is very low and/or that the inclination of fractures is significant in maintaining hangingwall block stability. It has been shown by Yow (1985) that apart from the discontinuity shear strength, the in-situ stress field around a block is the most critical condition affecting its stability.

By virtue of their geometry, blocks immediately adjacent to a wedge-shaped keyblock cannot have a similar shape. Hence failure of these blocks must occur by some falling/sliding combination. The loss of any particular keyblock must result in the relaxation of the confining stresses to the adjacent blocks, potentially rendering them unstable. A progression of such incidents may occur rapidly and spontaneously, resulting in a large amount of damage to the excavation and injury to personnel.

Equation 4.8 may be rearranged as follows to determine the resultant vertical force, F, on the block.

$$F = \sigma_h.h(\text{Tan } \gamma_1 + \text{Tan } \gamma_2) + F_c - W \qquad (4.10)$$

Where this force is positive, the block will remain in position and in fact a pullout force would be required to dislodge it. Where the force is negative however, the block is being pushed out of position and is

inherently unstable. A supporting force of the same magnitude would be required to keep the block in position. Figure 4.6 shows the relationship between the block geometry (as determined by the dip of the boundary planes) and the resultant force (F) acting on the block, normalized with respect to the block weight (W), for two values of horizontal confinement. The diverging lines indicate the decreasing dependence on the confinement as the fracture angles approach the vertical, in order to maintain stability. Figure 4.7 shows a comparison between the F/W ratio for the symmetrical, truncated, wedge-shaped block (Figure 4.2) and that for a similar block with one fracture plane vertical. A marked increase in stability in the latter case is immediately obvious.

4.4 Summary

This study has shown that vertically-oriented fractures bound rock blocks that are inherently less likely to fall and require less support than those between low-lying discontinuities. At steeper fracture inclinations the influence and necessity of the confining stresses in maintaining block stability is decreased. Attainment of one boundary discontinuity perpendicular to the confinement has been shown to provide significant improvements in block stability, maintaining a positive F/W ratio over almost the entire range of inclined fracture angles greater than the complement of the natural angle of friction.

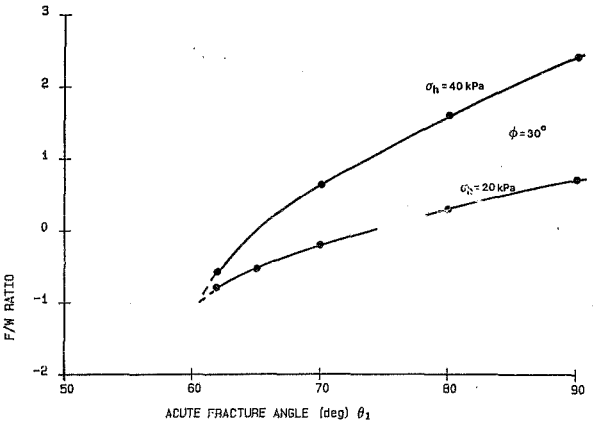

Figure 4.6 The relationship between the F/W ratio and symmetric block geometry for different values of horizontal confinement.

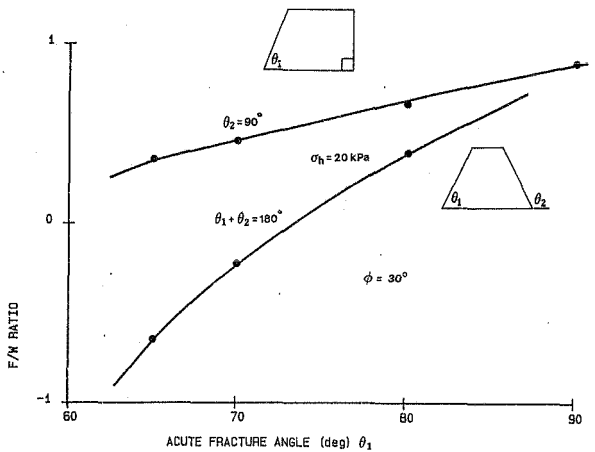

Figure 4.7 The relationship between the F/W ratio and block geometry for symmetric and non-symmetric blocks.

5 EXPERIMENTAL DETERMINATION OF HANGINGWALL STRATA BEHAVIOUR

It has been established that hangingwall stress relaxation can have beneficial effects on the stability and integrity of a stope hangingwall by virtue of the steeper inclinations of the newly-formed extension fractures ahead of the face. In addition it has been shown that hangingwall blocks with sides inclined close to the vertical are more stable than those bounded by low-inclination boundary discontinuities. The experimental work performed in the preparation of this dissertation involved the monitoring of two production stopes during conventional mining operations using timber supports, followed by a second period of monitoring after the installation of two different (hydraulic prop) support systems. With a view to achieving some stress relief in the hangingwall strata and the associated alteration in secondary fracture orientations to provide a more stable hangingwall, a face-parallel (dip) slot was cut in the stope hangingwall in both panels.

This chapter describes the instruments used in the underground monitoring programme, followed by a description of the experimental site and the experimental procedure adopted. The fourth part describes the laboratory test procedures and the results

obtained in determining the properties of the rock material in which the experiments were conducted.

5.1 Measurement and Instrumentation

5.1.1 Strain measurement

Stress (as opposed to strain) is an abstract quantity and as such cannot be directly measured. Strain on the other hand, defined as the elongation per unit length is readily measured. The calculation of stress from strain measurements makes use of the Young's modulus, E. Such theory employing Hooke's Law applied to rock therefore assumes purely elastic behaviour of the material. In the rock surrounding deep-level mining operations, this assumption may become invalid as the rock strata are almost invariably severely fractured, causing inelastic behaviour under load. In the context of the author's experimental work, it was deemed important to obtain some idea of the strains and hence stresses experienced by the rock strata and in the absence of an inelastic strain solution, the aforementioned theory was used.

Two-Dimensional Strain Measurement

One of the pioneers of rock stress measurement, Leeman (1964), has given several methods of determining stress in rock, including a detailed description of mathematical theory and measurement devices. In

particular he described strain measurements using a strain gauge rosette cemented on the flattened end of a borehole as previously attempted by Mohr (1956). Overcoring of similar devices, in order to measure absolute stresses was reported to have been achieved successfully by Olsen (1957) and Slobodov (1958).

A strain cell (known as the 'doorstopper') which incorporated three wire-resistance strain gauges was developed by Leeman (1964); this device has since been altered to include four such gauges at 45 degrees to each other. (Plate 5.1). The addition of the fourth gauge provides one redundant reading which allows estimates of error to be made. Such instruments were used fairly successfully in a number of experiments to determine the stresses in rock at depth (Leeman, 1964).

In a series of comparative tests using five different strain measuring devices (Gregory et al., 1983) it was found that doorstoppers provided the most consistent results and had the most convenient method of implementation. Following this recommendation which agrees with previous local experience, doorstoppers were selected for use in the author's experimental stopes to measure horizontal strain in the hangingwall strata.

It has been observed by several authors that considerable differences may occur between true stress magnitudes and those obtained by strain measurements on

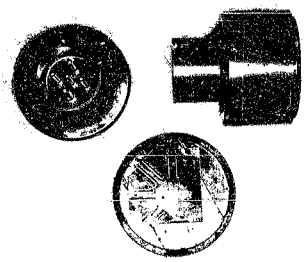

Plate 5.1 'Doorstopper' strain cells

the flattened end of a borehole. Continuum mechanics indicates that a concentration of the field stresses occurs at the end of a borehole but no analytical solution is available. A standard radial concentration factor of 1,53 was proposed by Leeman (1964). This was refuted by Bonnechère and Fairhurst (1968) who suggested a value of 1,25 to be more correct. Experimental and numerical analysis techniques have been performed by several authors (Gray and Barron, 1969; Crouch, 1969; Coates and Yu, 1970) primarily employing finite element solutions. While Crouch proposed a solution using axial and radial concentration factors, Coates and Yu added the effect of a tangential stress, resulting in three regression equations.

Substitution of Poisson's ratio of the order of 0,27 (as determined in laboratory tests) into the radial concentration equation (Coates and Yu, 1970) provides a concentration factor of 1,41 which lies well between the values of 1,53 and 1,25 suggested by Leeman and Crouch respectively. This factor was applied in all doorstopper solutions in the author's experimental work.

Three-Dimensional Strain Measurement

By making use of a three-dimensional strain measurement device, the complete state of stress may be determined in one operation. Several such instruments are available, all of which comprise an array of strain

gauges oriented so as to measure the complete strain change tensor. Amongst these are the low cost stressmeter of Peng et al. (1982), and the Commonwealth Scientific and Industrial Research Organization's (CSIRO) hollow inclusion triaxial strain cell. The CSIRO cell has been used extensively and has been shown to provide satisfactory results (Gregory et al., 1983). The availability of the CSIRO cell was the dominant factor in its selection for use in the author's triaxial strain measurement work (Plate 5.2).

The CSIRO cell has been well documented by Worotnicki and Walton (1976), the CSIRO field manual and Herrmann (1985) while the computational procedure to calculate the complete stress state has been presented by Duncan Fama and Pender (1980) and Brummer (1985). Further work on the theory of hollow inclusions and rock anisotropy as related to stress measurements has been published by Amadei (1984, 1985).

Both two-dimensional and three-dimensional strain measurements were taken using a Hottinger Baldwin Messtechnik (HBM) DMD 20 digital strain gauge monitor, in half-bridge configuration, with a dummy strain gauge maintained at a similar temperature to the measuring gauge to complete the bridge configuration. Attachment of the doorstoppers to the rock was achieved using HBM X-60 two-part adhesive while the CSIRO cells were fixed

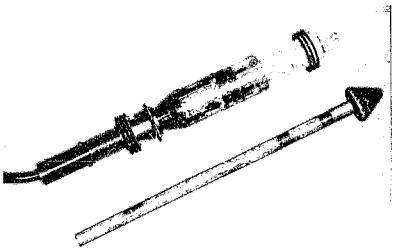

Plate 5.2 'CSIRO' triaxial strain cell

into their boreholes using Araldite BV 1055SA two-part epoxy.

Effects of Anisotropy on Stress Measurements

Several authors have published work on the effects of anisotropy on stress measurements notably Amadei (1982) and Amadei and Goodman (1982) and on stress concentration factors for anisotropic rocks (Rahn, 1984; Borsetto et al., 1984). In the present work, the effects of anisotropy were ignored and the rock was assumed to be at least transversely isotropic. The effect of this assumption on the results is considered to be small (Gay, 1987).

5.1.2 Vertical displacement measurement

Measurement of vertical strata displacement including bedding plane separation was performed using two types of extensometer.

The Sonic Extensometer

This instrument, developed by IRAD GAGE, Inc. consists of two parts: the sonic probe and the readout unit, (Plate 5.3), both of which are readily portable. Reference points in the form of P.V.C. (polyvinylchloride) anchors containing magnets must be installed in a BX sized (60 mm) borehole, at

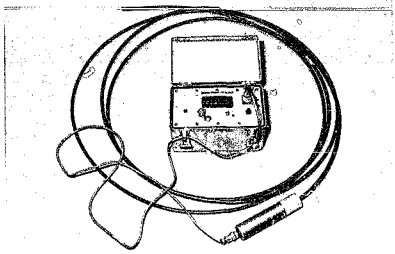

Plate 5.3 'IRAD GAGE' sonic probe and readout unit

pre-determined depths corresponding to the zones in which borehole axial movement is to be monitored (Plate 5.4). A continuous aluminium pipe passing through the centre of each anchor is used to guide the probe on insertion into the hole. The sonic extensometer operates on the principle of magnetic interference by the anchors of a current-generated strain wave in the probe, resulting in a reflected wave. The arrival time intervals of each such wave in a wave train is detected by the instrument and converted to a distance reading between magnetic reference points. An error analysis and full description of the equipment has been provided by Legge (1984), who recorded an accuracy of 0,1 mm over a range of incremental displacements between 0,1 mm and 1,0 mm. Errors were found to increase linearly with displacement yet averaging only 2,2% of the displacement value when this was greater than 10 mm. The equipment may be adversely affected by large 'steps' in the borehole pinching the guide tube and thereby preventing probe insertion. However, taking measurements is relatively simple and may be performed by unskilled personnel. The instrument was selected to monitor bedding separation in the immediate stope hangingwall.

The Wire Extensometer

This relatively simple instrument consists of small coil-spring anchors which are pushed into a borehole to a pre-determined depth, then released. Expansion of the

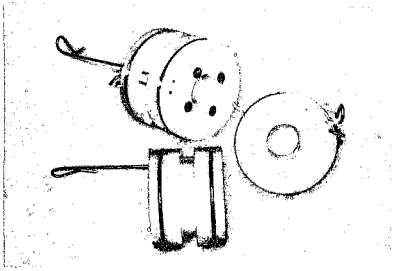

Plate 5.4 Magnetic anchors for use with sonic extensometer

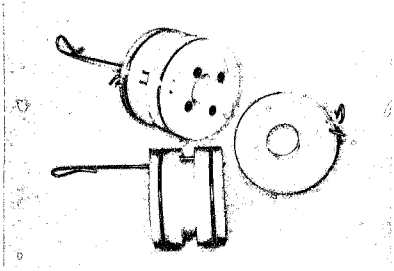

Plate 5.4 Magnetic anchors for use with sonic extensometer

spring firmly wedges the anchor against the sides of the hole. Attached to each anchor is a length of wire trace with a piece of steel measuring tape graduated in millimetres at its lower end, protruding from the borehole collar. The instrument is depicted in Plate 5.5. A small reference marker on the borehole collar is used to provide a fixed level on which to read the tape. Axial movements in the rock displace the anchors and hence the tape, on which the movement can be monitored. The instrument is useful in situations where large steps occur in the borehole, as the wire trace occupies little space in the hole and is unaffected except by very large steps of the order of one half the hole diameter. It is unfortunately not as accurate as the sonic probe extensometer, providing accuracy in the millimetre range. Monitoring the instrument is simple and does not require skilled personnel.

5.1.3 Closure and ride measurement

Relative movements of the stope hangingwall perpendicularly and parallel to the footwall are known as closure and ride respectively. Several methods of monitoring such movement have been used by various researchers, and that adopted by the author makes an addition to the list. The method makes use of the principle that three interpenetrating spheres ideally meet at a point. By employing three imaginary spheres of known radius, each centred at a fixed point in the



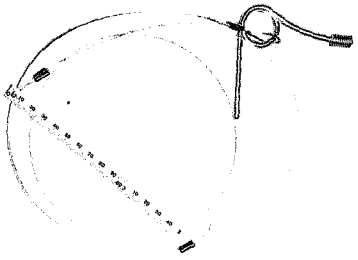

Plate 5.6 Wire extensometer

hangingwall, their point of intersection may be found. If the spheres are forced to intersect at a known point in the footwall, the relative position of that point with respect to the fixed hangingwall points may be found. With the mining activity in the stope, it was considered less harmful to the bolts to be in the hangingwall than in the footwall and hence at each monitoring station three masonry anchors were installed in the stope hangingwall in an orthogonal pattern; a central point, one point on strike and one point up dip. The bolts in the strike and dip directions were typically 600 mm from the central bolt. A fourth bolt was installed in the footwall below the central hangingwall bolt, as illustrated in Figure 5.1.

For analytical purposes it was assumed that only the footwall bolt moved relative to those in the hangingwall. Under this assumption it was only necessary to measure the change in distance between the footwall point and each point in the hangingwall in order to obtain values of closure and ride. This was performed using the Chamber of Mines (1987) Vernier Closure Meter and a simple algorithm.

5.1.4 Surface dilation measurement

In order to measure dilation of the hangingwall surface, use was made of the Chamber of Mines (1987) Vernier Surface Extensometer. This is simply a large (300 mm)

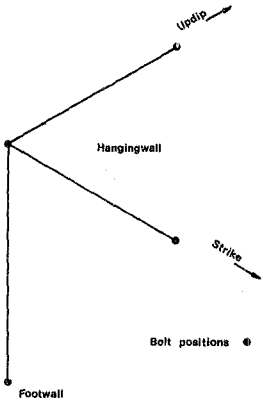

Figure 5.1 Schematic layout of a closure/ride monitoring station

vernier gauge with sharpened measuring prongs. The tips fit into centre-punched indentations on 20 mm square aluminium or stainless steel plates fixed to the hangingwall with putty. Two linear arrays of such points were aligned on strike on the hangingwall in each experimental panel. A comparison of the vernier-measured distances between the plates in the array over the time of the experiment provides a measure of the dilation of the rock surface.

5.1.5 Borehole observations

When conducting experimental work in rock, it is important to have an idea of the physical state of the material, its degree of fracturing and the presence of any bedding planes or geological structures passing through the region. A visual impression of the inside of a borehole drilled into the host rock may be obtained by a borehole television camera (BTC) or a petroscope. BTC's are expensive and bulky compared with a petroscope and the latter was used in the author's work. The petroscope, which has been described and used extensively in rock fracture observations by Adams and Jager (1979), consists of a small mirror inclined at 45° to the horizontal, mounted on a chassis which is pushed into the borehole using a series of steel rods. Observations of the borehole walls, via the mirror are simplified by making use of a small telescope (such as is found in a surveyor's dumpy level) although due to

visibility problems, range is limited to about five metres. A millimetre scale on the mirror allows an estimate of fracture widths to be made.

5.2 Location of the Experimental Site

5.2.1 Regional geology of the Klerksdorp Goldfield

The Vaal Reef, which is the major gold-bearing conglomerate reef in the Klerksdorp Goldfield is currently mined between 1 000 m and 3 000 m below surface. It lies near the middle of the Central Rand Group quartzites, which together with the underlying West Rand Group of shales and quartzites forms the Witwatersrand Supergroup. Above the latter, and separated from it by the Ventersdorp Contact Reef, lie the lavas of the Ventersdorp Group which range in thickness up to 2 000 m. A conglomerate band known as the Black Reef unconformably overlies the lavas and is itself overlain by surface dolomites of the Transvaal Supergroup, which have a maximum thickness of 1 900 m. All the above strata dip at approximately 10 degrees to the south-east.

5.2.2 Experimental site

An initial attempt in conducting the proposed fracture control experiment was made at the Chamber of Mines experimental site at 34 level south, 39 cross-cut at

4-shaft, Hartebeestfontein Gold Mine in the Klerksdorp Goldfield, at a depth of 2 100 m below surface. Two adjacent panels were prepared for the experimental work. The panels, known as panel 2 south and panel 3 south were advanced by conventional drill and blast methods into a remnant. The north side of the centre gully had been extensively mined-out some time previously, leaving initial stope spans in the region of 120 m and 50 m respectively. The average reef dip was 8 degrees to the west. A rockburst in the vicinity of this site and associated large falls of ground nullified the effects of the proposed slot-cutting in the hangingwall and the main experiment at that site was abandoned. However it was possible to investigate the influence of support on stresses in the hangingwall at this site, as follows:

A region of relatively smooth and competent hangingwall in the 0,6 m mat-pack supported back areas of panel 2 south was selected in which to perform support-induced stress and displacement measurements. Little site preparation was required other than a small amount of footwall excavation to permit access of the active support unit, a 1,6 MN barrier prop as described by Basson et al. (1984). The site, approximately 11 m behind the face, was centrally situated between the mat-pack supports, to minimize their effects on the region.

The alternative site selected in which to conduct the large-scale experimental work was the Chamber of Mines experimental site at 75 level north, 25 cross-cut at 6-shaft, Hartebeestfontein Gold Mine, at a depth of approximately 2 300 m below surface (Figure 5.2). The site as a whole comprised six panels, three either side of the centre gully, known as the north side and south side respectively. The bottom panel on the north side known as panel 8N was unmined both before and during the course of the experiment. The two panels immediately above it, panels 9N and 10N were used in the author's experimental work, while the region above panel 10N had been extensively mined-out some months previously. The south side was fairly similar in layout but was used for experimental work in mechanised mining by the Chamber of Mines Research Organization.

Ledging and early mining in panels 9N and 10N had been done using 0,6 m mat-packs at 2,0 m spacing for support in the stopes and waste-filled packs along the gullies. The waste-filled packs were found to be in poor condition and were replaced with 16-pointer 1,2 m packs.

Strike-parallel fracturing was found to occur near the top of panel 10N, which was attributed to the effects of the large lead above the panel. Hangingwall conditions in both panels were generally poor to average with regular shear fractures interspersed with fairly dense brittle or extension type fractures in the immediate

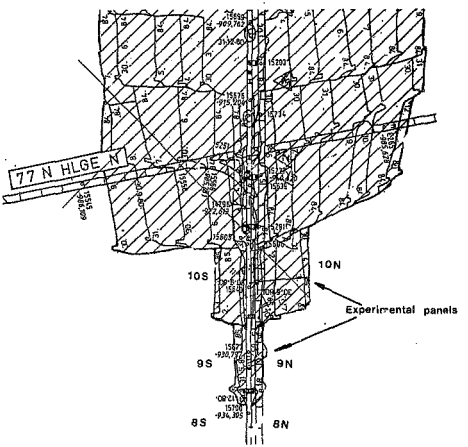

Figure 5.2 Plan of the experimental site, 6-shaft, Hartebeestfontein Gold Mine.

hangingwall. Local falls of ground were evident in the back areas. The reef dip in this area averaged 8 degrees to the south-east. Conventional drill and blast mining was employed on both panels 9N and 10N.

5.2.3 Local geology of the second experimental site

The geology of the rock mass immediately surrounding the experimental site may have a marked influence on the behaviour of that material. A detailed study of the hangingwall rock was carried out in order to determine its nature and properties. A 60 mm diameter (BX) borehole was drilled vertically into the hangingwall at the bottom of panel 10N, to a depth of 10 m and the core retained for inspection and logging. The borehole core log indicated that the overlying rock strata consisted primarily of coarse-grained quartzite bands, some argillaceous, interspersed with shaley argillaceous bedding planes. It was found to be extremely difficult to obtain solid pieces of core of any appreciable length, which was attributed to the highly stressed and fractured nature of the rock. The stratigraphic column is presented in Figure 5.3.

5.3 Experimental Procedure

Two primary experimental projects were performed. The first was devised to monitor the displacements and stresses induced in the hangingwall rock by a normal

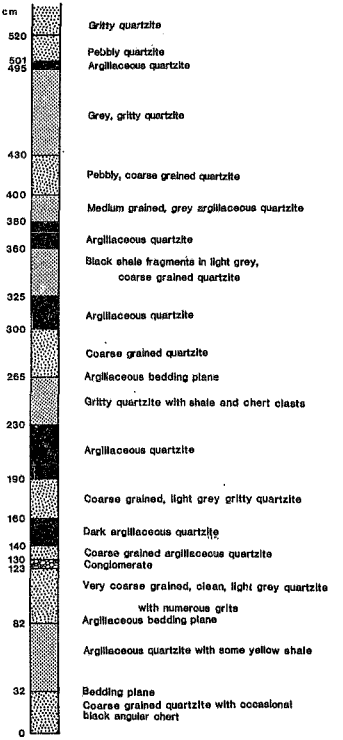

Figure 5.3 Stratigraphic column from stope hangingwall.

load applied to its surface. This experiment was performed at the 4-shaft site at Hartebeestfontein Gold Mine. In order to attain significantly high loads, a 1,6 MN hydraulic barrier prop was used. The load was applied in increments, while induced stresses and deformations were monitored.

The second experiment involved a study of the effects of differing stope support systems and geometrical alterations in the excavation layout on the fracturing and behaviour of the hangingwall. The procedure was lengthy and involved and thus will be described in some detail.

The Chamber of Mines experimental site at 6-shaft, Hartebeestfontein Gold Mine was newly developed with small stope spans either side of the centre (dip) gully. Similar experiments were conducted in both panels 9N and 10N, the only differences being due to relative face positions and the support systems installed.

Panel 10N, which had previously been mined for some 25 m from the centre gully using 0,6 m mat-pack support at 2,0 m centres on dip, advanced 5 m using wedge-prop supports at 1,2 m by 1,2 m spacings. This exposed relatively unfractured hangingwall close to the face, where in the approximate centre of the panel six BX sized boreholes were drilled to specific depths related

to their purpose. In all drilling procedures, the first hole completed was petroscoped to determine the position and extent of fractures and bedding planes, which in turn determined the depths to which the following holes were drilled. Extensometer holes were drilled to 5 m or 10 m depth dependent on the type of extensometer while the three stress measurement holes for doorstoppers were extended to such depths as to terminate within chosen bedding layers. The ends of these holes were flattened or polished to provide a smooth surface for attachment of the doorstopper.

It was found necessary to install the instrumentation immediately the drilling was completed due to adverse 'stepping' (due to slip on bedding planes) and fracturing of the boreholes. A vernier surface extensometer was placed on strike near the drilling site and closure-ride monitoring stations near the top, centre and bottom of the panel.

The face was advanced a further 8 m using wedge-prop support while the instrumentation was monitored regularly. At this stage a second complete set of instrumentation was installed in the hangingwall close against the face. In accordance with the mine's standards for 'caving', a 1 m deep footwall dip gully was blasted along the entire length of the panel just behind the first line of instrumentation in the mat-pack-supported region. This was followed by the

1,2 m high hangingwall dip slot cut directly above it. Face advance then continued, initially employing four rows of 200 kN rapid-yielding hydraulic props at 1,2 m on dip with rows spaced at 1,5 m on strike. After approximately 4 m of face advance the number of rows was reduced to three. This provided a support density of 111 kN/m^2. No further timber supports were installed and no attempt was made to either support the face side of the slot or to initiate hangingwall collapse between the slot and the back row of active support. The procedure is shown diagrammatically in Figure 5.4.

At the onset of preparations for the experiment, panel 9N had been mined for just 8 m from the centre gully and supported with 0,6 m mat-packs as in panel 10N. In order to maintain a practical mining layout, the face in panel 9N was advanced to a position in line with that of 10N, using wedge-prop support, whereupon the first line of instrumentation, identical to that of panel 10N, was installed. A similar procedure to that employed in panel 10N was then adopted until the final installation of the hydraulic prop support. This panel was intended to be stiffly supported and hence five rows of 400 kN rapid-yielding hydraulic props were installed at 1,2 m by 1,2 m spacings. This was reduced to four rows of support after some 4 m of face advance. The back row of support was stiffened by the inclusion between every second prop, of a 1,6 MN barrier prop (as described by Basson et al., 1984). This provided an

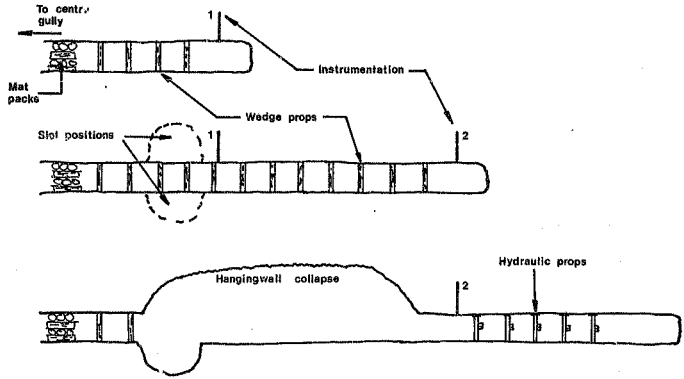

Figure 5.4 Schematic strike section of stope showing face progression and support systems used.

average support density of 463 kN/m^2. Throughout the experiment, the face in panel 9N was maintained some 3 m behind that in panel 10N. The same layout and support was used in this panel as in panel 10N. The results of all experimental work are presented in Chapter 7.

5.4 Laboratory Testing

Laboratory testing of materials forms an integral part of rock mechanics research work. It is imperative to know the properties and behaviour under load of the materials in which practical experiments are conducted.

A rock mass is a composite medium of rock material interrupted by joints, faults, fractures, dykes and intrusions, all of which influence its mechanical properties. With decreasing specimen size, progressively more of these discontinuities may be excluded, hence the behaviour of the rock mass differs from the behaviour of an intact sample. While a small test sample should not be considered as an exact representation of the rock mass it does at least provide some insight into the behaviour of the rock material.

The quartzites surrounding the gold-bearing reefs of the Witwatersrand are fundamentally brittle rocks characterized by work-softening in the post-failure state (Figure 5.5). The latter may be of importance as the immediate hanging- and footwalls of deep-level

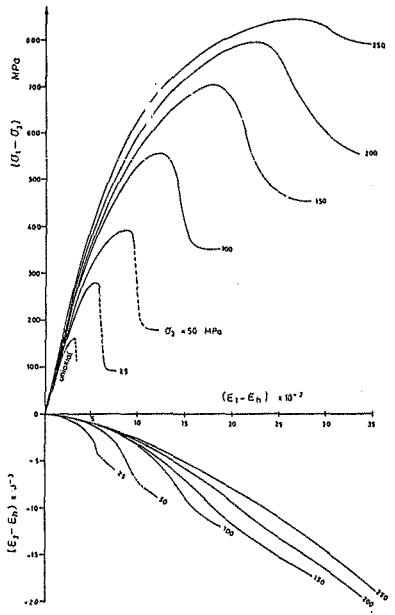

Figure 5.5 Constitutive behaviour of quartzite.

(After Stavropoulou, 1982)

excavations are extensively fractured. Laboratory tests on pre-fractured rock as on rock masses are, though important, difficult to perform.

Some work involving testing of pre-fractured rock was conducted by Smith et al. (1969) on granite which showed that under high confining pressures (triaxial tests) material properties differed only slightly from those of intact rock. Other researchers (Ladanyi and Don, 1967; Raphael and Goodman, 1979) have found that a modulus value of the order of 20 per cent of that of intact rock applies to broken rock. A significant amount of research was presented by Hojem and Cook (1968), Hojem et al. (1975), Bieniawski (1967) and Bieniawski et al. (1969) on brittle rocks such as Witwatersrand quartzites. Several other workers have provided further insights into the post-failure behaviour of rocks (Wawersik and Fairhurst, 1970; Wawersik and Brace, 1971; Wawersik, 1968). Much of the experimetal work performed by the author involved the initial fracturing of rock and thus post-failure testing of rock samples was ignored and only intact rock properties were determined from simpler laboratory tests.

5.4.1 Laboratory testing of rock samples

Sample Preparation

Selected pieces of standard diamond-drilled BX size borehole core were re-drilled to a smaller diameter, then ground on a lathe, thereby reducing them to solid cylinders. The ends of each sample were cut and ground to provide a sample of the required 3:1 length to diameter ratio, with flat, parallel ends. The allowed tolerance was 100 microns. Near absolute parallelity of the two flat surfaces was vital to eliminate platen loading effects and unwanted shear stresses in the sample. The resultant test specimen was a cylinder of height 76,2 mm and diameter 25,4 mm. Samples thus prepared were used in uniaxial and triaxial tests.

Similar cylinders of height 35 mm and diameter 70 mm were prepared for use in Brazilian tests.

Uniaxial Compression Tests

This is perhaps the oldest and simplest test, yet is a highly useful method of determining rock properties. It does however have some drawbacks.

Under uniaxial load ($\sigma_1 > \sigma_2 = \sigma_3 = 0$), the rock material expands in the transverse direction (by the Poisson effect) causing an interaction with the loading

platens on each end due to restrictions in lateral movement, thereby setting up shear stresses along the platen-sample interface. These stresses provide lateral confinement which appears to affect the sample for an axial distance approximately equal to its diameter.

Tests conducted in this work employed no additional factors to alleviate the shear problem, other than sample size. The tests were conducted in a two meganewton (2 MN) stiff testing machine. A complete description of the press, the significance of the stiffness of the machine, its effect on the test specimen and the mode of failure is beyond the scope of this work and has been reported by Hojem et al. (1975).

In order to increase the overall stiffness of the machine, cylindrical end pieces of tungsten carbide having the same diameter as the sample were inserted between the loading platens and the sample. The entire specimen was encased in a rubber sheath to prevent specimen disintegration after failure.

Brazilian Tests

The Brazilian or indirect-tensile test provides a simple means of estimating the uniaxial tensile strength of a material. By applying diametral compression to a rock cylinder, failure occurs by an extension fracture the

loaded diametral plane. Failure results from the tensile stresses induced normal to this plane by the applied load. Brazilian tests are of special interest in rock failure studies as the stress pattern involved (compressive and tensile) is thought to more closely resemble that obtained in underground extension fracturing than that obtained in uniaxial tension.

The Brazilian tests were conducted using the same 2 MN stiff testing machine as described in the section on uniaxial compressive tests. The samples were compressed between the steel loading platens of the machine.

Triaxial Extension Tests

The triaxial extension test, which may be seen as a reverse of the standard triaxial compression test as described by Jaeger and Cook (1979) does however provide similar information, namely Young's modulus, Poisson's ratio and a failure envelope for the material. It promotes extension-type fracturing or failure in the specimen as opposed to compressive shear failure and hence may be disadvantageous in certain cases when testing layered samples cut perpendicular to the bedding, due to inherent weaknesses between bedding planes. It is however regarded as a close approximation to the actual failure processes that occur in the rock in front of a stope face (Gay, 1987).

The test proceeds initially along a hydrostatic stress path $\sigma_1 = \sigma_2 = \sigma_3$ until a pre-determined level is reached. At this point while the confining pressure is held constant, the axial load is decreased, allowing axial extension of the sample until failure, $\sigma_1 = \sigma_2 > \sigma_3 > 0$. The load path followed is given in Figure 5.6.

The triaxial extension testing equipment consists of a triaxial cell connected to an hydraulic system capable of controlled flow in two directions. The system is fairly complex and will not be described in detail here. It has however been documented by Briggs (1982). Previous results of such testing programmes have been reported by Briggs and Vieler (1984).

Results

Uniaxial compressive tests were performed on quartzite core samples taken from the stope hangingwall at the first experimental site (4-shaft, Harteheestfontein Gold Mine), from approximately the same depth as that at which the CSIRO triaxial cells were installed. The core obtained was severely fractured and broken and provided only three samples of acceptable length and quality for use in such tests. One such sample, from the upper end of one hole was extremely argillaceous and failed under a uniaxial load of 107 MPa. The other two samples however were of similar rock type and quality and

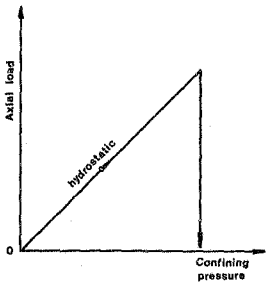

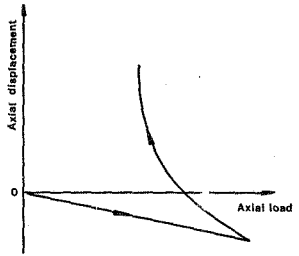

Figure 5.6 Load path followed in triaxial extension tests.

provided values for Young's Modulus of 64 GPa and 67 GPa. As no values for Poisson's ratio were obtained in the uniaxial compression tests, a value of 0,2 was assumed during stress calculations for the CSIRO cells.

A series of 20 uniaxial compression tests was performed on material taken from vertical boreholes in the stope hangingwall in both panels 9N and 10N at the 6-shaft site at Hartebeestfontein Gold Mine. A fairly wide range of uniaxial compressive strengths (U.C.S.) was found for the various samples, with an overall average U.C.S. of 154 MPa, which equates to that of a fairly argillaceous quartzite (Briggs, 1986). While some samples exhibited strengths as low as 107 MPa, stronger, cleaner quartzites found higher in the hangingwall had U.C.S. values of the order of 182 MPa.

Twelve Brazilian or indirect-tensile tests were performed on material samples from the quartzite hangingwall of the experimental site at 6-shaft. The results obtained were consistent, with an average tensile strength of 12,3 MPa and standard deviation of 0,9 MPa at failure.

A total of 46 triaxial extension tests were completed on similar material to that used in the uniaxial compression tests. Wherever possible a series of four tests was conducted on samples obtained from each specified depth into the hangingwall. Each series

comprised a uniaxial test as previously described and three extension tests at confining pressures of 200, 400 and 600 MPa, selected as reasonable values in order to obtain representative material properties (Briggs, 1986). In cases where sufficient samples existed, reasonably consistent failure envelopes could be drawn over the range of confining pressures from zero (the U.C.S.) to 600 MPa, as shown in Figure 5.7. A wide range of material strengths was obtained, with little correlation between the strengths of . les taken from similar depths in the strata. In cases where uniaxial and extension tests were performed on the same rock type, a greater value was obtained for Young's modulus (E) in the extension test samples. Values for Young's modulus and the bulk modulus (K) were measured directly from the load-deformation plots for each test and Poisson's ratio (v) was then determined from standard elastic formulae. Average values for E, of 59 GPa and v of 0,27 were obtained from the extension tests.

Laboratory test results for samples taken from the hangingwall at depths of less than 5 m are given in Table 5.1.

5.5 Summary

The laboratory testing programme comprising uniaxial compression and triaxial extension tests was intended to provide some properties of the rock materials in which

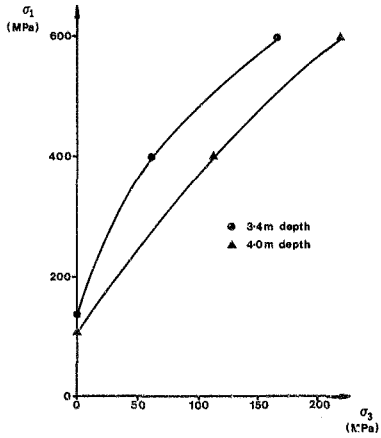

Figure 5.7 Failure envelopes for hangingwall quartzites.

the underground experiments were conducted. The quartzites in the hangingwall of both experimental sites were found to be generally argillaceous and interspersed with softer, shaley parting planes. Rock strengths slightly lower than those typically measured for Witwatersrand quartzites were obtained.

Table 5.1 Summary of Laboratory Test Results

Table 5.1(a) Uniaxial compression test results on hangingwall quartzites, panel 2S, 4-shaft site, Hartebeestfontein Gold Mine

Sample number	U.C.S (MPa)	Young's Modulus E (GPa)
1	241	64
2	238	67
3	107	48

Table 5.1(b) Uniaxial compression and triaxial extension test results, panel 9N, 6-shaft site, Hartebeestfontein Gold Mine

Depth into hangingwall (m)	σ_1 (MPa)	σ_3 (MPa)	K (GPa)	E (GPa)	ν
1,0	154	0		50	
1,0	200	9,6	39,7	57,4	0,26
1,0	400	73,4	46,2	70,1	0,25
1,0	600	174,6	42,1	53,1	0,29
1,4	143	0		46	
1,4	400	98,4	49,6	63,8	0,29
1,4	600	157,5	46,5	45,3	0,34
2,3	200	37,6	42,0	61,7	0,26
2,3	400	71,2	42,7	61,4	0,26
2,3	600	162,4	42,3	64,4	0,25
3,0	121	0		39	
3,4	138	0		48	
3,4	200	29,3	43,0	59,1	0,27
3,4	400	63,1	41,[illegible]	59,7	0,26
3,4	600	164,4	47,3	67,7	0,26
3,8	200	39,4	50,8	55,6	0,32
3,8	200	11,7	38,5	50,4	0,22
3,9	400	51,3	41,6	66,1	0,24
3,9	600	120,8	43,5	63,0	0,26
4,1	127	0		45	
4,1	157	0		53	

Table 5.1(c) Uniaxial compression and triaxial extension test results, panel 10N, 6-shaft site, Hartebeestfontein Gold Mine

Depth into hangingwall (m)	σ_1 (MPa)	σ_3 (MPa)	K (GPa)	E (GPa)	ν
1,0	400	103,3	49,6	61,9	0,21
2,4	171	0		55	
2,4	200	6,7	48,8	59,9	0,20
1,9	400	86,6	43,4	66,7	0,26
1,9	600	114,2	42,9	51,6	0,30
4,1	200	32,9	39,4	54,2	0,27
4,1	400	106.1	45,8	61,4	0,28
4,1	600	226,6	44,6	56,7	0,29
4,3	164	0		52	
4,3	200	8,6	42,7	60,5	0,26
4,3	400	62,9	42,9	59,8	0,27
4,3	600	145,9	45,8	62,7	0,27
4,5	175	0		57	
4,5	178	0		54	
5,1	159	0		49	
5,1	200	17,3	39,4	55,7	0,26

Table 5.1(d) Brazilian test results on hangingwall quartzites, 6-shaft site, Hartebeestfontein Gold Mine

Sample number	Max. Tensile stress (MPa)
1	12,2
2	11,8
3	13,2
4	12,6
5	12,8
6	11,4
7	11,1
8	11,4
9	11,3
10	13,0
11	13,1
12	13,9
Average	12,32
Std. deviation	0,91

6 NUMERICAL MODELLING

The ever-increasing depths at which mining operations are conducted, and the variety of mining layouts adopted have created a need for accurate numerical models to simulate both small- and large-scale rock behaviour. Such models should incorporate material constitutive relationships capable of predicting the actual behaviour of rock under load in both the far-field and near-field régimes. In terms of mine design, numerical modelling is necessary for achieving optimal layouts to increase production and provide safer working conditions. With this in mind, simulations of the proposed slot-cutting experimental work were performed using a finite element suite, to predict the stresses and deformations likely to occur in the stope hangingwall. The following sections describe the finite element code used in the analyses, followed by numerical predictions of the stresses and displacements induced in the hangingwall both with and without the presence of a dip slot.

6.1 The 'GOLD' Finite Element Suite

The 'GOLD' finite element code was developed by the Chamber of Mines Research Organization in conjunction with the University College of Swansea for use in the analysis of mining-related problems, with particular emphasis on deep-level operations in quartzites. These brittle rocks display work-softening behaviour in the

post-failure state, an attempt at simulating which has been incorporated in the finite element code as an elasto-viscoplastic material model. A physical representation of an elasto-viscoplastic material is shown in Figure 6.1. The formulation assumes elastic material behaviour up to a yield point (governed by a chosen criterion) followed by time-dependent plastic flow until the stress state has returned to the yield surface.

The 'GOLD' code incorporates four failure criteria, namely Tresca, Von Mises, Drücker-Prager and Mohr-Coulomb. The latter, being suited to rock material was employed in all analyses in the author's work. In order to simulate tensile cracking of rock materials, a 'no- or limited tension' criterion has been included in the code, which limits the tensile stress in the material by permitting visco-plastic flow in the direction of the stress once the tensile limit has been exceeded. The Mohr-Coulomb failure envelope with a 'limited-tension' constraint is shown in Figure 6.2.

The presence of thin shaley layers in the quartzitic host rocks surrounding gold-mine stopes has been simulated by the inclusion of joint elements in the finite element code. These elements allow large localized shear displacements corresponding to relative lateral slip on the shaley planes. Infinite elements account for the great depths at which the modelled

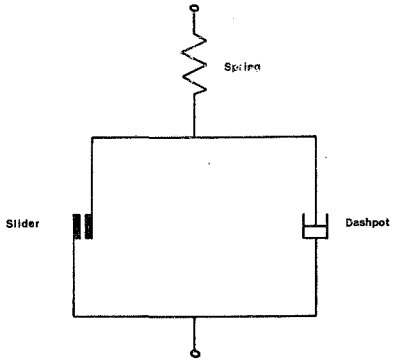

Figure 6.1 Rheological analogue for elasto-viscoplastic material behaviour.

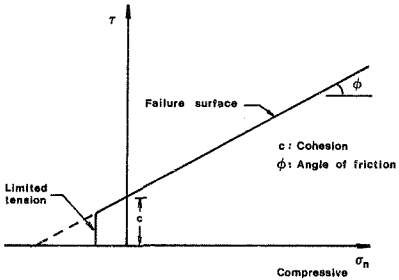

Figure 6.2 Mohr–Coulomb failure envelope with tension cut–off.

excavations occur and obviate the need for representation of the ground surface and the far-field in the finite element mesh. In its present form the code employs four-noded quadrilateral, joint and infinite elements using one-, two- and four-point integration schemes respectively.

6.2 Finite Element Analyses

The 'GOLD' code was used to predict the behaviour of the stope hangingwall rock under various geometrical constraints and support types. The geometry of the stope layout at the Hartebeestfontein 6-shaft site was considered too severe to model using finite elements due to the large stope span-to-width ratio and the associated large number of elements required. In order to obtain qualitative predictions of the behaviour of the hangingwall rock a simplified representation of a small-span stope in two dimensions employing the plane strain condition was used. To simplify the layout a stope extending 9 m either side of the centre gully was modelled and use was made of two planes of symmetry. The hangingwall slot and subsequent progressive collapse of the strata were represented by the removal of a 1 m x 1 m element 6 m behind the face. A horizontal line of joint elements displaying material properties similar to those of a shale was introduced at the upper limit of the slot, extending along the span of the stope. The far-field continuum was represented by

infinite elements. The mesh used in the analysis is shown in Figure 6.3.

Stresses of 67,5 MPa and 33,75 MPa were applied vertically and horizontally respectively to the unrestrained boundaries, representative of the overburden stresses at a depth of 2 500 m and assuming a vertical to horizontal stress ratio of 2. The rock mass itself was modelled as a continuum with a friction angle of 25 degrees, a nominal cohesion of 20 MPa, Young's modulus of 60 GPa and Poisson's ratio of 0,25.

6.3 Effects of Slot-Cutting

6.3.1 Influence on stresses

The predicted principal stress plot for a conventional stope under the above loading is given in Figure 6.4. The stresses immediately above the excavation are predominantly compressive and horizontal, indicating block confinement.

Figure 6.5 shows the principal stress plot for a similar stope layout with the inclusion of a hangingwall slot. In this diagram it may be seen that the horizontal stresses above the stope have been relaxed and the magnitudes of the minor principal stresses in the rock ahead of the stope face and above the reef are reduced. The resultant stress on a particular rock element is

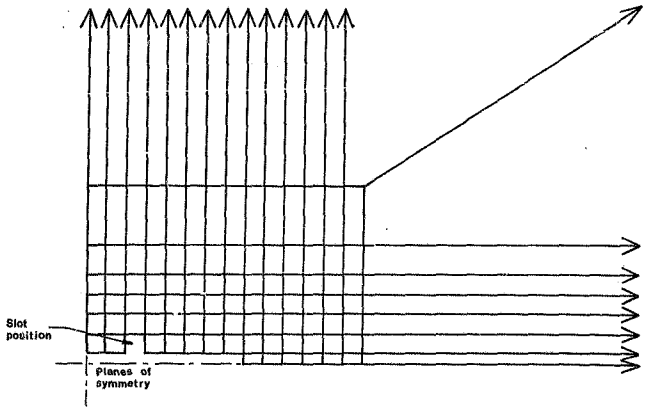

Figure 6.3 Finite element mesh for stope analysis.

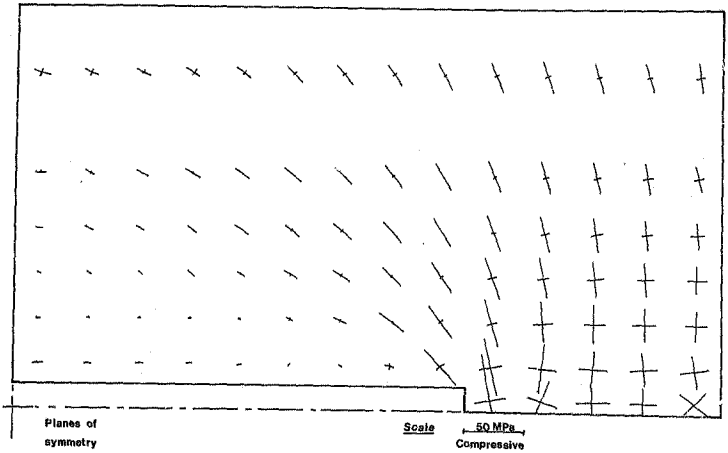

Figure 6.4 Principal stress plot for conventional stope layout.

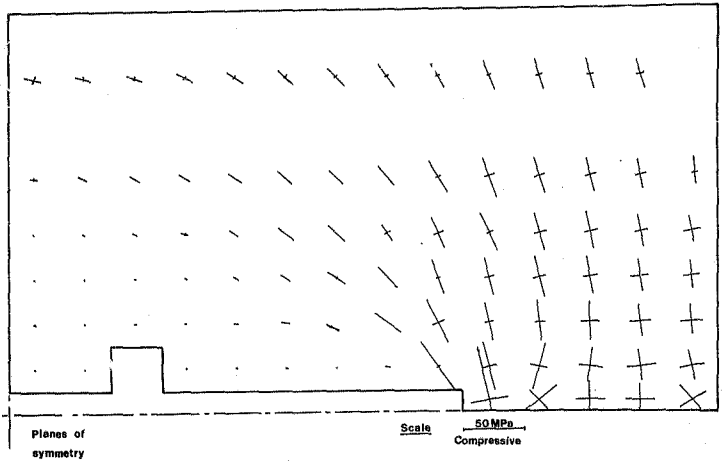

Figure 6.5 Principal stress plot for slope with hangingwall slot.

thus more closely aligned with the major principal stress, being approximately vertical in front of the stope face. When related to the formation of extension fractures this would result in fracture inclinations closer to the vertical.

The predicted vertical and horizontal stresses in the stope hangingwall at 0,5 m depth both with and without the slot are shown in Figure 6.6. Lower stresses in both directions are predicted in the case of the hangingwall with the slot. The difference between the two horizontal stress levels represents the 'instantaneous' release of confining stresses within the rock due to cutting of the slot. The magnitude of stress relaxed is of the order of 10 MPa to 20 MPa, immediately ahead of the excavation.

6.3.2 Influence on displacements

The absolute horizontal displacement of the hangingwall surface ahead of the slot is illustrated in Figure 6.7. In this diagram the lower curve, representing hangingwall surface movements under a conventional stope geometry, indicates gradually increasing dilations of the rock continuum away from the solid zone, reaching a peak some 4 m in front of the face. This is followed by a rapid decrease in displacement of the rock further ahead of the excavation.

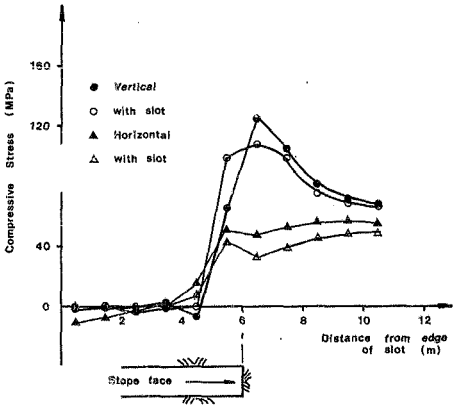

Figure 6.6 Vertical and horizontal stresses in stope hangingwall, with and without the slot.

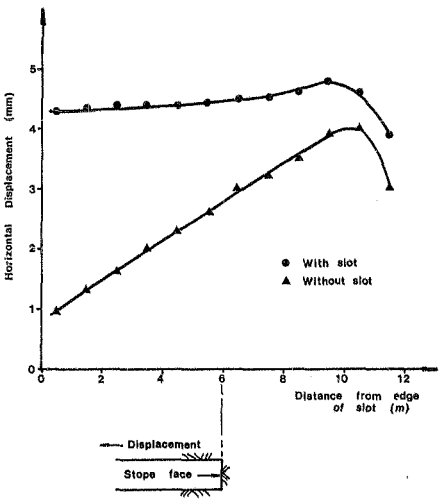

Figure 6.7 Horizontal displacement of the hangingwall surface.

The zone of greatest dilation corresponds fairly closely with the expected region of high stresses and rock fracture in the underground situation. It is however 2 m to 3 m ahead of the predicted point of maximum vertical stress (Figure 6.6). This failure mechanism results in expansion of the mass as a whole, which is unable to dilate into the solid rock ahead of the face and thus compresses the blocky material above the excavation and the rock ahead of the face. In turn this provides additional horizontal confinement to the rock mass which causes rotation of the resultant stress towards the horizontal. Fractures thus formed are inclined closer to the horizontal.

In contrast, the upper curve in Figure 6.7 indicates fairly uniform movement of the entire immediate hangingwall stratum towards the excavated slot. The small peak approximately 4 m ahead of the stope face corresponds with the region of rock fracture described above. Uniform dilation of the rock stratum would provide for relaxation of the confined horizontal stresses without inducing additional loads. In the zone of rock fracture ahead of the face, the high propensity for horizontal movement would allow relaxation of any confinement and thus create fractures inclined more closely with the (vertical) major principal stress.

Although the above results indicate qualitative agreement between the numerically-predicted rock

behaviour and that typically observed underground, in quantitative terms, despite the smaller excavation dimensions, the predictions are inaccurate. Figure 6.8 shows the absolute dilation profile for the rock directly ahead of a stope face as derived by Brummer (1986a). Although it strictly applies to the particular large-span conventional layout stope in which the measurements were made by Legge (1984), the author feels that the orders of magnitude of the derived absolute displacements are representative of most deep-level stopes and thus may be used for comparison with numerical solutions. The absolute dilation profile was attained by simple integration of the relative displacements measured by extensometers installed into the rock ahead of the face.

The separation of the two curves at any point illustrates the incremental dilation towards the excavation of the rock at that point after a face advance of 1 m. For example, the rock 6 m ahead of an advancing face remains undisturbed. Following a 1 m face advance, that particular rock element is now 5 m ahead of the face and has moved towards the face by 4 mm. After the next 1 m of face advance the element moves another 9 mm in the same direction. The cumulative dilation of the rock after any particular face advance is given by the lower curve, with respect to the axis system.

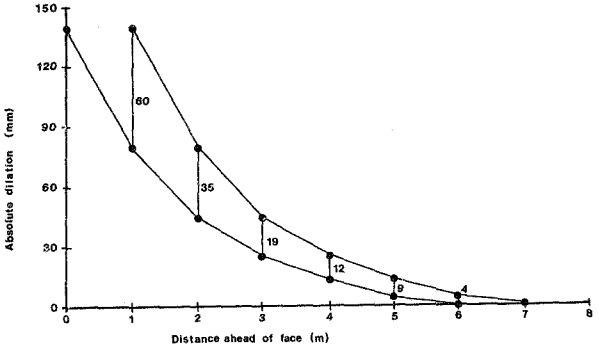

Figure 6.8 Absolute dilation profile for rock ahead of a stope face. (After Brummer, 1986a)

It is obvious that horizontal displacements of the order of 4 mm as predicted by the finite element solution occur only in the region some 5 m to 6 m ahead of the face and that the numerical code is unable to cope with the large displacements that occur closer to the excavation. Unfortunately no measurements of the horizontal dilation in the rock ahead of the face were made in the experimental stopes and thus no direct comparisons can be made.

Figure 6.9 shows the stope closure as determined by the finite element solution. As the model assumed a horizontal plane of symmetry along the stope centre-line, the values of predicted closure have been doubled to account for footwall heave and to provide more accurate values for comparative purposes.

The numerical solution predicts greater closure under a conventional stope layout than in one with a hangingwall slot. This disagrees with the expected result as the slot ought to relax confinement and thus allow sag of the unsupported strata. Predicted closure values of the order of 20 mm to 30 mm some 2 m behind the face were obtained for the slot solution, which in terms of typical stoping conditions are not unreasonable. The small movements ahead of the stope face are associated with elastic deformation and crushing of the rock under high vertical stresses.

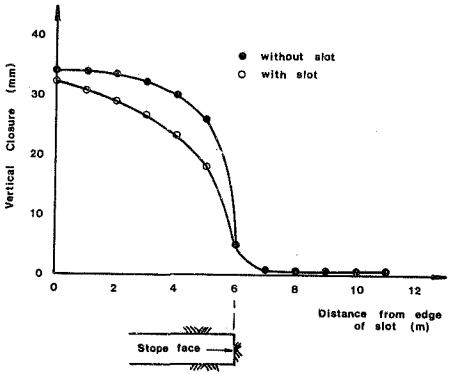

Figure 6.9 Predicted stope closure.

6.4 Effects of Support Systems

In order to obtain some idea of the effects of stiffer support systems on the stope hangingwall, a material having Young's modulus, E of 100 MPa was introduced to fill the excavation ahead of the slot position. No other changes were made to the mesh.

6.4.1 Influence on stresses

Figure 6.10 illustrates the vertical stress profiles in the immediate hangingwall 0,5 m above the stope and ahead of the slot position, both with and without the presence of a hangingwall slot. For comparative purposes the corresponding curve indicating the vertical stress profile without stope support and without a slot is included.

Above the excavation the support system may be seen to allow the formation of compressive vertical stresses both with and without the slot. Ahead of the face only marginal differences in compressive stresses are noted, the difference diminishing rapidly some 3 m into the unmined rock. The curve indicated by triangles, representing the conventional mining situation, predicts a greater stress peak just ahead of the face than those representing the case of a mass-filled stope. The reduction in peak compressive stress in the filled stopes may be due to the supportive effects of the fill

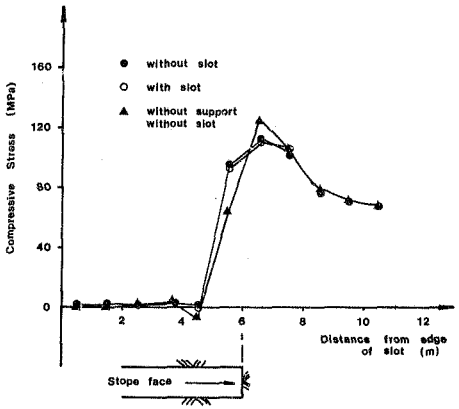

Figure 6.10 Vertical stress profiles in the immediate hangingwall.

absorbing some of the load, which otherwise would rest on the rock at the edges of the excavation.

The horizontal stresses for the same region are shown in Figure 6.11. The major significant effect of the stiffer support system is that higher compressive horizontal stresses are predicted in the rock ahead of the stope face than in the conventional situation lacking the support resistance. This indicates that some restriction in horizontal dilation of the strata is present which may directly affect the failure mode of the rock. Above the excavation similar differences in the horizontal stresses exist. Compressive stresses are predicted in the immediate stope hangingwall in the presence of the mass support system, which would tend to clamp blocks together and improve the stability of the stratum as a whole. The 'instantaneous' release of confining stresses due to cutting the hangingwall slot is of much smaller magnitude than in the unsupported case, here of the order of 4 MPa to 6 MPa just ahead of the face. The stresses relaxed in the rock above the supported stope due to the slot are of similar magnitude. It should be noted however that the differences in stress magnitudes predicted are relatively small and in the underground situation such marginal differences may be inconsequential.

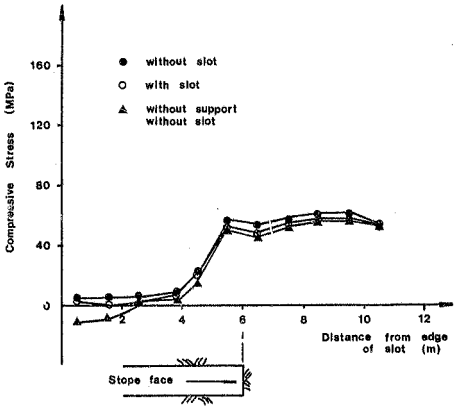

Figure 6.11 Horizontal stress profiles in the immediate hangingwall.

6.4.2 Influence on displacements

The predicted horizontal displacement of the supported hangingwall stratum is shown in Figure 6.12. In contrast with the unsupported dilations (Figures 6.7 and 6.8) the finite element model indicates displacement of the rock above the excavation towards the face (away from the slot). This movement rapidly decreases nearer to the face, finally resulting in more conventional dilations towards the slot, some 2 m ahead of the face. Such displacements would cause a build-up of horizontal compressive stresses in the stratum and appear to be unaffected by the inclusion of the slot. Some frictional resistance between the support system and the overlying rock may account for this phenomenon. The magnitude of the predicted displacements is again somewhat less than what may be expected in an underground situation. In addition, the differences in predicted displacements both with and without the hangingwall slot are small and unimportant.

Figure 6.13 depicts the vertical closure profile as determined by the finite element code. In a similar fashion to that obtained in Figure 6.9, the predicted closure is less in the stope with a hangingwall slot than in one without. The support system appears to have restricted closure to some extent particularly near to the face, where a comparison with Figure 6.9 shows a difference of a few millimetres in the combined

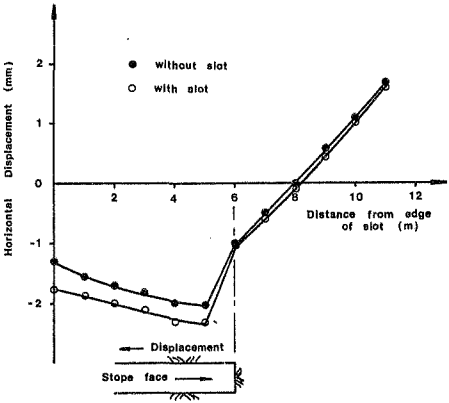

Figure 6.12 Predicted horizontal displacement of the hangingwall with stope support.

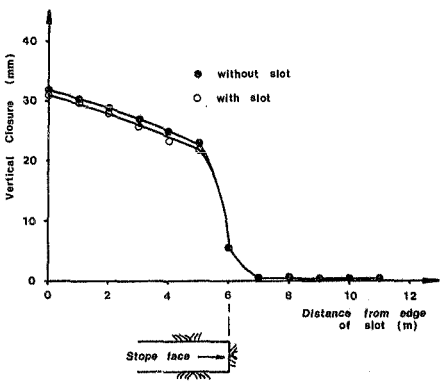

Figure 6.13 Closure profile with stope support.

hangingwall and footwall displacements. As in the case of horizontal displacements, the differences between the predicted closure values with and without the hangingwall slot are small.

6.5 Summary

The above analyses and results show that the GOLD finite element code is able to predict qualitative behaviour of the rock surrounding deep-level stopes but it is far from realistic in quantitative analyses. Predicted values of both stresses and displacements unfortunately showed small differences between conventional and non-conventional mining layouts, which in the underground situation would be regarded as marginal and unimportant. Although the finite element mesh used in the analyses was not representative of the actual situation, it is felt that the trends obtained from the solutions do provide an indication of the actual behaviour to be observed underground. Further development and application of the code is recommended in order to obtain closer agreement between numerical solutions and reality.

7 RESULTS AND DISCUSSION

In the previous chapters the motivation for performing the slot-cutting and support system experiment was presented, along with numerical analyses of the proposed layout in order to obtain some idea of the stresses and deformations that may be expected. The results of the experimental investigations at both the 4-shaft and 6-shaft sites at Hartebeestfontein Gold Mine are now documented, together with some discussion on the effects of the support systems and geometrical alterations on the hangingwall strata. The chapter commences with the results of the experimental work conducted at the 4-shaft site in determining the influence of a single active (hydraulic prop) support load on the fractured hangingwall, which is followed by the results of the slot-cutting experiment at the 6-shaft site.

7.1 Individual Support Load Effects

7.1.1 Determination of the structure of the hangingwall

The structural nature of the rock in which the experiment was conducted was determined by means of a surface fracture map using a technique described by Rorke and Brummer (1985) and shown in Figure 7.1 and the borehole petroscope log, Figure 7.2. The map showed two prominent shear fractures on either side of the proposed

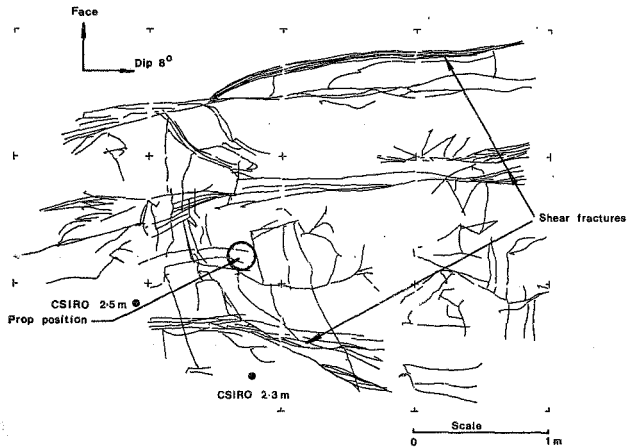

Figure 7.1 Stereographic fracture map of the hangingwall surface, panel 2S

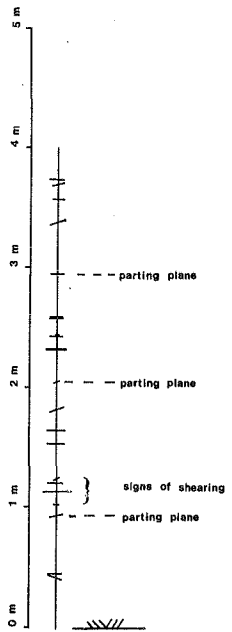

Figure 7.2 Petroscopic observations of fractures intersecting the hangingwall borehole, panel 2S.

prop position, parallel to each other and separated by a region of relatively solid rock, traversed by a small number of extension fractures. The absence of major fracture zones indicated that the block between the shear fractures could be regarded as solid.

The nature of the rock above the hangingwall surface and the depth and extent of fracturing were determined from petroscope observations in a vertical borehole. With the exception of the first metre or so, which was largely unfractured, the strata were observed to be lightly fractured, predominantly in the horizontal direction with solid regions of the order of 10 cm to 30 cm between fractures. Closed parting planes were observed at 0,9 m and 2,05 m depths, with a slightly wider layer occurring at 3 m which showed some signs of separation.

7.1.2 *Induced stresses* in the hangingwall

Two CSIRO cells, installed at depths of 2,30 m and 2,50 m into the hangingwall in separate boreholes as shown in Figure 7.1, were monitored to determine the magnitude and direction of the induced stresses in the hangingwall, due to the applied load. The instrument installed at 2,5 m depth initially performed adequately but at higher loads displayed some drift and irregularities in readings, possibly due to adverse influences from fractured ground. The lower cell

however produced consistent readings. Measurements of the relative positions of the prop and the borehole collar and the surface position and inclination of the intervening shear fracture have shown that this instrument was installed in the same block as that on which the prop acted (Figure 7.3).

The relevant boundary shear fractures and typical load-induced principal stress orientations are depicted on an upper hemisphere stereonet in Figure 7.4. This diagram shows that the induced major principal stress was nearly parallel to the dominant bounding fracture planes. The minor induced principal stress, σ_3, with a dip of 5° was oriented nearly perpendicularly to the fractures, while the intermediate component, σ_2, having a shallow dip of some 4°, was sub-parallel to the fracture planes. The relationships between the measured induced stresses and applied loads are shown in Figure 7.5, while the altitudes (which indicate the dip or plunge) and azimuths of the measured stresses are given in Figures 7.6 and 7.7 respectively.

From Figure 7.5 it can be seen that rapid increases in measured stresses for the first 200 kN of load were followed by a gradual 'tailing off' of the measured stress, which eventually reached an asymptote of constant stress in the rock under some 600 kN to 800 kN of load. The 'tailing off' may be attributed to compression and closing of the fractures within the

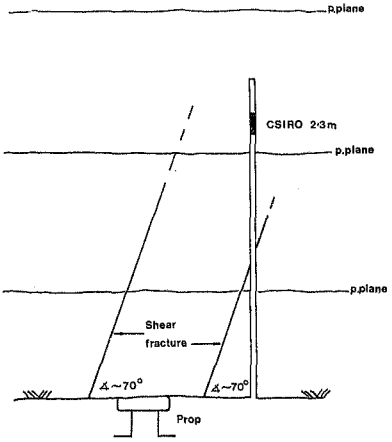

Figure 7.3 Sectional layout of stress measurement site

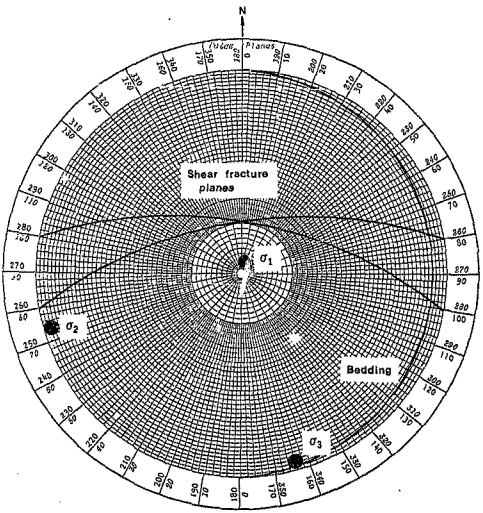

Figure 7.4 Upper hemisphere polar stereonet showing dominant fracture and measured principal *stress* orientations

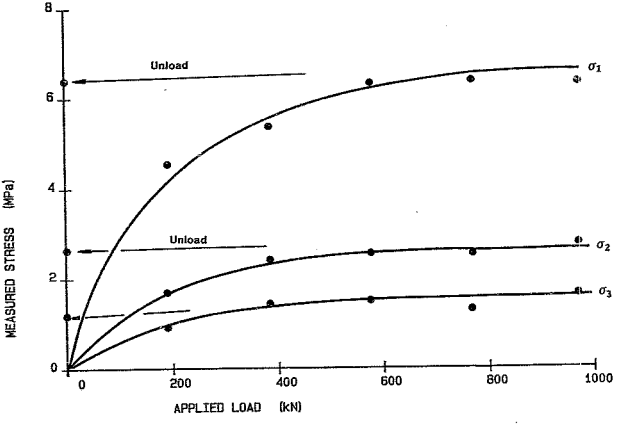

Figure 7.5 Relationship between the applied surface loads and induced stresses at 2,3m depth.

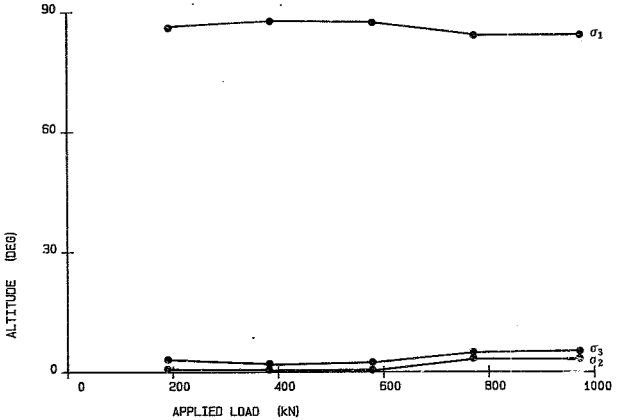

Figure 7.6 Altitudes c. the induced principal stresses at 2,3m depth.

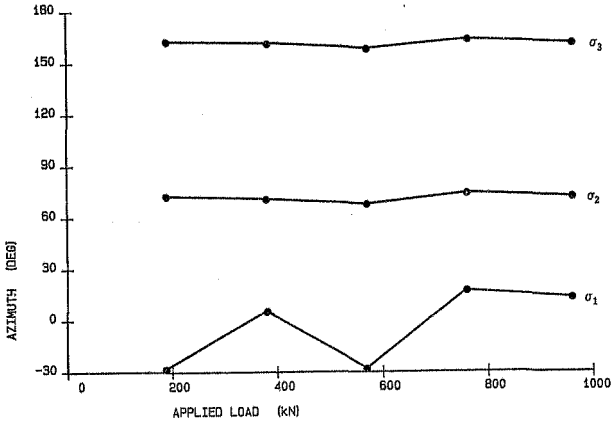

Figure 7.7 Azimuths of the induced principal stresses at 2,3m depth.

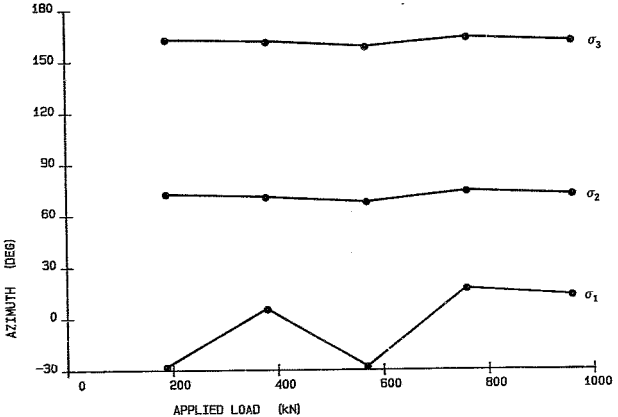

Figure 7.7 Azimuths of the induced principal stresses at 2,3m depth.

block accompanied by some slip on the block side interfaces, eventually reaching a stable frictional limit. At this stage, any increase in the applied load resulted in a further incremental displacement of the block, relieving the stress build-up. Unfortunately the actual dimensions and mass of the 'block' could not be ascertained as its boundaries were invisible. Judging from the observed fractures and parting planes, the block was estimated to be approximately 1 m square at its base and some 3 m in height.

Relaxation of the applied load did not result in immediate relaxation of the induced stresses, but rather a partial relaxation with the remaining stresses 'stored' within the rock. This in itself indicates a large amount of inelastic behaviour within the rock mass, in this case probably due to shearing of interface asperities. For reasons explained, no confirmation of such phenomena could be obtained. The loaded rock block may have been forced or wedged between adjacent blocks, increasing its confinement and preventing further elastic response on unloading, assisted by non-linear restraints provided by the interface material and geometry. This situation may be compared to the analogy of a cork being squeezed into the neck of a bottle.

It is interesting to note that the measured stresses in the hangingwall, both vertical and horizontal were of the order of megapascals (MPa), which is well in excess

of the required confinement (kPa) to maintain the stability of a typical hangingwall block as determined in Chapter 4. This indicates that active support loads may, if correctly positioned, significantly improve block stability. At this point however, it is worth bearing in mind that incorrect positioning of such a load could also have adverse effects, loosening otherwise stable blocks.

It may be seen that the major principal stress, σ_1, which reached 6 MPa, maintained a vertical orientation (Figure 7.6) and fluctuated around a mean azimuth or horizontal direction (Figure 7.7) throughout the incremental load application. The intermediate and minor principal stresses, σ_2 and σ_3, which were of the order of 1 MPa to 3 MPa, maintained constant altitudes and azimuths. The reason for the differences in magnitude between the intermediate and minor principal stresses is uncertain but has been attributed to anisotropy of the material and the effects of discontinuities in stress distribution. The orientations and inclinations of the block boundary fractures must influence the stress distribution within the block, providing confinement or allowing relaxation, depending on their position. Relaxation of stresses in the σ_3 direction due to the softer, sheared material at the block interfaces may account for the difference in magnitude between the intermediate and minor principal stresses.

Figure 7.8 shows the Boussinesq solutions for a point load corresponding to the barrier prop head-piece, acting on the surface of a semi-infinite elastic medium. It is immediately obvious that a significant difference in magnitude exists between the vertical and horizontal induced stresses, which correlates with experimental data, and that the theoretical stress changes are two orders of magnitude lower than the experimental values. The discontinuous nature of the rock and the associated non-linear behaviour combined with local peaks and stress concentrations must account for this discrepancy.

7.1.3 Induced displacements in the hangingwall

Displacements caused by the barrier prop acting on the hangingwall were measured in two separate areas. The relative displacements of the rock strata above the stope were measured with a spring anchor wire-type extensometer extending to 4 m in the hangingwall, with additional anchor points at 2,5 m, 1,2 m and 0,5 m depths. This instrument was found to have insufficient accuracy for the magnitude of movements to be measured and no definitive results were obtained. Many of the readings indicated movements of the order of 1 mm which unfortunately fell within the limits of accuracy of the instrument, rendering them suspect. Difficulties in

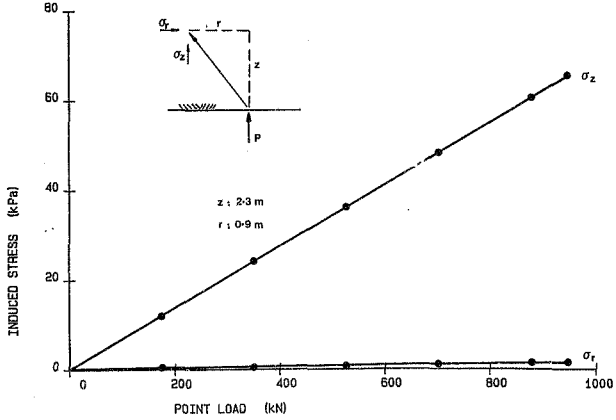

Figure 7.8 Point load effects on an elastic medium.

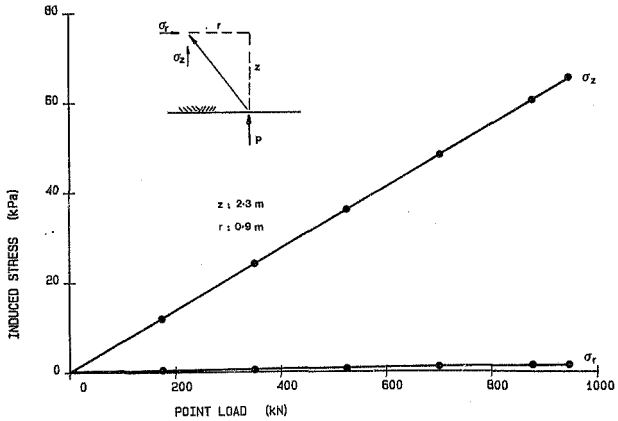

Figure 7.8 Point load effects on an elastic medium.

obtaining repeatable results caused by uneven extensions of the wire traces and tapes provided another source of error.

A summary of the results (not presented here) indicated that the upper sections of the rock mass under examination, between 2,5 m and 4,0 m depth were not displaced by the active load. Some shortening (2 mm) of the borehole was measured between the 1,2 m and 2,5 m anchors under high applied loads of the order of 950 kN, probably due to closing of a small fracture or parting plane. Due to the inadequacies of this instrument, such movement could not be distinguished from hangingwall surface deformations which would have the same influence on readings.

Relative separation of the hanging- and footwall surfaces was monitored over several stations, measurements being taken between installed masonry bolts. A single vernier closure meter had to be attached to each measuring station separately for each set of readings obtained. This movement caused discrepancies in readings and thus introduced a source of error. A continuous or permanent monitoring device attached to each bolt would have produced more accurate results. A plan of the bolt positions is given in Figure 7.9 and a summary of the results for bolts that remained undamaged by stoping activity is presented in Figure 7.10. It may be seen that whereas bolt 'A'

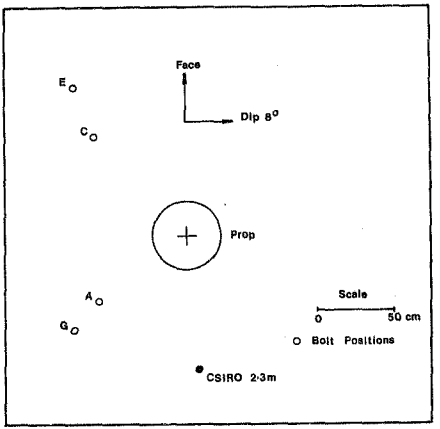

Figure 7.9 Plan of relative bolt positions.

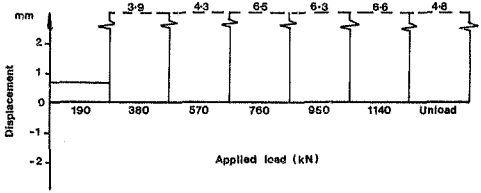

Bolt 'A'

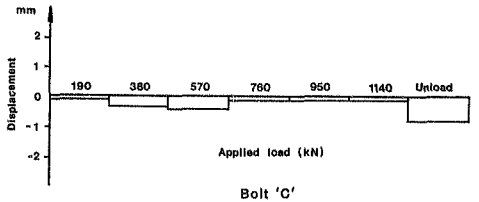

Bolt 'C'

Figure 7.10 (a) Relative surface deformations around the active support load.

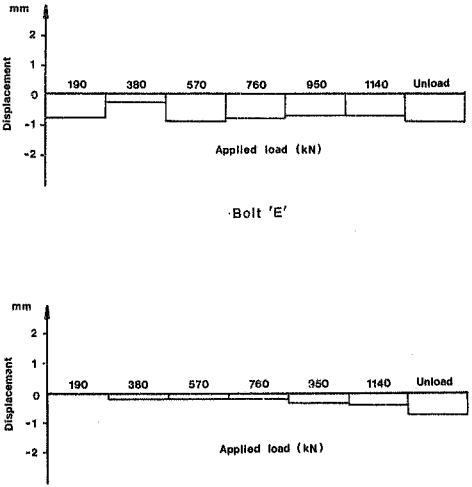

Figure 7.10 (b) Relative surface deformations around the active support load.

exhibited fairly large upward movements when the barrier prop was activated, the other bolts, such as 'G', displayed downward movements (of smaller magnitude). This is particularly interesting as it indicates differential movement (slip or rotation) between adjacent blocks separated by the narrow extension-type fracturing observed on the hangingwall surface. It may be argued that such behaviour may apply to much larger blocks in an intensely fractured production stope hangingwall where the imposition of a stiff, high-load support may provide sufficient disruption to dislodge adjacent blocks.

Bolt 'A' was selected for further analysis since it was fairly close to the centre of the disturbance and seemingly in the same continuous block as that on which the prop acted, as shown by its deformational consistency. Figure 7.11 shows the load-deformation characteristics of the rock at that position with the dotted line indicating the response on unloading the prop. The displacement recovery was only 27% with the remaining displacement being permanent (or time-dependent). This provides further evidence for the inelastic, non-linear response of the fractured strata to support loads. For comparative purposes a similar cyclic loading curve for rock joints displaying residual displacement, (after Sun et al., 1985) is shown in Figure 7.12.

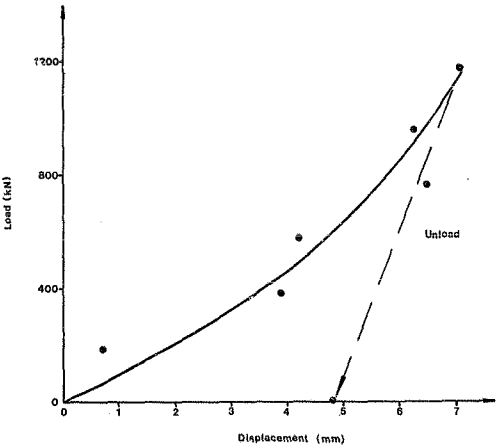

Figure 7.11 Load–deformation characteristics for hangingwall as measured at bolt 'A'

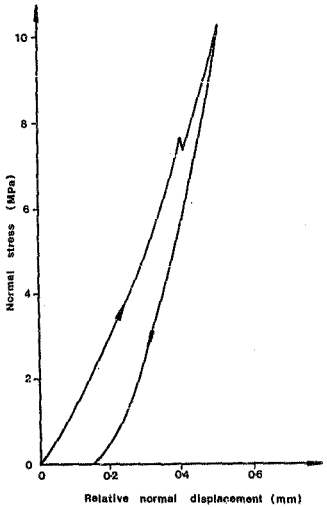

Figure 7.12 Load-deformation curve for rock joints.
(After Sun et al.,1985)

The displacement magnitudes measured by the author, even at some 700 mm from the prop centre, are more than two orders of magnitude greater than those predicted by elastic theory (Figure 7.13).

7.1.4 Young's modulus for broken rock

It has been the aim of much research to determine a value of the stiffness and strength parameters for broken rock. Researchers such as Ladanyi and Don (1967) and Raphael and Goodman (1979) have proposed modulus values in the region of 20% of that for intact rock. Such determinations must largely depend on the degree of fracturing, the orientation of the fractures and the proportions and positions of voids within the rock mass sample, making a consistent value impossible to obtain. Such work was also based on shallow or near-surface rock which may have been weathered and is not applicable to South African mining situations.

Substitution of relevant values obtained from the above measurements employing bolt 'A', into the elastic Boussinesq equation for displacement, provides a value for E in the region of 0,2% of that expected for solid material. It can be seen that the range of values for the modulus of broken rock is large and the author is of the opinion that no unique average value can be universally adopted.

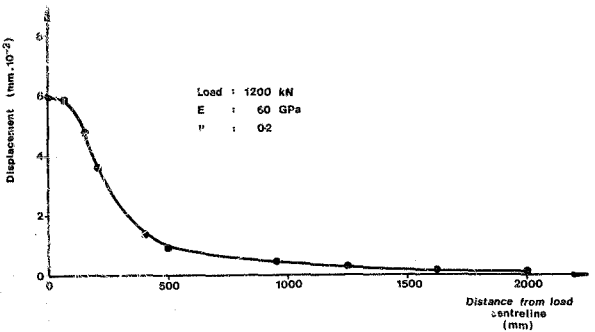

Figure 7.13 Predicted elastic deformations for rock surface.

7.2 Support System Effects

7.2.1 Inclination of hangingwall fractures

The inclinations of the hangingwall extension fractures were measured over the entire face length of both panels 9N and 10N, sampling the newly exposed fractures near the face after every 2 m of face advance. In the course of the experiment both faces were advanced over 40 m; this provided ample opportunity for alteration of fracture orientations due to the geometrical constraints imposed. A least squares linear interpretation (Figure 7.14) of Kersten's (1969) data by Brummer (1986a) indicated very little overall change in the inclination of the primary or shear fractures (Class III) in the hangingwall, formed ahead of a caving stope. Observations of the extension-type fractures (Class I) in the same stope showed a general increase in their dip, from a low-inclination 68° to the horizontal and towards the solid, to a much steeper 82° after some 30 m of face advance. Kersten (1969) noted that the fracture inclinations tended to increase with face advance or distance from the line of initiation of caving and that a sudden change in the dip of fractures was closely associated with that line.

The author's measurements in panel 9N, with a support density of 400 kN/m^2 are shown in Figure 7.15. It may be seen that behind the face position at the time of

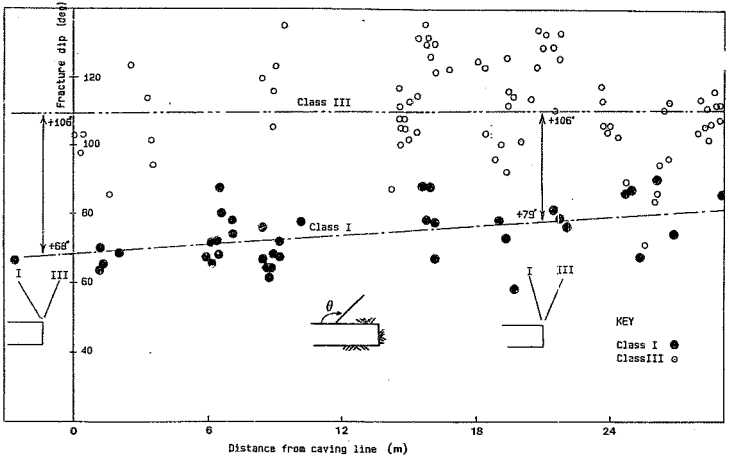

Figure 7.14 Inclinations of shear and extension fractures based on Kersten's (1969) observations. (After Brummer, 1986a)

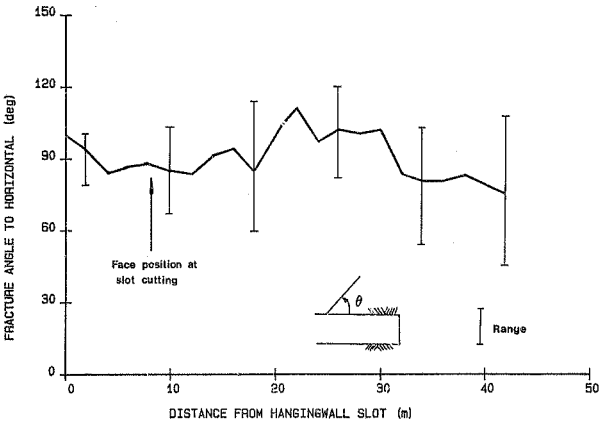

Figure 7.15 Hangingwall extension fracture inclinations, panel 9N

cutting the slot the hangingwall fractures were inclined fairly steeply at 80° (dipping away from the solid) to 100° (dipping towards the solid) from the horizontal. According to the block stability analysis in Chapter 4, such fractures provide for stable hangingwall conditions. A sudden decrease in the inclination of the fractures formed ahead of the face occurred some 8 m ahead of the face position at the time of cutting the slot. This change which may have been due to the associated stress relaxation and hence redistribution ahead of the face, occurred over a distance of only 2 m and altered the fracture angles some 10°, changing their dip from towards the solid zone to away from it. With further face advance the fractures formed tended to dip towards the solid zone approximately 5° to 12° from the vertical.

At a distance of 30 m from the slot position and after 20 m of face advance the hangingwall fractures reverted to inclinations between 80° and 90° to the horizontal, dipping towards the mined-out zone. Approximately 10 m ahead of this area the fractures in the hangingwall became more intense, irregular and deviated from their trends, which has been attributed to the influence of the opposing stope face advancing towards the experimental panel. Holing through the intervening pillar occurred some 50 m ahead of the slot position.

It should be remembered that the mining process continually increases stope span and thus alters the stresses on the rock ahead of the face. In addition, the remaining 'pillar' between the experimental stope and the opposing excavation was reducing in size and thus, particularly in the latter stages of the experiment, abnormal and high stresses would have occurred in that rock.

Throughout the 40 m or so that the hangingwall fracture angles were measured in this panel, they averaged almost exclusively within 10° of the vertical although individual variations of up to 30° from the average were encountered. No significant overall changes were measured. The hangingwall conditions may have been described as 'fair' before the slot-cutting but showed a marked improvement thereafter, providing a competent, clean, regularly fractured but smooth hangingwall.

The back unsupported region remained as a large intact slab extending over almost the entire panel length and typically for 4 m to 6 m behind the back row of support. This 'cantilevered beam' periodically broke 1 m behind the back row of support. Despite a slot height of 1,2 m, the fallen hangingwall slab was only approximately 50 cm thick indicating a weak parting plane at that level. The process of slab formation (with face advance) and collapse was cyclic although some variation in the unsupported span occurred. In one

instance, the hangingwall remained unsupported for 17 m into the back areas, indicating very competent and stable strata immediately above the stope. This phenomenon may have been aided by the high loads exerted on the strata by the stiff support system, in particular the back row of hydraulic props enhanced by barrier props. The support system, in forming a more rigid support for the overhanging slab may have had the effect of moving the effective solid face nearer the actual [illegible], thereby extending the permissible length of [illegible]antilevered beam further into the back a[illegible]. Additional block confinement by the support-induced horizontal stresses may have contributed to the axial thrust required for such beam stability.

No falls of ground occurred in the supported region of the stope once the slot had been cut and face advance resumed. Mining operations became easier as the hangingwall stability improved and the necessity for additional local support dwindled.

Panel 10N, with a 'softer' support system (exerting only 100 kN/m^2), exhibited more noticeable trends in fracture orientation (Figure 7.16). Behind the initial face position, the extension fractures had formed at angles averaging between 70° and 80° to the horizontal, dipping towards the excavation. During the initial mining period, local fallout of hangingwall blocks occurred particularly in the central and upper portions of the

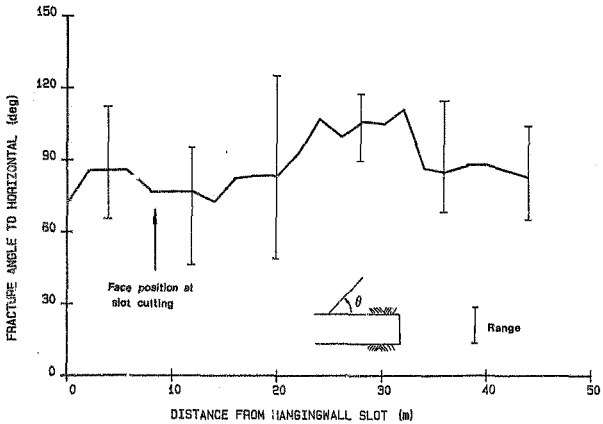

Figure 7.16 Hangingwall extension fracture inclinations, *panel 10N*

panel. The majority of these blocks were formed between two fractures, dipping towards and away from the excavation respectively. Such instability is predicted by the block analysis described in Chapter 4.

A substantial number of fractures inclined at low angles of the order of 60° to 70° were measured in the hangingwall just ahead of the first line of instruments. The rock some 3 m to 4 m ahead of the face at the time of cutting the slot, exhibited a similar sudden decrease in fracture inclinations as that experienced in panel 9N. Following a similar trend, the average extension fracture angle then increased with face advance, becoming first vertical, then lying at over 10° from the vertical dipping towards the solid zone. The author is uncertain of the cause of this occurrence but it may be attributed to a local change in stress distributions, material strengths or geological structure. No noticeable change in the immediate hangingwall rock type was observed and no external or geometrical influence had been applied.

At approximately the same distance from the hangingwall slot position as in panel 9N, after some 30 m of mining, the extension fractures in the hangingwall reverted quite suddenly to a steeper dip, averaging 85° to 90°. Unfortunately the mining rate during the course of the experiment was not constant and such occurrences may have been due to delays in face advance. However, panel

10N was mined approximately 3 m ahead of panel 9N and the similarity in positions of the change in fracture inclinations may dispute the above argument. A further lowering of the average fracture inclination accompanied by an increase in individual variation occurred as the panel was advanced into the remnant left by the opposing stope face and the hydraulic prop support system was replaced by 0,6 m mat packs at 3 m centres, due to difficulties in prop removal caused by intensive and irregular fracturing.

In contrast to panel 9N, panel 10N showed a definite alteration in the extension fracture inclinations, from initially relatively low angles of 70° to 80° to steeper fractures of 85° to 90° after the slot cutting. With the exception of the zone 20 m to 30 m ahead of the slot, where fractures dipped towards the solid material and some hangingwall blocks became unstable particularly near the top of the panel, the stability and condition of the hangingwall strata was excellent. The lower stratum surface was not as smooth as that in the adjacent panel (9N) but presented no support or instability problems and mining proceeded unhindered.

The greatest visual difference between the two panels was the occurrence and form of back-area hangingwall collapse. As previously described, the region between the slot and the last row of hydraulic props was left unsupported. In panel 9N this left a long shallow

cantilevered beam projecting over the back areas but in panel 10N the converse occurred. The hangingwall in this panel collapsed regularly, often after every blast following the advance of the support system. The collapse occurred right up to the back line of supports without over-running them and to a height of over 1 m, resulting in a typical 'caving stope' operation. The regular 'caving' of the hangingwall may have been enhanced by the 'softer' support system allowing block separation and collapse due to the lower confinements induced.

A detailed map of all hangingwall fractures on a 5 m long, strike-parallel line performed in panel 9N did not display the cyclic pattern observed by Kersten (1969) in a caving stope at Hartebeestfontein Gold Mine. It did however reinforce his data on the general difference in inclination between the shear and extension fractures in the hangingwall (Figure 7.17). Observations by the author in the south side panels, mining away from panels 9N and 10N, where no geometrical constraints were applied have shown a distribution of extension fracture angles well below the vertical and all dipping towards the excavation.

Measurements of extension fracture angles in the hangingwall at the abandoned 4-shaft site at Hartebeestfontein Gold Mine are shown in Figure 7.18. Due to the mining difficulties and frequent hangingwall

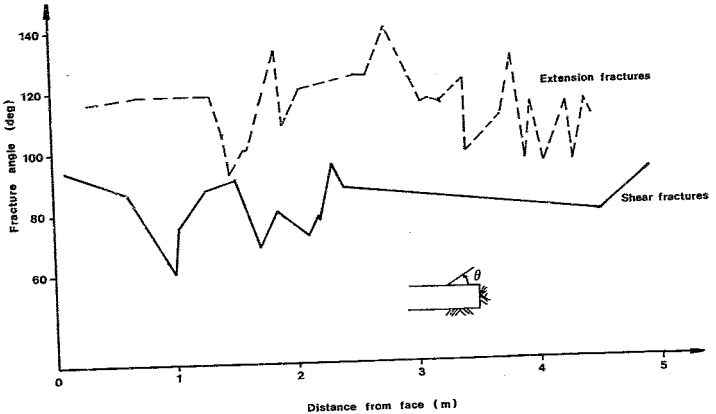

Figure 7.17 Inclinations of hangingwall shear and extension fractures on a 5m strike line.

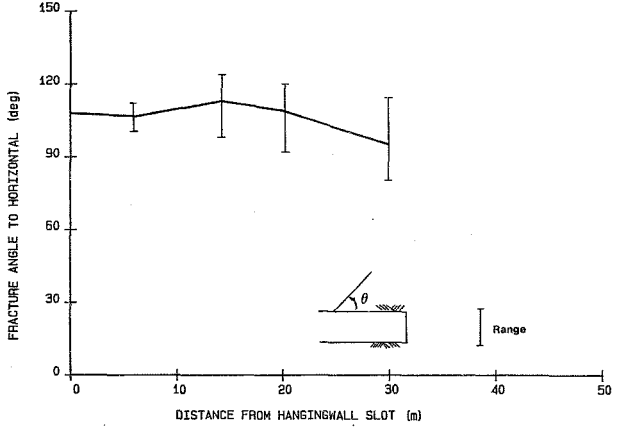

Figure 7.18 Hangingwall extension fracture inclinations, panel 3S

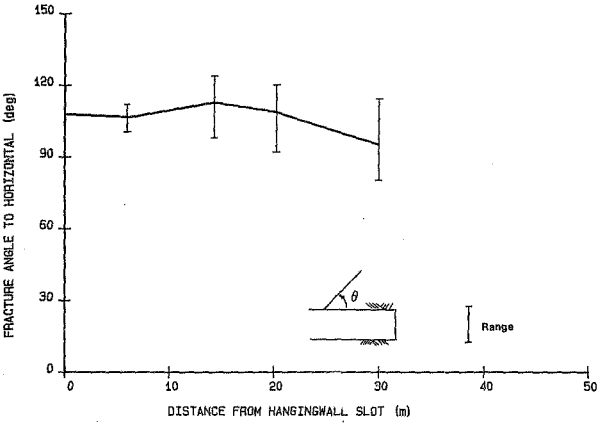

Figure 7.18 *Hangingwall extension fracture inclinations, panel 3S*

collapse, only a few measurements were taken over the 30 m of face advance, yet a definite trend is visible in the inclination of the fractures formed. At commencement of the observations the total stope span was of the order of 90 m and the hangingwall fractures were inclined at an average of 20° to the vertical, dipping towards the solid rock. The collapse of the hangingwall effectively simulated a dip slot with the fractures becoming oriented more towards the vertical as mining progressed. Such occurrences may have been major contributors to the improved stability of the hangingwall strata, which became apparent after 30 m to 40 m of face advance.

Kersten (1969) observed that the dip of fractures tended to increase with an increase in stope span. The author's own observations at the above site dispute this as is borne out by the low angle fractures in abundance at a stope span of 90 m. However, in agreement with Kersten's data, the initiation of caving or a geometrical constraint having similar effects can significantly alter and increase the dip of extension fractures in the hangingwall.

7.2.2 Stress relaxation

The strike-parallel dilation of the rock ahead of an advancing face has been discussed in Chapter 3. If inhibited, these dilations are likely to cause

significant compressive stresses in the strata. Relaxation of these stresses thus may affect the principal stress orientations ahead of the stope which in turn alter the in-situ fracture formation processes. In tandem with the measurement of hangingwall fracture inclinations associated with the cutting of the hangingwall slot, relative changes of the horizontal stresses in the hangingwall both before and after the slot-cutting were measured. This was performed using three doorstoppers installed at such depths into the hangingwall as to coincide with the bedding layers separated by the more prominent parting planes (See Figures 7.19a and 7.19b). The gauges were positioned so as to avoid fractured rock which would adversely affect their response.

In order to illustrate the significance of the slot and subsequent collapse of the hangingwall on the stresses in the strata, the measured strains have been converted to *stresses assuming elastic material behaviour*. This assumption is not entirely valid as inelastic deformations could have occurred in the rock during the measurement period, resulting in non-linear responses in the strain gauges.

Due to the irregular blasting cycle in the stopes which on occasion led to each face being advanced only every 5 days, the following data has been related primarily to time rather than to face advance. All measurements have

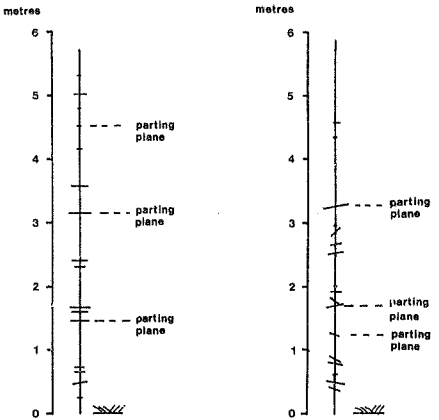

(a) panel 9N (b) panel 10N.

Figure 7.19 Petroscopic observations of fractures in the stope hangingwall

indicated a continual change with time, which was not markedly affected by the occurrence of blasting on the face.

The cumulative hangingwall stress changes (all data related to relative zero at the start of each monitoring cycle) obtained over a period of some 50 days of conventional mining in panel 10N are shown in Figure 7.20. This time span corresponds to a face advance of approximately 8 m. The lower hangingwall, extending to nearly 1,3 m before being broken by a shaley parting plane, exhibited a gradual stress relaxation (curve 1) during the first half of the mining sequence. Subsequently the stratum was compressed before the instrumentation was destroyed during initiation of the hangingwall slot. The bedding layer immediately above this stratum, extending to just over 3 m, showed a similar trend of stress relaxation followed by re-compression (curve 2). The rock above these two layers exhibited purely compressional behaviour, a total change of 70 MPa being recorded (curve 3).

The stress changes measured at similar depths into the hangingwall, under similar mining conditions, in panel 9N are shown in Figure 7.21. In contrast to the relaxation pattern obtained in panel 10N, the lower strata indicated the development of large compressive stresses without the initial relaxation as occurred in panel 10N. The lowest strain gauge rosette recorded the

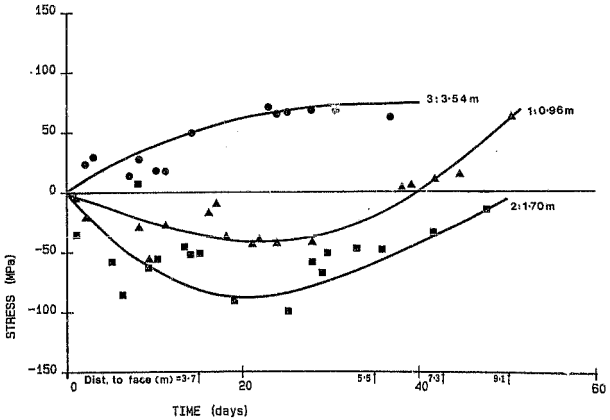

Figure 7.20 Strike – parallel stress changes under conventional mining, panel 10N.

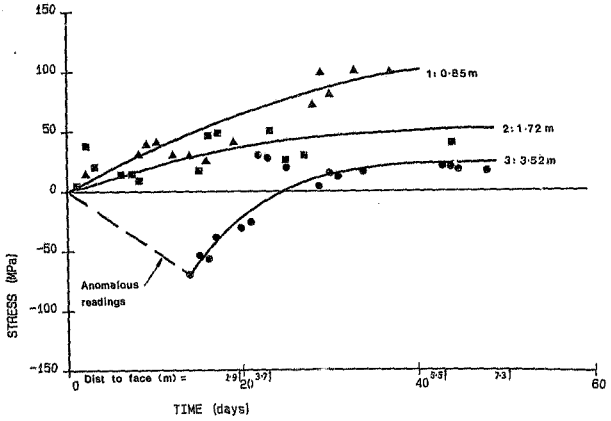

Figure 7.21 Strike – parallel stress changes under conventional mining, panel 9N.

largest variation in computed stresses (curve 1), probably due to interblock contact irregularities in the highly fractured and discontinuous stratum. Smaller changes in compressive stresses were measured in the second bedding layer where a fairly gradual increase was measured (curve 2), before some form of partial relaxation occurred. The curve representing the stress changes in the upper stratum, at 3,5 m depth, appears to be vertically displaced. This is probably due to irregularities in the measured strain values during the early period, which may have been due to interference from water ingress during the drilling of subsequent boreholes. Alternatively an error may have been accumulated early in the monitoring history. The curve however displays a continual compressive trend at a very similar rate (particularly in the latter stages) and of a similar magnitude to the corresponding curve for panel 10N.

After cutting the hangingwall dip slot, large strike-parallel tensile strains were measured in both panels, in the strata below the parting plane at approximately 3 m. The calculated stress relaxations for panel 10N are illustrated in Figure 7.22. The figure shows a similar trend to that obtained before cutting the slot for the lowest stratum - a gradual increase in the stresses relaxed, reaching a peak around 50 MPa, followed by a more gradual tailing-off. Unfortunately measurements beyond this point were not

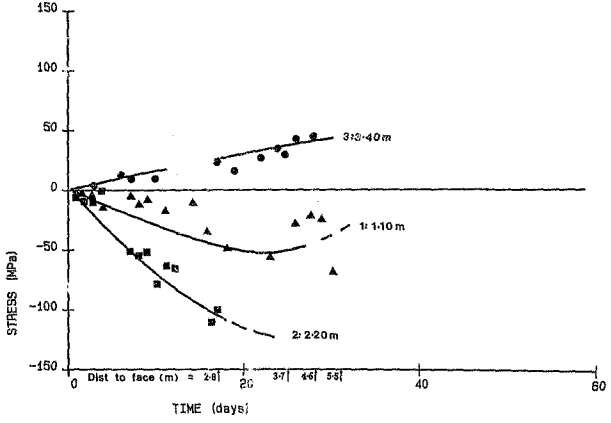

Figure 7.22 Strike – parallel stress changes after cutting the slot, panel 10N.

obtained due to collapse of the hangingwall and destruction of the instrumentation. In the same fashion as in Figure 7.20, measurements in the bedding layer above 1,3 m into the hangingwall indicated larger stress releases than in the lower layer. It appears that this intermediate zone, being less blocky than the lower region is able to contain and thus relieve itself of applied stresses more easily than the lower stratum. Large cumulative stress releases of the order of 100 MPa were calculated for this zone. These values are rather large and probably indicate the presence of inelastic strains in the rock. The rock above the 3,2 m parting plane exhibited no stress release but rather showed a continual, gradual increase in compression.

Figure 7.23 illustrates the calculated stresses obtained from measurements in panel 9N after the hangingwall slot was cut. The lowest instrument recorded a marked rapid release of contained compressive stresses followed by a period of re-compression once mining was re-established. Following the trend observed in panel 10N, larger cumulative relaxations were measured in the second prominent stratum above the excavation, in this case reaching approximately 100 MPa. This peak preceeded a period of gradual re-compression or re-confinement which continued until the instruments became unserviceable. The third doorstopper, some 3,4 m into the hangingwall exhibited a continual increase in confinement at a similar rate and of a similar magnitude

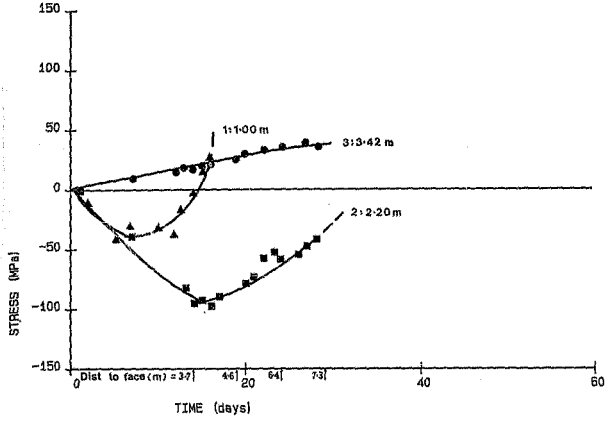

Figure 7.23 Strike – parallel stress changes after cutting the slot, panel 9N.

to the corresponding instrument in panel 10N. It is interesting to note that, prior to re-compression, the curves for the upper- and intermediate-level doorstoppers (curves 2 and 3) are very similar for both panels during this mining stage. This implies that the stiffer support system (400 kN/m²) in panel 9N, was having little additional influence on the upper hangingwall strata over the support in panel 10N (100 kN/m²). The behaviour of the doorstoppers installed in the lower bedding layers (curves 1 and 2), which in panel 9N indicated fairly rapid re-compression, may be due to the induced confinement and restrictions in dilation caused by the stiff support system.

An examination of the curves obtained from panel 10N (Figures 7.20 and 7.22) shows that the behaviour of the lower hangingwall in each layer did not differ greatly during the conventional mining and caving phases of the experiment. This implies that the strata were severely fractured and blocky, which permitted significant dilations and hence stress release. The fact that the upper doorstopper indicated compressional changes in both cases suggests that these severely fractured layers did not extend beyond the second prominent parting plane (3,2 m).

In contrast, the hangingwall in panel 9N showed large differences in the measured stresses during both phases of the experiment. Large stress relaxations in the

lower layers were followed by rapid re-compression, possibly due to the stiffer support system in that panel restricting strata dilation.

It is possible to deduce from the results obtained after the hangingwall slot was cut, that while the strata in the immediate hangingwall are affected by the disturbance, the range of influence of the slot may extend into the hangingwall strata above the slot. In the measurements obtained at the Hartebeestfontein site, it may be noted that the slot's influence extended to the upper limit of the bedding layer in which the slot terminated. It is of interest that the bedding plane above this upper boundary was not affected by the slot, which may be attributed to the intermediate parting plane facilitating sliding and the associated discontinuity in transmitted shear stresses and stress relaxation. This phenomenon is in accordance with the effective stope width concept proposed by Brummer (1986a).

The relatively highly fractured, discontinuous and blocky nature of the lower hangingwall as compared with the rock further away from the stope may cause irregularities in the stress patterns expected in that (lower) layer. The formation of such fractures alters the rock mass as a whole, effectively reducing the stiffness and thus the magnitude of contained stresses

induced by a particular value of strata dilation. This accounts for the lower values of relaxed stresses measured in this layer.

Results from Section 7.1 have indicated that the high-load, stiff supports employed in panel 9N may have increased the horizontal confinement in the hangingwall. The initial relaxation of mining-induced stresses following the blasting of the dip slot may have been counteracted by the horizontally-induced stresses of the support system, thus reducing the overall tensile dilation or strain of the rock mass. Compressive zones formed on the underside of transversely loaded cantilevered beams, formed by the hangingwall strata between the face and the unsupported slot, may account for much of the observed re-compression, as indicated by the measured stresses, of the relaxed hangingwall strata.

The compressive stresses measured in panel 9N before the slot was cut agree conceptually with elastic theory - restricted dilations must result in compressive stresses. The stresses measured in the lower strata of panel 10N however, can only be explained as a direct consequence of the intensely fractured and blocky material permitting dilation of the entire stratum. The previously mined region of panel 10N adjacent to the centre gully had experienced many large falls of ground, facilitating such dilations. The gradual re-compression

of the lower strata may have resulted from the improved lateral confinement provided by the reduction in the number and extent of falls of ground and the compression induced by bending of the strata.

7.2.3 Bedding separation

The stratified rock around the stopes has a tendency to separate, under gravitational or other loading, on the weak parting planes between layers. This separation results in stope closure rates in excess of those predicted by elastic analyses. Bedding separation was measured in panels 9N and 10N to a height of 10 m by wire extensometers (Roberts, 1986b) and to a height of just over 3 m by sonic extensometers. The latter instruments were intended to monitor movement in the immediate stope hangingwall, under what was assumed to be the direct influence of the support, while the former, on a less accurate basis, monitored larger-scale separations over greater intervals. Unfortunately the wire extensometers installed in the first line of instrumentation in both panels were unreliable and no data was collected.

Figure 7.24 shows the axial extensions measured in the sonic extensometer borehole for panel 10N while those for panel 9N are shown in Figure 7.25. The hangingwall in the centre of panel 10N showed some separation, of the order of 1,5 mm between 1,8 m and 2,3 m and

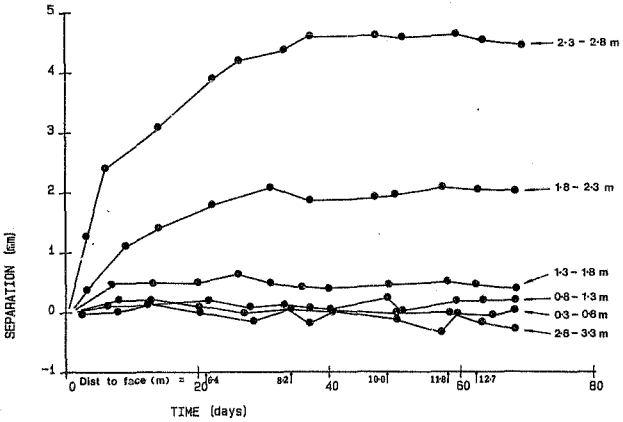

Figure 7.24 Borehole axial extensions as measured by sonic extensometer, panel 10N.

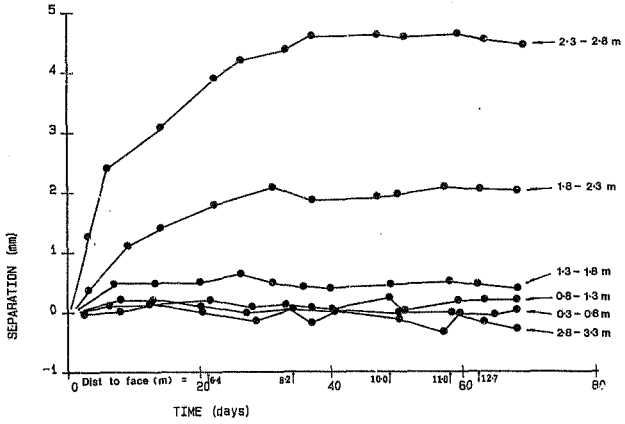

Figure 7.24 Borehole axial extensions as measured by sonic extensometer, panel 10N.

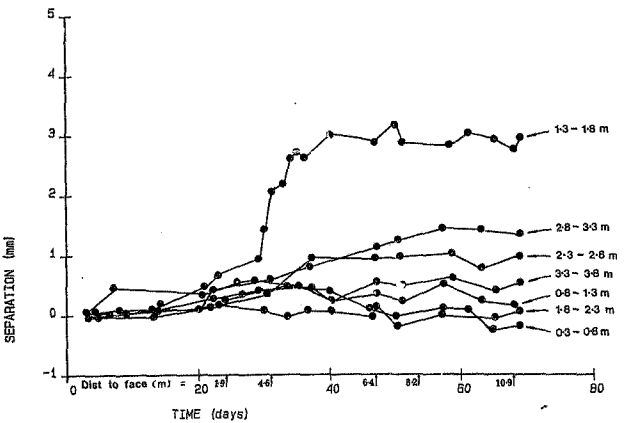

Figure 7.25 Borehole axial extensions as measured by sonic extensometer, panel 9N.

approximately 4,5 mm between 2,3 m and 2,8 m above the stope. These separations occurred after only 20 days and remained fairly constant for a further 50 days, when measurements ceased. Other zones showed no significant vertical separation. As all of the extensometers were installed behind the face, some separation had probably already occurred between bedding layers, which was not measured. Petroscopic observations of the hangingwall could not distinguish between fractures and small aperture openings on parting planes.

Panel 9N exhibited one major zone of separation between 1,3 m and 1,8 m above the stope, where some 3 mm of extension was measured. This occurred quite suddenly approximately 30 days after installation when the face had advanced approximately 4 m. Small amounts of borehole axial extension were recorded over the remaining zones of the instrument, reaching a maximum of just over 1 mm in the zone between 2,8 m and 3,3 m above the excavation. Such measurements may be attributed to minor bedding separation and elastic expansion of the strata.

The zone of significant axial borehole extension measured in panel 9N contained an observed parting plane (Figure 7.19) on which the separation may have occurred. Obstruction of the boreholes by the monitoring instrumentation prevented visual confirmation being made. In panel 10N, a possible parting plane

(marked in Figure 7.19) was identified at 1,7 m depth in a separate observation hole; this plane corresponds closely with the lower limit of the zone of measured elongation between 1,8 m and 2,3 m depth. Irregular hangingwall surface profiles and parting planes could account for the discrepancy in depth measurements. No parting plane was observed between 2,3 m and 2,8 m depth, where the largest separation was measured. Although the magnitude of the measured separations was small, significantly larger elongations were recorded in panel 10N than in panel 9N. This may be due to the supportive effects of the solid abutment immediately down-dip of panel 9N, as opposed to the mined-out stope up-dip of panel 10N. This stope would have experienced considerable bedding separation and would have influenced similar stratum layers above the monitored stopes, with diminishing magnitude as the solid (and therefore compressed) abutment was approached.

Figure 7.26 and Figure 7.27 show the separations recorded by wire extensometers in panels 9N and 10N respectively after the hangingwall slots were cut and differing support systems implemented. The results are plotted relative to the upper anchor (at 10 m above the stope) which was assumed to have remained stationary throughout the experiment. On-going measurements by Roberts (1986b) have detected bedding separation some distance above this and hence the values obtained are not absolute. In panel 10N, separations were recorded

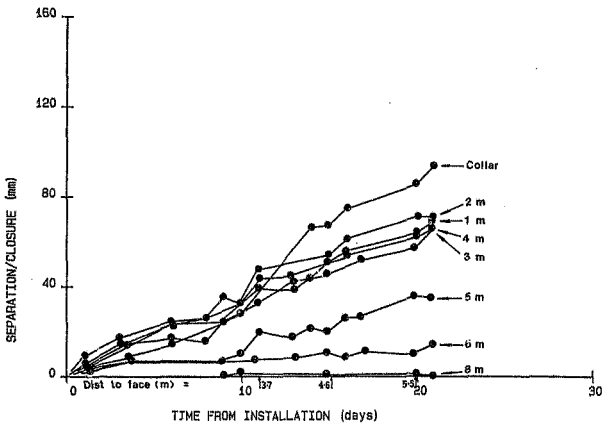

Figure 7.26 Wire extensometer measurements of borehole axial elongation, panel 9N.

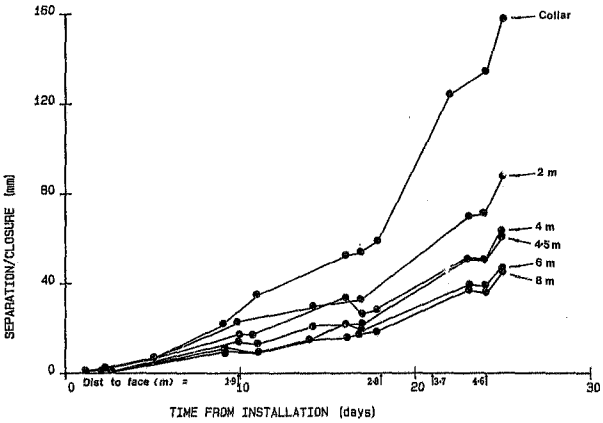

Figure 7.27 Wire extensometer measurements of borehole axial elongation, panel 10N.

between the collar of the hole and 2 m, between 2 m and 4 m, 4 m and 6 m and between 8 m and the upper anchor at 10 m above the stope. The borehole axial elongations measured varied between 47 mm and 160 mm over a period of only 25 days during which the face advanced some 6 m.

In panel 9N, separations were measured between the collar and 2 m, 4 m and 5 m, 5 m and 6 m and between 6 m and 8 m into the hangingwall. Face advance in this panel was approximately 7 m over the same time period. Smaller borehole elongations were measured in this panel (between 0 mm and 93 mm of extension), than in panel 10N, which may be attributed to the combined effects of the solid abutment downdip of panel 9N and the stiffer support system in the stope.

The combination of 400 kN hydraulic props and 1,6 MN barrier props in panel 9N provided an average support resistance of over 400 kN/m^2 which should support the hangingwall (on deadweight) to a height of 15 m. Separation of the order of 90 mm between the borehole collar and the uppermost anchor at 10 m, indicates that the support system was not operating at its pre-supposed capabilities, or that bedding plane separation is not caused by gravity alone.

The zones of separation in the lower hangingwall above panel 10N coincide with the positions of parting planes up to the limit of observation but only the lowest

observed parting plane in panel 9N corresponds to a zone of measured borehole elongation. Difficulties in visually identifying parting planes before any separation occurred, may have led to the omission of such items in the petroscopic borehole log. Core recovered from boreholes was generally badly broken and thus visual inspections yielded little information.

The support density of approximately 100 kN/m^2 in panel 10N should support nearly 4 m of hangingwall deadweight. As in the lower panel, this was not achieved as is evident from the large separations of 70 mm measured between the borehole collar and an anchor 2 m into the hangingwall. An increase in the rate of bedding plane separation as the face advanced and the collapsing hangingwall approached the measurement site is clearly shown in Figure 7.27. At this stage the overlying strata would have moved out of the supporting influence of the face and the lack of support from the back areas may have encouraged the separation of strata.

Figure 7.28 and 7.29 show the separations measured in the second line of instrumentation above panels 9N and 10N respectively by the sonic extensometers. In both cases the magnitudes of measured separations were greater than those obtained in the undisturbed hangingwall, before the slot was cut. In a similar

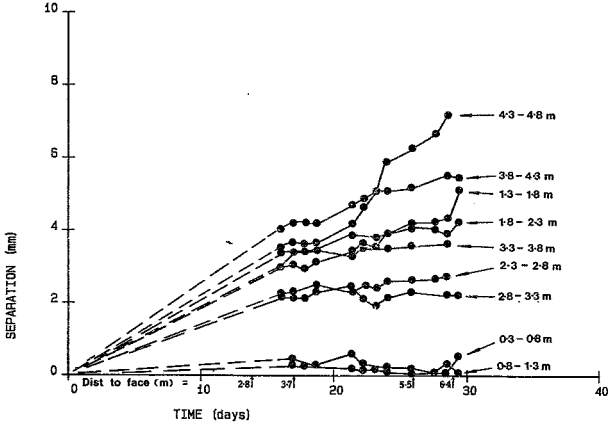

Figure 7.28 Borehole axial extensions as measured by sonic extensometer after slot-cutting, panel 9N.

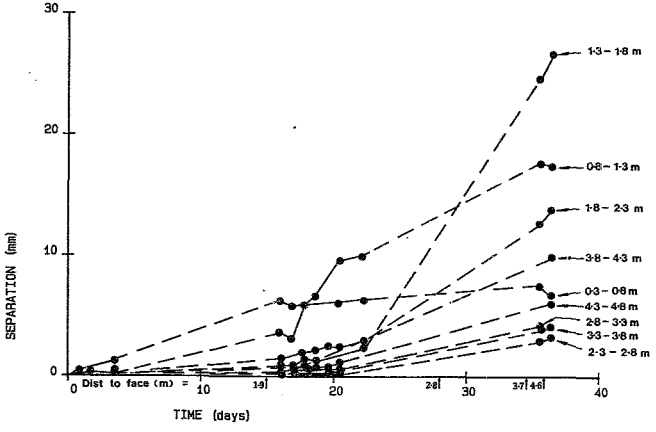

Figure 7.29 Borehole axial extensions as measured by sonic extensometer after slot-cutting, panel 10N.

fashion to the measurements obtained using the wire extensometer, significantly larger values were obtained in panel 10N than in panel 9N.

7.2.4 Closure and ride

Closure and ride, both parallel and perpendicular to strike, were monitored at three stations in each panel both before and after the hangingwall slot was cut.

The measured closures in panels 9N and 10N during conventional mining are shown in Figures 7.30 and 7.31. Initially slow closure rates increased rapidly as face advance continued, thereby increasing the stope span. Average closure rates of between 3,5 mm and 3,8 mm per day were obtained for both panels with panel 10N tending to have slightly higher rates than panel 9N.

Subsequent to the cutting of the hangingwall dip slot, closure rates in both panels were observed to increase dramatically (Figures 7.32 and 7.33). Panel 10N experienced an average rate of 13 mm/day whereas the closure rate in panel 9N was slower, averaging 10 mm/day. Both these values were far in excess of the predicted elastic closure rate which varied between zero at the abutment below panel 9N and approximately 6 mm/day at the upper end of panel 10N, adjacent to the extensively mined-out region. The magnitude of the bedding separations measured above the stopes provide an

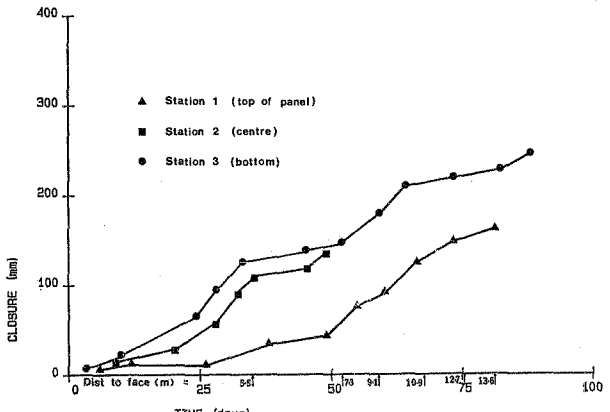

Figure 7.30 Measured stope closure under conventional layout, panel 9N.

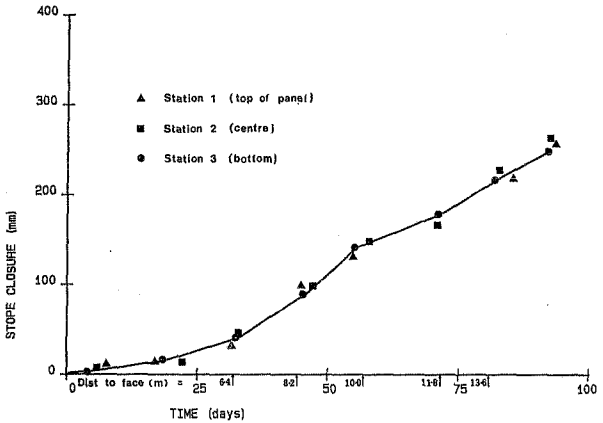

Figure 7.31 Measured stope closure under conventional layout, panel 10N.

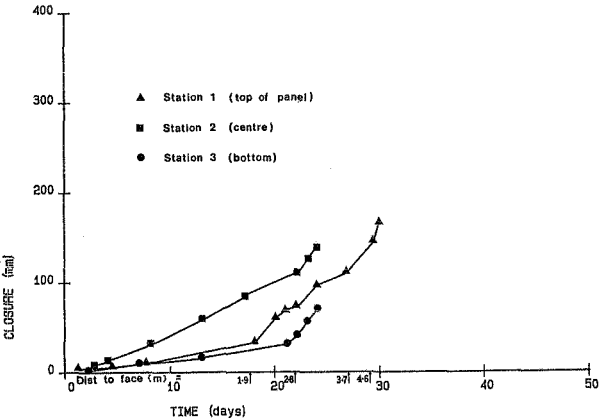

Figure 7.32 Measured stope closure under 'caving' conditions, panel 9N.

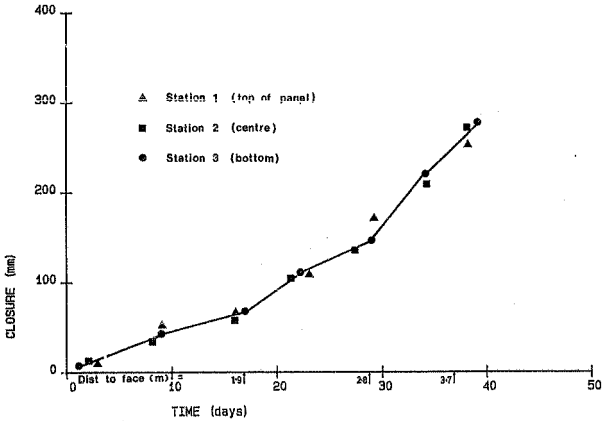

Figure 7.33 Measured stope closure under 'caving' conditions, panel 10N.

explanation for this rapid closure. The small difference in measured closure rates between the two panels of 3 mm/day does not justify the use of a more complicated or more dense support system, if its purpose is to influence closure. In fact, the difference in closure may be attributed to the effect of the surrounding excavations and abutments.

From the measurements taken, it appears that the support systems did not affect the hangingwall strata to any significant degree other than some compression of opening parting planes in the immediate stope hangingwall. Such observations have shown that large deadweight carrying capacities of support systems are possibly unnecessary as the strata are largely unaffected by them, borne out by the similar closure rates observed in the two panels. From observations and measurements such as these, it would appear feasible to provide sufficient stope support only to maintain and uphold the blocky strata in say, the first 3 m of hangingwall. By maintaining the stability of these blocks, stability of the entire hangingwall could be achieved. However, a system such as this would probably not be able to withstand rockburst conditions and loading. Similar conclusions have since been published by Jager and Roberts (1986).

Calculated values of ride in the dip direction indicated down-dip movement of the footwall relative to the hangingwall in both panels during the first stage of the experiment. This was facilitated by strike gullies excavated below reef level at the lower end of each panel, allowing movement of the footwall strata. Figure 7.34 shows the average measured ride of the footwall in both panels 9N and 10N for this period. Movement in the upper panel was significantly less than that in the lower panel. The situation was reversed after installation of the hydraulic prop supports and alteration of the stope geometry by cutting of the hangingwall dip slot, as shown in Figure 7.35. Down-dip ride of the footwall in panel 9N was decreased to less than one-half of its previous value, although the 'ride rate' was increasing shortly before the measurements ceased due to collapse of the hangingwall. On the other hand, the down-dip ride of the footwall in panel 10N increased slightly over its previous value.

Figure 7.36 illustrates the ride in the strike direction (away from the face) of the footwall relative to the hangingwall for both panels before the slot-cutting. The data from panel 10N showed a large scatter in individual values while definite trends were obvious from the data of panel 9N. Horizontal movement of the strata was small, reaching only 150 mm in panel 9N after 80 days, corresponding to some 12 m of face advance.

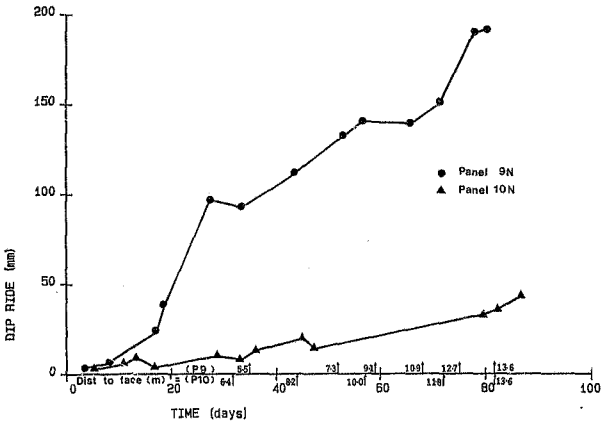

Figure 7.34 Relative downdip ride of the footwall under conventional mining conditions.

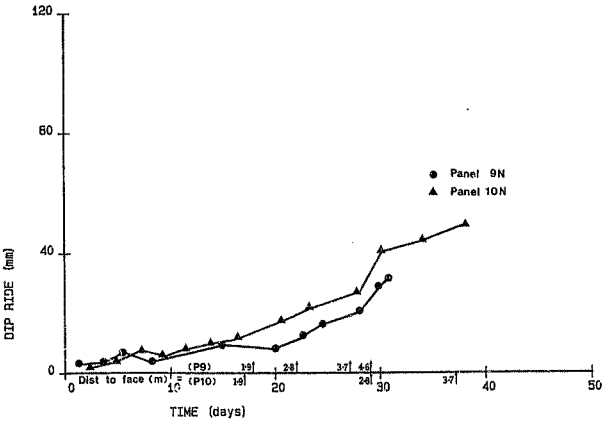

Figure 7.35 Relative downdip ride of the footwall after cutting the hangingwall slot.

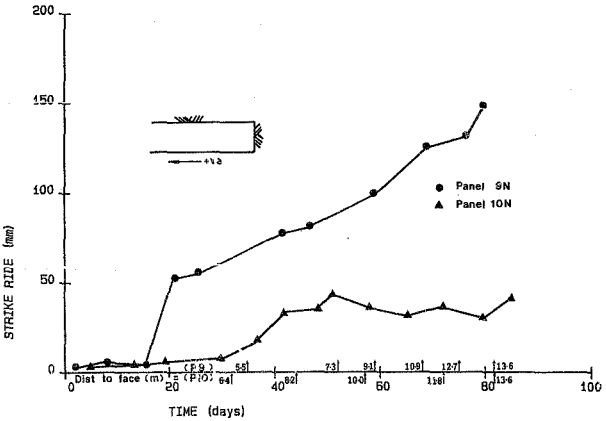

Figure 7.36 Strike ride of the footwall under conventional mining conditions.

This was less than that measured in the dip direction. In both panels, the relative strike ride occurred with the footwall moving away from the face.

After cutting the hangingwall slot, strike-parallel displacement of the footwall relative to the hangingwall occurred to a similar magnitude in both panels (Figure 7.37), averaging some 80 mm in under 40 days, corresponding to 5 m of face advance. This movement was not relative hangingwall displacement away from the face as may have been anticipated, but in fact was footwall dilation. The dip gully excavated in the footwall, directly below the hangingwall slot, would have provided the required mechanism for such displacement. The expected hangingwall movement may have taken place but to a lesser extent than that in the footwall and hence was not detected.

7.2.5 Surface dilations

The strike parallel dilation of the hangingwall surface was monitored using the vernier surface extensometer. Two parallel lines of measuring points were installed on the hangingwall in each panel. The total linear extensions of each line are shown in Figure 7.38 for panel 9N and Figure 7.39 for panel 10N. Results for panel 10N show very little dilation of the hangingwall whereas a gradual compression (negative values) of the immediate hangingwall stratum is evident in panel 9N.

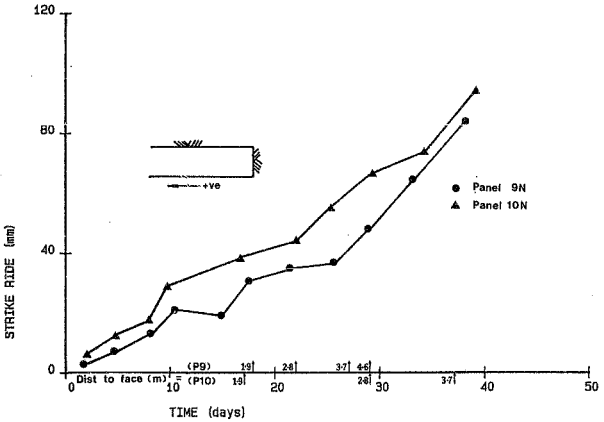

Figure 7.37 Strike ride of the footwall after cutting the hangingwall slot.

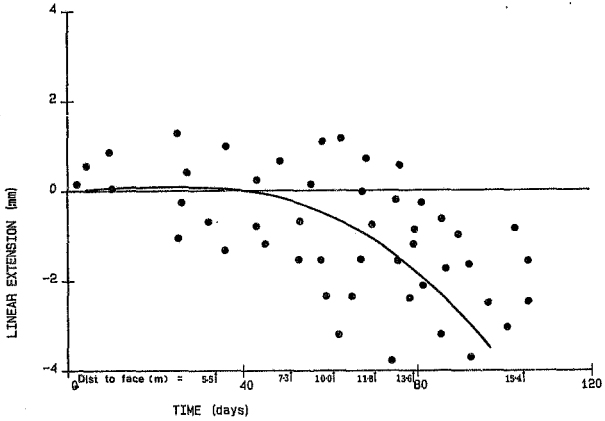

Figure 7.38 Total linear extension of the hangingwall surface, panel 9N.

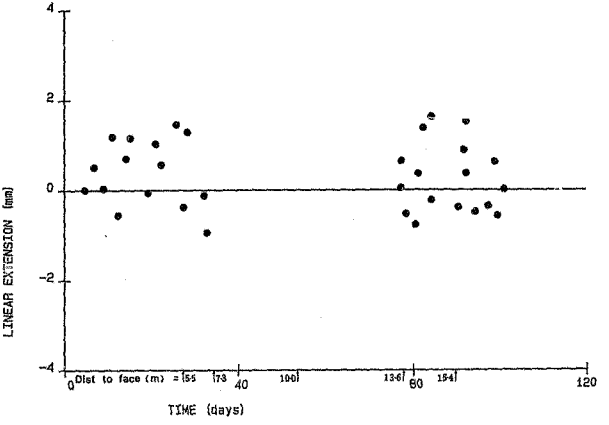

Figure 7.39 Total linear extension of the hangingwall surface, panel 10N.

This may have been due to the dilation of the fractured rock ahead of the face, in turn compressing the material above the excavation. Bending of the cantilevered strike-parallel beam over the stope would have induced compressive stresses in its lower surface which would contribute to the contraction of the measuring grid. Although a compressional trend is obvious in the results, a large scatter in values occurred. In neither panel was positive dilation of the hangingwall measured.

Similar linear measuring points were installed in both panels just prior to the initiation of the hangingwall slot. These provided few measurements before they were damaged during mining operations and no meaningful results were obtained. Thus no comparisons between strata dilation before and after the slot-cutting or under different support systems were possible.

7.3 Summary of Results

This chapter has presented the results obtained from the underground experimental determination of the influence of an active load on fractured rock strata and the effects of two different stope support systems in conjunction with a hangingwall dip slot on the stability of roof strata. Much data was collected and this section provides a brief summary of the salient results.

A triaxial strain cell installed in the same block of rock to which an active load (hydraulic prop) was applied, showed that internal hangingwall stresses increased with the applied load until some limit was reached, whereupon they maintained a constant level. This has been attributed to sliding on the block side interfaces, after shear forces exceeded the frictional limit. Some inelastic behaviour of the block was noted after relaxation of the load, as a 'containment' of the induced stresses. The measured stresses in the block were in the region of two orders of magnitude greater than those predicted by elastic theory. Measurements of the separation of the stope hanging- and footwalls around the hydraulic prop showed that while the loaded block was displaced upward, adjacent blocks moved downwards, indicating some disruption in the block assemblage. In a similar fashion to the stresses, some inelastic displacements of the block were measured after relaxation of the load.

The effects of two different support systems on the condition of the hangingwall strata were studied in conjunction with the cutting of a dip slot in the back areas, to provide stress relief in the overlying rock. Measurements of extension fracture inclinations in panel 9N showed a small decrease in the average fracture dip after cutting the slot, although no major changes were noted. Fractures in panel 10N showed a greater change

in inclination, steepening considerably after the slot was cut. Both panels showed a marked improvement in hangingwall stability as mining progressed.

Stress measurements in the strata above panel 9N indicated that the rock is continually compressed as the face advances, unless some form of relaxation is permitted. In such cases the stresses relaxed were of the order of 50 MPa. The stiffer support system in panel 9N appeared to provide some restrictions on hangingwall strata movement and hence affected internal stresses and stratum stability, although differences between the two panels were relatively small. Bedding separation and closure rate in both panels showed a large increase after the hangingwall slot was cut, while the support systems proved unable to withstand even their pre-supposed deadweight carrying capacity. A summary of measured parameters for both panels 9N and 10N are presented in Table 7.1.

Table 7.1 Measured Parameters for the Experimental Panels

Parameter Description	Panel 9N (400 kN/m²)	Panel 10N (100 kN/m²)
Extension fracture fluctuation	80° - 100°	70° - 110°
Max stress change in hangingwall layer : before (after) 'caving'		
lower	92 (- 40) MPa	- 42 (- 50) MPa
intermediate	50 (- 90) MPa	- 85 (-110) MPa
upper	25 (38) MPa	70 (42) MPa
Total bedding separation to 10 m in hangingwall after 'caving'	96 mm	155 mm
Average closure before (after) 'caving' at 30 days	65 (165) mm	40 (155) mm
Strike ride before (after) 'caving' at 30 days	75 (52) mm	25 (68) mm
Hangingwall surface dilation before 'caving'	- 4 mm	nil

8 CONCLUSIONS AND RECOMMENDATIONS

This work has described the effects of some support systems and of 'caving' of the hangingwall in a deep-level mine. The attitudes of fractures in the stope hangingwall allow the formation of blocks or wedges of rock in the strata, which under certain conditions become unstable and fall, resulting in injury to personnel, damage to the excavation and delays in production.

A block stability analysis has shown that block geometry and the block boundary fracture inclinations are important in determining the stability of that block. It has been shown that blocks with sides inclined at angles close to the vertical make full use of the available frictional and confining forces and thus are more stable than those with sides inclined at less steep orientations. The significance of the horizontal confining stresses in maintaining block stability is reduced as the bounding fracture planes approach the vertical. The horizontal stresses required to maintain the stability of a typical hangingwall block are of the order of kilopascals (kPa) which is significantly lower than the theoretical mining-induced stresses in the rock at the depths considered.

The shape of the loaded block may have a significant effect on the support-induced stresses within it and hence on the adjoining blocks. Imposition of an active load on a wedge-shaped block may force it upwards, increasing the lateral confinement of the block and its neighbours. As demonstrated in Chapter 4, this may improve the overall stability of the blocky stratum. A similar load acting on an inverted wedge will have the opposite effect, relaxing horizontal confinement and allowing collapse of unstable blocks. Use of a larger headpiece on the support could alleviate this problem. A parallel-sided block will be forced between its neighbours, initially being compressed, but reaching an equilibrium state in which further loading causes slip on the block interfaces, the internal stresses remaining constant. Such behaviour, similar to that of a cork in the neck of a bottle, occurred in the loaded rock block in the stope hangingwall as described in Section 7.2.

The individual active support load used in the author's experimental work produced compressive stresses in the blocky hangingwall, far in excess of those predicted by elastic theory. This indicates that not only does the hangingwall behave in a highly non-linear fashion, but that support loads may have an important effect on block- and thus stratum stability by virtue of the horizontal stresses induced.

The orientations of the block boundary fractures may affect the stress distribution within the block. Fractures themselves are planes of weakness which allow stress relaxation between adjacent blocks. Thus lower induced stresses in rock blocks may be expected normal to their major boundary discontinuities. Such behaviour was found to occur in the experimental block in the stope hangingwall at the Hartebeestfontein 4-shaft site, where stress changes normal to the major boundary discontinuities were found to be only one half of those parallel to the discontinuity.

The importance of inter-block friction and boundary discontinuity stiffnesses in controlling the relative displacement of adjoining blocks has been determined by deformational measurements. Stiffer block boundaries with a higher friction coefficient will result in a more uniform curve of the hangingwall surface under load, tending towards the elastic solution. Blocks that are relatively rigid when compared to their interface material will provide step-like transitions in displacement between blocks. The measured deformations not only indicated upward movement of the loaded block, but downward displacements of adjoining ones, suggesting some loosening of blocks in the stratum. In addition, some permanent (or possibly time-dependent) deformation of the loaded block was measured; further evidence for the non-linear response behaviour of the blocky medium.

Predictions of the effects of slot-cutting in the back areas of stopes and the associated collapse or 'caving' of the unsupported hangingwall were performed with the aid of the 'GOLD' finite element code. These analyses showed that the large horizontal compressive stresses in the strata above the stope and ahead of the face are partially relaxed by the introduction of the hangingwall slot. This provides a rotation toward the vertical of the resultant stress on a particular rock element ahead of the face and the associated change in the orientation of the fractures formed. The deformational results obtained from the finite element analyses were much smaller in magnitude but nevertheless showed the same trends as those expected, namely a general dilation of material away from the solid zone and towards the hangingwall slot position.

Inclusion of a mass supporting material in the excavation produced irregular deformations and reduced values of the horizontal stresses relaxed. The predicted deformations did not agree with expected results and some irregularity in the analysis is suspected. Alternatively the model may be inappropriate in the complex zone near to the excavation. On the whole, differences in numerically-predicted values for situations with and without the hangingwall slot and the mass supporting material were small and insignificant in terms of the underground situation. Further development of the code and its constitutive laws is recommended,

followed by stringent tests to check their validity. The development of a new purpose-built code for the analysis of the behaviour of fractured rock near to the stope may be a viable alternative.

The actual effects of a hangingwall slot and subsequent collapse of the unsupported strata above the stope were studied utilising two different support systems.

Introduction of a stiff, high-load support system near to the face theoretically may increase the lateral confinement of the strike-parallel hangingwall beam, improving its stability and reducing its tendency to collapse. Observations in the experimental stopes showed however that although a larger span remained unsupported above the back areas of such a stope, the condition of the hangingwall was similar to that under lower support densities.

Laboratory tests have shown that rock samples under triaxial loading tend to fail along a plane inclined at some angle to the major principal stress. The inclination of this failure plane can be steepened by removing the lateral confinement and allowing failure under uniaxial compression. This principle was employed in the underground stress relaxation experiment in order to alter the inclinations of extension-type hangingwall fractures.

The mining process and subsequent dilation of the rock towards the excavation causes a build-up of horizontal compressive stresses in the hangingwall. Due to the discontinuous nature of the rock immediately above a stope, any attempt at relaxing such stresses may provide only a reduction rather than complete removal of the confinement, thus allowing a change in fracture orientation while maintaining sufficient pressure to hold blocks in place. A reduction of the horizontal confinement above a stope by introducing a dip slot in the hangingwall was found to provide a significant change in the hangingwall strata condition. Such relaxation steepens the inclination of the extension-type fractures in the immediate hangingwall strata, thus providing more competent, stable hangingwall conditions.

The lower hangingwall strata are generally extensively fractured and thus allow some degree of stress relaxation. The bedding planes slightly higher in the hangingwall are less severely broken and are under some confinement, and thus may contain higher compressive stresses. Cumulative measurements of the strike-parallel horizontal stress changes developed in the hangingwall strata above an advancing stope have shown that these compressive stresses may reach magnitudes greater than 50 MPa. Similar values were measured for the cumulative relaxation of stresses after cutting a hangingwall dip slot. In addition, the results have shown that rock strata above the level of

the excavation are continually compressed during face advance, unless some relaxation is permitted. *Recompression of the lower strata in the hangingwall at* a distance of some 4 m behind the face suggests that bending of the strata occurs as a cantilever over the stope.

The separation of bedding layers on parting planes has been observed in several instances. Stiff support systems, contrary to expectations, have been shown to be unable to prevent such movements, even at depths into the hangingwall well within the supposed deadweight support capabilities of the system. Similarly neither stope closure rates (which were greater than predicted by elastic theory) nor general mining conditions were significantly altered by the presence of a stiff, high-load support system. It thus appears that under semi-static conditions the advantages of employing a stiffer support system are small in comparison with the extra cost and effort involved in installing it. Under rockburst conditions however, as determined by Wagner (1982), high support resistances are required.

The author's work has shown that the stress relaxation procedure adopted does have advantageous effects on the condition and stability of the immediate hangingwall rock. It has been demonstrated that successful mining of a narrow tabular excavation with no back area support is feasible. In turn, this procedure should provide

beneficial psychological attitudes amongst the mineworkers in working under a more competent stratum. It has been shown that the horizontal compressive stresses in the hangingwall strata and those induced by (active) support loads are more than sufficient to maintain block stability, provided that the inclinations of the block edges to the vertical are not greater than the interface material angle of friction.

The South African gold mining industry employs several different mining methods utilising and combined with several different support systems. The work described in this dissertation has provided an insight into just one such combination. Further work is necessary in both similar and alternative mining situations to determine the behaviour and influences of support systems on the hangingwall strata on an industry-wide basis.

9 REFERENCES

Adams, G.R. and Jager, A.J. (1979). Petroscopic observations of fracturing of rock ahead of stope faces in deep-level gold mines. Research Report no.17/79, Chamber of Mines of South Africa, Johannesburg.

Adams, G.R., Jager, A.J. and Roering, C. (1981). Investigations of rock fracture around deep-level gold mine stopes. Proceedings of the 22nd U.S. Symposium Rock Mechanics, Massachusetts Institute of Technology, June, pp.213-218.

Amadei, B. (1982). The influence of rock anisotropy on measurement of stresses in-situ. Ph.D thesis, University of California, Berkeley, 472 pp.

Amadei, B. (1984). In-situ stress measurements in anisotropic rock. International Journal of Rock Mechanics and Mining Sciences and Geomechanics Abstracts, vol.21, no.6, pp 327-338.

Amadei, B. (1985). Applicability of the theory of hollow inclusions for overcoring stress measurements in rock. Rock Mechanics and Rock Engineering, vol.18, pp.107-130.

Amadei, B. and Goodman, R.E. (1982). The influence of rock anisotropy on stress measurements by overcoring techniques. Rock Mechanics, vol.15, pp.167-180.

Auchtmuty, R.L. (1931). Subsidence and ground movement in a limestone mine caused by longwall mining in a coal bed below. American Institute of Mining and Metallurgy, Technical Publication no.396.

Barton, N., Lien, R. and Lunde, J. (1974). Engineering classification of rock masses for the design of tunnel supports. Rock Mechanics, vol.6, pp.189-236.

Bass[illegible]y, N.C., Jack, B. and Wagner, H. (1984). The pe[illegible]nce of rapid-yielding hydraulic barrie[illegible] props as stope support in a deep level mine. Research Report no.13/84, Chamber of Mines of South Africa, Johannesburg.

Batty, G.B. and Bell, J.H.C. (1945). Stope caving. Association of Mine Managers of South Africa, Papers and Discussions, vol.1, pp.421-432.

Beer, G. and Meek, J.L. (1982). Design curves for roofs and hangingwalls in bedded rock based on 'voussoir' beam and plate solutions. Transactions of the Institute of Mining and Metallurgy (sect. A: Mining Industry), vol.91, January.

Belytschko, T., Plesha, M. and Dowding, C.H. (1984). A computer method for stability analysis of caverns in jointed rock. International Journal for Numerical and Analytical Methods in Geomechanics, vol.8, pp.473-492.

Bieniawski, Z.T. (1967). Mechanism of brittle fracture of rock. D.Sc thesis, University of Pretoria.

Bieniawski, Z.T. (1976). Rock mass classification in rock engineering. Exploration for Rock Engineering, Bieniawski Z.T. ed. (Cape Town, Rotterdam : A.A. Balkema), vol.1, pp.97-106.

Bieniawski, Z.T., Denkhaus, H.G. and Vogler, U.W. (1969). Failure of fractured rock. International Journal of Rock Mechanics and Mining Sciences and Geomechanics Abstracts, vol.6, no.3, pp.323-341.

Bonnechère, F.A. and Fairhurst, C. (1968). Determination of the regional stress field from doorstopper measurements. Journal of the South African Institute of Mining and Metallurgy, vol.68, July, pp.520-544.

Borsetto, M., Martinetti, S. and Ribacchi, R. (1984). Interpretation of in-situ stress measurements in anisotropic rocks with the doorstopper method. Rock Mechanics and Rock Engineering, vol.17, pp.167-182.

Brace, W.F., Paulding, B.W. and Scholz, C. (1966). Dilatancy in the fracture of crystalline rocks. Journal of Geophysical Research, vol.71, no.16.

Brekke, T.L. (1968). 'Blocky and seamy rock' in tunnelling. Bulletin of the Association of Engineering Geologists, vol.5, pp.23-66.

Briggs, D.J. (1982). Mechanical properties of quartzites and associated rock types. Research Report no.13/83, Chamber of Mines of South Africa, Johannesburg.

Briggs, D.J. (1986). Personal communication. Chamber of Mines Research Organization, Johannesburg.

Briggs, D.J. and Vieler, J.D.S. (1984). Microfracture studies of quartzite in triaxial extension. Research Report no.12/84, Chamber of Mines of South Africa, Johannesburg.

Briggs, H. (1929). Mining subsidence, London, Arnold.

Briggs, R.C. (1963). Discussion on 'Concentrated stoping at Stilfontein mine', by Morgan, J.N. and Theron, D.J. Association of Mine Managers of South Africa, Papers and Discussions, vol. I, pp.323-405.

Brummer, R.K. (1985). Stress calculations, rotations, principal stresses and errors for analysis of 'CSIRO' cell results. Research Report no.14/85, Chamber of Mines of South Africa, Johannesburg.

Brummer, R.K. (1986a). Fracturing and deformation at the edges of tabular gold mining excavations and the development of a numerical model describing such phenomena. D. Ing thesis in preparation, Rand Afrikaans University, Johannesburg.

Brummer, R.K. (1986b). Personal communication. Chamber of Mines Research Organization, Johannesburg.

Brummer, R.K. and Crook, A.J.L. (1985). The development and application of finite element techniques for modelling the inelastic behaviour of rock around mining excavations. Proceedings of the 5th International Symposium on Finite Element Methods in South Africa, University of Stellenbosch, February.

Brummer, R.K. and Herrmann, D.A. (1986). Finite element applications in mining engineering. Proceedings of the 6th International Symposium on Finite Element Methods in South Africa, University of the Witwatersrand, Johannesburg, February.

Brummer, R.K. and Rorke, A.J. (1984). Mining induced fracturing around deep gold mine stopes. Research Report no.38/84, Chamber of Mines of South Africa, Johannesburg.

Bucky, P.B. (1956). Fundamental considerations in block caving. *Quarterly of the Colorado School of Mines*, vol.51, no.3, July, pp.129-146.

Chamber of Mines (1987). A catalogue of instrumentation for use in geotechnical investigations in mines. Chamber of Mines Research Organization, Johannesburg.

Chan, Lap-Yan and Goodman, R.E. (1983). Prediction of support requirements for hard rock excavations using keyblock theory and joint statistics. Proceedings of the 24th U.S. Symposium on Rock Mechanics, College Station, TX, June, pp.557-576.

Coates, D.F. and Yu, Y.S. (1970). A note on the stress concentrations at the end of a cylindrical hole. International Journal of Rock Mechanics and Mining Sciences and Geomechanics Abstracts, vol.7, pp.583-588.

Cook, N.G.W. (1962). A study of failure in the rock surrounding underground excavations. Ph.D thesis, University of the Witwatersrand, Johannesburg.

Cording, E.J. and Mahar, J.W. (1974). The effect of natural geologic discontinuities on behaviour of rock in tunnels. Proceedings of the 1974 Rapid Excavation and Tunnelling Conference, San Francisco, California, June, vol.1, pp.107-138.

Crawford, A.M. (1982). Rock wedge stability. Proceedings of the 23rd U.S. Symposium on Rock Mechanics, University of California, Berkeley, August.

Crawford, A.M. and Bray, J.W. (1983). Influence of the in-situ stress field and joint stiffness on rock wedge stability in underground openings. Canadian Geotechnical Journal, vol.20, pp.276-287.

Crook, A.J.L., Hoe, Y.C., Hinton, E. and Stagg, K.G. (1984). Development of a finite element package for rock mining problems. Report no.C/M/187/84, University of Wales, Swansea.

Crouch, S.L. (1969). A note on the stress concentrations at the bottom of a flat-ended borehole. Journal of the South African Institute of Mining and Metallurgy, December, pp.100-102.

Crouch, S.L. (1970). The influence of failed rock on the mechanical behaviour of underground excavations. Ph.D thesis, University of Minnesota.

Crouch, S.L. (1976). Analysis of stresses and displacements around underground excavations : an application of the displacement discontinuity method. Geomechanics Report, Department of Civil and Mineral Engineering, University of Minnesota, 268pp.

Crouch, S.L. and Starfield, A.M. (1983). Boundary element methods in solid mechanics. George Allen and Unwin, London, 332 pp.

Cruden, D.M. (1978). Discussion on 'A method of distinguishing between single and double plane sliding of tetrahedral wedges' by Hocking G. International Journal of Rock Mechanics and Mining Sciences and Geomechanics Abstracts, vol.15, p.217.

CSIRO. Hollow Inclusion Stress Gauge, Field Manual. Rock Instruments, Queensland, Australia, unpublished.

Cundall, P.A. (1971). A computer model for simulating progressive large scale movements in blocky rock systems. Proceedings of the International Symposium on Rock Fracture, Nancy, France, Paper II-8.

Cundall, P.A. (1980). UDEC - A generalised distinct element program for modelling jointed rock. European Research Office, United States Army, London, England.

Cundall, P.A. and Hart, R.D. (1983). Development of generalised 2-D and 3-D distinct element programs for modelling jointed rock. Final Technical Report, Itasca Consulting Group, Inc., Minneapolis, Minnesota.

Deacon, D.D. (1963). Discussion on 'Concentrated *stoping at Stilfontein mine*', by Morgan, J.N. and Theron, D.J. Association of Mine Managers of South Africa, Papers and Discussions, vol. I, pp.323-405.

Deacon, D.D. (1965). Stoping at Zandpan. Association of Mine Managers of South Africa, Papers and Discussions, pp.379-409.

Deist, F.H. (1966). The development of a non-linear continuum approach to the problem of fracture zones and rockbursts and feasibility study by computer. Ph.D thesis, University of the Witwatersrand, Johannesburg.

Dinsdale, J.R.C. (1937). Ground failure around excavations. Transactions of the Institute of Mining and Metallurgy, vol.46.

Duffett, G.A., Griffin, T.B., Martin, J.B., Mercer, C.D., Reddy, B.D. and Resende, L.N. (1983). Nostrum - A finite element program ' non-linear structural mechanics. Technical Report 18B, UCT/CSIR Non-linear Structural Mechanics Research Unit, University of Cape Town.

Duncan Fama, M.E. and Pender, M.J. (1980). Analysis of the hollow inclusion technique for measuring in-situ rock stress. International Journal of Rock Mechanics and Mining Sciences and Geomechanics Abstracts, vol.17, no.3, pp.137-146.

Elisovetskii, I. Ya, Solov'ev, V.S., Sergeev, V.V. and Samusenko, A.K. (1978). Analysis of the causes of caving of the flanks and roof of rooms during mining-out of underworked ores at the Mayak Mine of the Talnakh Deposit. Soviet Mining Science, vol.14 no.2, March-April.

Elsworth, D. (1986). Wedge stability in the roof of a circular tunnel : plane strain condition. International Journal of Rock Mechanics and Mining Sciences and Geomechanics Abstracts, vol.23, no.2, pp.177-181.

Evans, W.H. (1941). The strength of undermined strata. Transactions of the Institute of Mining and Metallurgy, 15th Session, vol.50.

Gay, N.C. (1987). Personal communication. Chamber of Mines Research Organization, Johannesburg.

Goodman, R.E. (1976). Methods of geological engineering in discontinuous rocks. West, St. Paul, 472 pp.

Goodman, R.E. and Shi, Gen-hua (1982). Geology and rock slope stability - application of the keyblock concept for rock slopes. Proceedings of the 3rd International Conference on Stability in Surface Mining : Society of Mining Engineers, American Institute of Mining, Metallurgical and Petroleum Engineers, Inc., New York, pp.347-373.

Goodman, R.E. and Shi, Gen-hua (1985). Block theory and its application to rock engineering. Prentice-Hall, Inc., Englewood Cliffs, New Jersey, 338 pp.

Goodman, R.E., Shi, Gen-hua and Boyle, W. (1982). Calculation of support for hard jointed rock using the keyblock principle. Proceedings of the 23rd U.S. Symposium on Rock Mechanics, University of California, Berkeley, August, pp.883-898.

Gorrie, C. and Scott, G. (1970). Some aspects of caving on powered support faces. The Mining Engineer, August, pp.677-691.

Gray, W.M. and Barron, K. (1969). Stress determination from strain relief measurements on the ends of boreholes; planning, data evaluation and error assessment. Proceedings of the International Symposium on the Determination of Stresses in Rock Masses, Lisbon, 19-21 May, pp.183-199.

Gregory, E.C., Rundle, T.A., McCabe, W.M. and Kim, K. (1983). In-situ stress measurement in a jointed basalt : the suitability of five overcoring techniques. Proceedings of the Rapid Excavation and Tunnelling Conference, Chicago, Illinois, June, pp.42-61.

Herrmann, D.A. (1985). Practical guidelines for using 'CSIRO' hollow inclusion stress gauges. Research Report no.22/85, Chamber of Mines of South Africa, Johannesburg.

Herrmann, D.A. and Johnson, R.A. (1987). The use of finite elements for the analysis of the inelastic behaviour of rock in mining. Proceedings of the 7th International Symposium on Finite Element Methods in South Africa, University of Cape Town, January.

Heywood, G.R. (1945). Some aspects of mining practice. Association of Mine Managers of the Transvaal, Papers and Discussions, vol.II, pp.959-1045.

Hocking, G. (1976). A method for distinguishing between single and double plane sliding of tetrahedral wedges. Technical Note, International Journal of Rock Mechanics and Mining Sciences and Geomechanics Abstracts, vol.13, July, pp.225-226.

Hoek, E. (1977). Structurally controlled instability in underground excavations. Proceedings of the 18th U.S. Symposium on Rock Mechanics, Keystone, Colorado, June, pp.5A6-1 - 5A6-5.

Hojem, J.P.M. and Cook, N.G.W. (1968). The design and construction of a triaxial and polyaxial cell for testing rock specimens. The South African Mechanical Engineer, vol.18, no.2, September, pp.57-61.

Hojem, J.P.M., Cook, N.G.W. and Heins, C. (1975). A stiff, two meganewton testing machine for measuring the work-softening behaviour of brittle materials. The South African Mechanical Engineer, vol.25, September, pp.250-270.

Irresberger, H. (1981). Strata control in the face. Glückauf, vol.177, no.2, pp.69-71.

Jaeger, J.C. and Cook, N.G.W. (1979). Fundamentals of rock mechanics. Third edition, June, Chapman and Hall, London, 593 pp.

Jager, A.J. and Roberts, M.K.C. (1986). Support systems in productive excavations. Gold 100, Proceedings of the International Conference on Gold, vol.1 : Gold Mining Technology, SAIMM, Johannesburg.

Jooste, C.L. (1963). Stoping with steel friction props and caving at Free State Geduld Mines Ltd. Association of Mine Managers of South Africa, Papers and Discussions, vol.II, pp.673-692.

Kendorski, F.S. (1978). The cavability of ore deposits. *Mining Engineering, AIME, June, pp.628-631.*

Kendrick, R. (1970). Induction caving of the Urad Mine. Mining Congress Journal, October, pp.39-44.

Kersten, R.W.O. (1969). Structural analysis of fractures around underground excavations on a Witwatersrand gold mine. M.Sc dissertation, University of Pretoria.

Kidybinski, A. (1977). Roof rock stability tests and powered support selection systems for longwalls. State of the Art Report, USDI/CMI Joint Research Report, Project No. 14-01-0001-1450, Report no. 2.

Kidybinski, A. (1979). Experience with hand rock penetrometers used for mine rock stability predictions. Proceedings of the 4th International Congress on Rock Mechanics, Montreux, vol.2, pp.293-310.

Kidybinski A. (1982). Critical roof span approach to selection of proper coal-mining systems. Proceedings of the 2nd Conference on Ground Control in Mining, July 19-21, Morgantown, WV.

King, R.V. (1945). A study of geologic structure at Climax in relation to mining and block caving. Transactions of AIME, vol.163, pp.145-155.

Ladanyi, R. and Nguyen Don (1967). A 'cell test' with rock. Proceedings of the Geotechnical Conference, Oslo, pp.283-288.

Leeman, E.R. (1958). Some underground observations relating to the extent of the fracture zone around excavations in some Central Rand mines. Journal of the South African Institute of Mining and Metallurgy, vol.59, pp.357-384.

Leeman, E.R. (1964). The measurement of stress in rock - parts I, II and III. Journal of the South African Institute of Mining and Metallurgy.

Legge, N.B. (1984). Rock deformation in the vicinity of deep gold mine longwall stopes and its relation to fracture. Ph.D thesis, Univ[illegible] Wales, Cardiff, 293 pp.

Lorig, L.J. (1984). A hybrid computational model for excavation and support design in jointed media. Ph.D thesis, University of Minnesota, 237 pp.

Lorig, L.J. and Brady, B.H.G. (1983). An improved procedure for excavation design in stratified rock. *Proceedings of the 24th U.S. Symposium on Rock* Mechanics, College Station, TX, June, pp.577-585.

Mahtab, M.A., Bolstad, D.D. and Kendorski, F.S. (1973). Analysis of the geometry of fractures in San Manuel Copper Mine, Arizona. RI 7715, U.S. Bureau of Mines, 24 pp.

Mahtab, M.A. and Dixon, J.D. (1976). Influence of rock fractures and block boundary weakening on cavability. Transactions of the Society of Mining Engineers, AIME, vol.260, March, pp.6-12.

McGarr, A. (1971). Stable deformation of rock near deep-level tabular excavations. Journal of Geophysical Research, vol.76, no.29, pp.7088-7106.

Mohr, H.F. (1956). Measurement of rock pressure. Mine and Quarry Engineering, May, pp.178-189.

Morgan, J.N. (1945). Discussion on 'Some aspects of mining practice', by Heywood, G.R. Association of Mine Managers of the Transvaal, Papers and Discussions, vol. II, pp.959-1045.

Morgan, J.N. and Theron, D.J. (1963). Concentrated stoping at Stilfontein Mine. Association of Mine Managers of South Africa, Papers and Discussions, vol.I, pp. 3-405.

Olsen, O.J. (1957). urement of residual stress by the strain relief od. Quarterly of the Colorado School of Mines, vol.52, July, pp.185-204.

Owen, D.R.J. and Hinton, E. (1980). Finite elements in plasticity - theory and practice. Pineridge Press, Swanse 594 pp.

Panet, M. (1969). Discussion of 'Graphical stability analysis of slopes in jointed rock', by John, K.W. Journal of the Soil Mechanics and Foundation Division, Proceedings of ASCE, vol.95, SM2, pp. 685-686.

Pariseau, W.G., Voight, B. and Dahl, H.D. (1970). Finite element analyses of elastic-plastic problems in the mechanics of geologic media : an overview. Proceedings of the 2nd Congress, ISRM, Belgrade, vol.2, Paper 3-45, pp.311-323.

Pearson, R.S. (1963). Stoping with steel friction props and caving on President Steyn Gold Mining Company Ltd. Association of Mine Managers of South Africa, Papers and Discussions vol.I, pp.569-587.

Peirce, A.P. (1981). Unpublished notes. Chamber of Mines Research Organization, Johannesburg.

Peirce, A.P. (1983). The applicability of the non-linear boundary element method in the modelling of mining excavations. M.Sc dissertation, University of the Witwatersrand, Johannesburg.

Peirce, A.P. and Ryder, J.A. (1983). Extended boundary element methods in the modelling of brittle rock behaviour. Proceedings of the 5th International Congress on Rock Mechanics, Melbourne, pp.F159-F168.

Peng, S.S., Su, W.H. and Seisuko Okubo (1982). A low cost stressmeter for measuring complete stress changes in underground mining. Geotechnical Testing Journal, GTJODJ, vol.5, no.1/2, March/June, pp.50-53.

Priest, S.D. (1980). The use of inclined hemisphere projection methods for the determination of kinematic feasibility, slide direction and volume of rock blocks. International Journal of Rock Mechanics and Mining Sciences and Geomechanics Abstracts, vol.17, pp.1-23.

Rahn, W. (1984). Stress concentration factors for the interpretation of 'doorstopper' stress measurements in anisotropic rocks. International Journal of Rock Mechanics and Mining Sciences and Geomechanics Abstracts, vol. 21, no.6, pp.313-326.

Raphael, J.M. and Goodman, R.E. (1979). Strength and deformability of highly fractured rock. Proceedings of the Geotechnical Engineering Division, ASCE, vol.105, no.GT11, November, pp.1285-1300.

Resende, L. (1984). Constitutive modelling and finite element analysis in geomechanics. Ph.D thesis, University of Cape Town.

Reyes, S.F. and Deere, D.U. (1966). Elastic-plastic analysis of underground openings by the finite element method. Proceedings of the 1st Congress, ISRM, Lisbon, Paper 7-42, pp.477-483.

Roberts, M.K.C. (1986a). Personal communication. Chamber of Mines Research Organization, Johannesburg.

Roberts, M.K.C. (1986b). Report in preparation. Chamber of Mines Research Organization, Johannesburg.

Roering, C. (1978). Confidential Report to the Chamber of Mines Research Organization, Johannesburg.

Roering, C. (1979). Confidential Report to the Chamber of Mines Research Organization, Johannesburg.

Rorke, A.J. and Brummer, R.K. (1985). A stereographic mapping technique. Research Report no.6/85, Chamber of Mines of South Africa, Johannesburg.

Ryder, J.A. and Napier, J.A.L. (1985). Error analysis and design of a large-scale tabular mining stress analyser. Proceedings of the 5th International Conference on Numerical Methods in Geomechanics, Nagoya, Japan.

Ryder, J.A. and Officer, N.C. (1964). The elastic analysis of strata movement in the vicinity of inclined excavations. Journal of the South African Institute of Mining and Metallurgy, vol.64, pp.219-244.

Salamon, M.D.G. (1963). Elastic analysis of displacements and stresses induced by the mining of seam or reef deposits - Part I. Journal of the South African Institute of Mining and Metallurgy, vol.64, pp.128-149.

Salamon, M.D.G. (1964). Elastic analysis of displacements and stresses induced by the mining of seam or reef deposits - Part II. Journal of the South African Institute of Mining and Metallurgy, vol.64, pp.197-218.

Salamon, M.D.G. (1974). Rock mechanics of underground excavations. In 'Advances in Rock Mechanics', Proceedings of the 3rd Congress, ISRM, vol.I, Part B.

Salamon, M.D.G., Ryder, J.A. and Ortlepp, W.D. (1964). An analogue solution for determining the elastic response of strata surrounding tabular mining excavations. Journal of the South African Institute of Mining and Metallurgy, vol.65, pp.115-137.

Schaller, S. (1979). Strata behaviour under caving conditions in the Sydney Basin Coalfields. BHP Technical Bulletin, vol.23, no.2, November, pp.27-34.

Shepherd, R. (1970). Discussion on 'Some aspects of caving on powered support faces', by Gorrie, C. and Scott, G. The Mining Engineer, August, pp.677-691.

Shi, Gen-hua and Goodman, R.E. (1981). A new concept for support of underground and surface excavations in discontinuous rocks based on a keystone principle. Proceedings of the 22nd U.S. Symposium on Rock Mechanics, Boston, MA, pp.310-316.

Slobodov, M.A. (1958). Test application of the load-relief method for investigating stresses in deep rock. Ugal, vol.7, pp.30-35. (D.S.I.R. Russian Translation RTS 1068).

Smith. J.L., de Vries, K.L., Bushnell, D.J. and Brown, W.S. (1969). Fracture data and stress-strain behaviour of rocks in triaxial compression. Experimental Mechanics, vol.9, pp.348-355.

Sofianos, A.I. (1986). Stability of rock wedges in tunnel roofs. International Journal of Rock Mechanics and Mining Sciences and Geomechanics Abstracts, vol.23, no.2, pp.119-130.

Stravropoulou, V. (1982). Constitutive laws for brittle rocks. Ph.D thesis, University of the Witwatersrand, Johannesburg.

Sun, Z. Gerrard, C. and Stephansson, O. (1985). Rock joint compliance tests for compression and shear loads. International Journal of Rock Mechanics and Mining Sciences and Geomechanics Abstracts, vol.22, no.4, pp.197-213.

Swaisgood, J.R., McMahon, B.K. and West, L.J. (1972). Rock mechanics in the planning and control of block caving. Joint Meeting, MMIJ-AIME, Tokyo, May, Print no.T IIa2, 14 pp.

Thorneycroft, W. (1931). Effect on buildings of ground movement and subsidence caused by longwall mining. American Institute of Mining and Metallurgy, Technical Publication no.398.

Timoshenko, S.P. and Goodier, J.N. (1970). Theory of Elasticity, McGraw-Hill, New York.

Unrug, K. and Szwilski, A.B. (1982). Methods of roof caveability prediction. In 'State of the Art of Ground Control in Longwall Mining and Mining Subsidence', Y.P. Chugh and M. Karmis (eds.), AIME, 1982.

Wagner, H. (1982). Support requirements in rockburst conditions. Proceedings of the 1st International Congress on Rockbursts and Seismicity in Mines, N.C. Gay and E.H. Wainwright (eds.), Johannesburg, pp.209-218.

Walsh, J.B., Leyde, E.E., Whit and Carragher, B.L. (1977). Stope closure stud. West Driefontein Gold Mine. International Journal of Rock Mechanics and Mining Sciences and Geomechanics Abstracts, vol.14, pp.277-281.

Warburton, P.M. (1981). Vector stability analysis of an arbitrary polyhedral rock block with any number of free faces. International Journal of Rock Mechanics and Mining Sciences and Geomechanics Abstracts, vol.18, pp.415-427.

Wawersik, W.R. (1968). Detailed analysis of rock failure in laboratory compression tests. Ph.D thesis, University of Minnesota.

Wawersik, W.R. and Brace, W.F. (1971). Post-failure behaviour of granite and diabase. Rock Mechanics, vol.3, pp.61-85.

Wawersik, W.R. and Fairhurst, C. (1970). A study of brittle rock fracture in laboratory compression experiments. International Journal of Rock Mechanics and Mining Sciences and Geomechanics Abstracts, vol.7, no.5, September, pp.561-575.

Worotnicki, G. and Walton, R.J. (1976). Triaxial hollow inclusion gauges for the determination of rock stresses in-situ. Proceedings of the ISRM Symposium on Investigation of Stress in Rock and Advances in Stress Measurement, Sydney, Supplement, pp.1-8.

Yow, J.L. (1985). Field investigation of keyblock stability. Ph.D thesis, University of California, Berkeley, 228 pp.

Zienkiewicz, O.C. (1977). The finite element method. McGraw-Hill, (UK), 787 pp.

Zienkiewicz, O.C., Best, B., Dullage, C. and Stagg, K.G. (1970). Analysis of non-linear problems in rock mechanics with particular reference to jointed rock systems. Proceedings of the 2nd Conference, ISRM, Belgrade, Paper 8-14, pp.501-509.

Zienkiewicz, O.C., Valliappan, S. and King, I.P. (1968). Stress analysis of rock as a no-tension material. Géotechnique, vol.18, pp.56-66.

Author Herrmann Dean Albert
Name of thesis Fracture control in the hangingwall and the interaction between the support system and the overlying strata. 1987

PUBLISHER:
University of the Witwatersrand, Johannesburg
©2013

LEGAL NOTICES:

Copyright Notice: All materials on the University of the Witwatersrand, Johannesburg Library website are protected by South African copyright law and may not be distributed, transmitted, displayed, or otherwise published in any format, without the prior written permission of the copyright owner.

Disclaimer and Terms of Use: Provided that you maintain all copyright and other notices contained therein, you may download material (one machine readable copy and one print copy per page) for your personal and/or educational non-commercial use only.

The University of the Witwatersrand, Johannesburg, is not responsible for any errors or omissions and excludes any and all liability for any errors in or omissions from the information on the Library website.